



Department of Mechanical and Aerospace Engineering

**Thermal Mass Modelling in Whole Building
Simulation Tool, For Model Predictive Control of
Peak Demand Limiting and Peak Load Shifting**

Author: Dereje Muluneh Workie

Supervisor: Dr Paul Strachan

A thesis submitted in partial fulfilment for the requirement of the degree
Master of Science
Sustainable Engineering: Renewable Energy Systems and the Environment
2015

Copyright Declaration

This thesis is the result of the author's original research. It has been composed by the author and has not been previously submitted for examination which has led to the award of a degree.

The copyright of this thesis belongs to the author under the terms of the United Kingdom Copyright Acts as qualified by University of Strathclyde Regulation 3.50. Due acknowledgement must always be made of the use of any material contained in, or derived from, this thesis.

Signed: Dereje M Workie Date: 08/09/2015

Abstract

Building integrated thermal mass systems, such as hollow-core concrete slabs, can be used as effective heat storage systems to maintain room air conditions for comfort. By using Model Predictive Control (MPC), hollow-core thermal systems can be configured to reduce demand and shift heating or cooling loads to off-peak time periods, thereby reducing costs.

This thesis presents an investigation of the thermal and economical characteristics of roof-integrated hollow-core slabs modelled using IES-VE building simulation software. Two case studies are also presented focussing on the impact of conventional controls and MPC on these characteristics, especially the cooling loads and their associated cost.

The results show that the efficacy of MPC is strongly dependent on the precooling duration, the zone set-point trajectory and the duration of the demand limiting control period. The total peak cooling demand can be reduced by up to 50% using optimised MPC over conventional control systems and the optimal precooling duration is approximately 3 hours before the onset of occupancy. This lowers the peak demand and can maintain comfortable air conditions for a longer duration over the occupancy period.

Acknowledgement

I would like to thank my project supervisor Dr Paul Strachan, for his continued support and guidance throughout my study. I also would like to take this opportunity to thank the senior management and my work colleagues for their continued support during my studies.

My special thanks goes to Dr M E Bennett, Dr G Aird, Darragh Gleeson, Michael Pollock, Lord G McVey, Dr Birthe Klebow, Aleksandar Nikoloski and Douglas Bell; for their valuable comments & inputs or support on Optimise tool, ModelIT tool and the HVAC tool.

Last but not least, I would like to thank my entire family for standing by me while I juggled work, family and study.

Table of Contents

Abstract.....	3
Acknowledgement	4
Table of Contents.....	5
List of Figures.....	9
List of Tables	13
1 Introduction	15
1.1 Energy in Buildings.....	15
1.2 Thermal Mass.....	16
1.3 Air Activated Hollow Core Slab	17
1.4 Peak Demand Limiting and Peak Load Shifting.....	18
1.5 Model Predictive Control.....	18
1.6 Aims and Objectives	19
2 Literature survey, Thermal Mass and Modelling	22
2.1 Thermal Mass.....	22
2.1.1 Thermal Mass and Thermal Mass Activation.....	22
2.1.2 The Building Fabric as Thermal Storage.....	22
2.1.3 Thermal Mass Characterisation	23
2.1.4 Active Thermal Mass Performance & the key parameters	26
2.1.5 Classification of Thermal Mass	26
2.1.6 Historical use of Thermal Mass for Comfort.....	26
2.1.7 Passive heating strategies that employ the use of thermal mass.....	28
2.1.8 Direct Gain System.....	30
2.1.9 Passive cooling strategies that employ the use of thermal mass.....	30
2.1.10 Active Heat Storage Strategies Employing Thermal Mass.....	31

2.1.11	Phase Change Material (PCM) as a Thermal Mass	32
2.1.12	Thermal Mass Modelling	34
2.2	Heat Transfer Modes in Buildings	35
2.2.1	Convective heat transfer	35
2.3	Hollow Core Ventilated Slab System.....	36
2.4	Active Thermal Mass, Hollow Core Slab, Modelling.....	38
2.5	Conclusion.....	44
3	Literature Survey – Optimal Thermal Mass Control, Peak Demand Limiting and Peak Load Shifting	45
3.1	Optimal Control of Building Thermal Storage System.....	45
3.1.1	Thermal Mass control Systems	46
3.1.2	Air Flow Control in Buildings	47
3.1.3	Thermal Mass Control Strategies.....	47
3.1.4	Optimal Control of Hollow Core Slab	50
3.1.5	Building Level or Supervisory Controls	51
3.1.6	Model Predictive Control.....	52
3.1.7	MPC in Building Sector	55
3.1.8	Previous Work on Optimal Control in Buildings:	56
3.2	Peak Demand Limiting and Peak Load Shifting.....	57
3.2.1	Demand Response.....	58
3.2.2	Zone Temperature Adjustments and Zone Temperature Optimal Trajectories	59
3.3	Previous work on Zone temperature adjustment, Demand limiting and Load Shifting	62
3.4	Thermal Comfort models	65
3.5	Conclusion.....	66

4	Model Development and Validation.....	67
4.1	Model development.....	67
4.1.1	Previous Modelling detail of Hollow core slab, by Ren, 1997 and Winwood, et al, 1994	67
4.1.2	Air film resistance calculation	69
4.1.3	Modelling of the hollow core slab in Virtual Environment, the VE™	71
4.1.4	Bend Geometry	72
4.1.5	Model Parameters	73
4.2	Model Validation.....	74
4.2.1	Step Input Test	76
4.3	Refinement of the model	77
4.3.1	The use of THERM™ to determine effective conductivity.....	77
4.3.2	Bend Study.....	79
4.3.3	Number of core utilisation	82
4.3.4	Conclusion	83
5	Case Study-I Conventional Control Strategies.....	84
5.1	Introduction	84
5.2	Conventional Control Strategy.....	84
5.2.1	Discussion of Results.....	88
5.2.2	Conclusion	88
5.3	Conventional Control Strategies with Recirculation & Heat Recovery.....	90
5.4	Parameterisation of the Conventional Control Strategies	92
5.4.1	A Brief Introduction to the Optimise™ Tool	93
5.4.2	Time of Use Cost Structure.....	93
5.4.3	Zone Temperature Set Point Trajectory and Demand Limiting	93

5.4.4	Precooling start and end times	96
5.4.5	Coil Leaving Air Temperature or Slab core Entering Temperature	96
5.4.6	Core Entering Air Flow Rate	97
5.5	Results	97
5.5.1	The Base Line System	98
5.5.2	Precooling Start time.....	100
5.5.3	Pre Cooling Temperature Set point.....	104
5.5.4	Slab Core Air Volume Flow	106
5.5.5	Slab Core Entering Temperature	107
5.6	Results Summary.....	108
5.7	Conclusion.....	109
6	Case Study-II Model Predictive Control (MPC)	111
6.1	Introduction	111
6.2	Simulation Framework Concept description.....	112
6.3	Implementation of MPC.....	114
6.3.1	Assumptions.....	114
6.3.2	Economic Optimisation Model.....	114
6.3.3	Cost Function	115
6.3.4	Optimisation Using Exhaustive Search Method	116
6.3.5	Terms of Reference for MPC.....	117
6.4	Results	117
6.5	Discussion of results.....	118
6.5.1	Conclusion	119
7	Conclusion.....	127
7.1	Modelling a Hollow Core Slab.....	127

7.2	Parametric Study	127
7.3	The Use of Whole Building Simulation Tool and MPC	128
7.4	Future Work	129
	References.....	131

List of Figures

Figure 1.0	Hollow core slab as described by Ren, 1997.....	18
Figure 2.0:	Time lag and decrement factor (the Concrete centre)	24
Figure 3.0:	Representation of time lag ϕ and decrement factor f (Asan, 2005), f is the ratio of the amplitude of the temperature fluctuation between the maximum and minimum temperature ranges within the 24 hour.....	24
Figure 4:	Korean Gudeul or heated stone (Sourbron, 2012).....	27
Figure 5:	Roman hypocaust, under floor heating (Sourbron, 2012)	27
Figure 6:	Mass Wall (Psarompas, 2001).....	28
Figure 7.0:	Trombe Wall, showing radiation and convection as mechanisms for heat transfer between the mass wall and the indoor environment (Psarompas, 200)	29
Figure 8:	water wall (Psarompas, 2000)	29
Figure 9:	Thermosiphonic panel, heated air moves up the vent inducing stack flow that brings cold room air into the siphone, causing convection in the room .(Psarompas, 200) ...	30
Figure 10:	Direct gain (sun room) Psarompas, 2001	30
Figure 11.0:	Elements of a PCM Solar wall	33
Figure 12.0:	Temperature of PCM wall's inner surface with different heat of fusion and melting temperature (Y. Zhang et al, 2007).....	34

Figure 13.0: Possible configurations of ventilated slab (Chae & Strand, 2013) (in slab and zone configuration, the slab core air is supplied to the zone, whereas in slab only configuration, the core air does not get supplied to the zone)	37
Figure 14.0: Hollow core concrete system (supply air makes three passes through three cores, there by exchanging heat with slab core, before being supplied to the room) Barton et al, 2002.....	37
Figure 15: Four sided hollow core slab model (Winwood et al,1994)	39
Figure 16.0: Experimental response to diurnal range (Winwood et al, 1994).....	40
Figure 17.0: Hollow core slab surface temperature and core air temperature at the bend during cooling mode (Barton et al., 2002).....	41
Figure 18.0: The effect of time constant τ on cooling load ratio (Yang and Li, 2008)	42
Figure 19: MPC controller operation (adopted from Smith, 2012)	54
Figure 20- Comparison of night setup, load shifting and demand-limiting control (Braun and Lee, 2007)	61
Figure 21 - Example of demand-limiting building set point temperature control (adopted from Braun & Lee, 2007)	63
Figure 22: Illustration of the weighted average method (a) Load & (b) zone temperature (adapted from Lee & Braun, 2007).....	65
Figure 23: Ventilated hollow core slab, R-C model	68
Figure 24: Illustration of the approximation process	68
Figure 25.0: Actual Dimensions (mm) of hollow core slab modelled in VE	71
Figure 26: Cross-section of the VE model showing the hollow core slab.....	71
Figure 27: Bend Geometry.....	73
Figure 28: Model validation HVAC network assembly	75
Figure 29: Air temperatures results of the model simulation	76

Figure 30: Unit step test based on Willis and Wilkins (1993).....	77
Figure 31: Illustration of the THERM modelling	78
Figure 32: Results showing the THERM modelling.....	79
Figure 33: Bend and straight section heat transfer comparison (the bends are located at 4.4 m and 8.88 m)	80
Figure 34: Temperatures profiles along the core path (at the bends, 4.4 and 8.8 m the increase in slab surface temperature is pronounced)	81
Figure 35: Bend and straight section heat flux and delta T between zone surface and room temperature (the heat flux axis is -ve).....	81
Figure 36: Comparison of 3 core vis-a-vis 6 core pass.....	82
Figure 37: Basic network for conventional strategies simulation (see table 8 for the description of network).....	85
Figure 38: Zone air temperature with different conventional strategies.....	87
Figure 39: The HVAC network used (air flows clockwise from the green inlet arrow)	90
Figure 40: Time of Use Energy Cost	93
Figure 41: Zone temperature set point trajectory driving profile	95
Figure 42: Demand limiting start and end times illustration for polynomial zone temperature set point trajectory as an example (12:00-16:00, 12:00-17:00, 13:00-16:00, 13:00-17:00, 14:00-16:00, 14:00-17:00, 15:00-16:00 & 15:00-17:00).....	96
Figure 43: Various precooling start time illustration (the lines at the left show various precooling start times).....	96
Figure 44: Base line energy profile for conventional studies (not used for MPC).....	99
Figure 45: Baseline cooling set point and zoon temperature during occupancy (the black colour is zone temperature, whereas the blue colour is the zone temperature set point	99

Figure 46: Periods of interest in the study (demand limiting start times are 12:00, 13:00, 14:00 and 15:00; where as demand limiting end times are 16:00 and 17:00; precooling times are from 00:00 to 12:00) 100

Figure 47: Normalised Peak Cost ratio as a function of precooling times for demand limiting period of 12:00 to 17:00 (the different colours represent the different discharge control trajectories. Precooling start time of 03:00 is optimal when discharged through exponential path of Exp_2)..... 101

Figure 48: Peak cost ratio as a function of precooling time (DL 12:00-17:00), precooling start time of 03:00 is optimal with trajectory Exp_2 101

Figure 49: Number of peak time "Chiller off" hours as a function of precooling time (for demand limiting period of 12:00 to 17:00) 102

Figure 50: The effect of demand limiting start times on peak cost ratio; the first half (12:00 & 13:00) of the demand limiting start time span shows better performance than the second half (14:00 & 15:00)..... 103

Figure 51: Peak cost ratio as a function of precooling (demand limiting running between 15:00-17) showing sub-optimal performance 103

Figure 52: Normalised Cost Ratio as a function of Precooling Temperature set point check 104

Figure 53: Average Peak Time PMV as a function of Precooling Temperature set point 105

Figure 54: Normalised Peak Cost Ratio as a function of Precooling Temperature set point (it appears the precooling temperature does not seem to make huge difference between the different temperatures used) 105

Figure 55: Average Peak Time PMV as a function of Precooling Temperature set point 106

Figure 56: Peak time chiller off time as a function of air flowrate (please note that for lower flow rates, the chillers are on during the entire peak time)..... 106

Figure 57: Average Peak Time PMV as a function of Air Flow (lower air flow rates seem to exhibit higher percentage of PMV outside the range -0.5 to 0.5).....	107
Figure 58: Peak cost ratio as a function of slab core entering air temperature	108
Figure 59.0: Receding horizon.....	112
Figure 60.0: MPC with IESVE	113
Figure 61 MPC Result showing load shifting and peak demand limiting (the red area is the MPC result while the blue area represents the baseline). The dry bulb temperature for the day is shown and it seems the energy consumption is shows correlation to it.	120
Figure 62: Result of MPC showing demand limiting and peak shifting, compared to the baseline. It also shows the zone temperature for the day. (red baseline, blue MPC)	121
Figure 63: MPC result for Monday (day one of simulation) showing peak load reduction and shifting to off peak hours (red MPC, blue baseline).....	122
Figure 64: MPC result for Tuesday day two of simulation. Almost all the chiller load has been taken during early mornings (the lines are for dry bulb temperature) (red MPC, Blue, baseline)	123
Figure 65: MPC result for Wednesday, day 3 of simulation (red MPC, blue baseline)	124
Figure 66: MPC result for Thursday, day 4 of simulation (red MPC, blue baseline).....	125
Figure 67: MPC result for Friday day 5 of the simulation (red MPC, blue baseline) On Friday, although there is chiller load during peak time for MPC, its peak value is less than the baseline's peak value.	126

List of Tables

Table 1.0 - Properties of building material	25
Table 2: Example of rule based control of thermal mass.....	47
Table 3: Model parameters	73

Table 4: Model inner and outer surfaces.....	74
Table 5: Room Conditions (these make the hollow core inside and hence will be in contact with the forced air with properties of: density of 1.2 kg/m ³ , specific heat capacity of 1008 J/Kg.K, laminar viscosity of 1.58 x 10 ⁻⁵ m ² S ⁻¹ and thermal conductivity of 0.0255W/mK).	74
Table 6: Boundary conditions of the THERM modelling	78
Table 7: Heat transfer coefficient multiples.....	79
Table 8: Heat flux along the length of the path of the core air	80
Table 9: Network description.....	85
Table 10: Conventional Strategies parameter (controller dead band used is 2 °C, strategy #2 uses free cooling and no mechanical cooling at night)	86
Table 11: HVAC network description table	91
Table 12: Low level control logic description	92
Table 13: Problem variables, range and resolution for parametric study	92
Table 14: Result variables.....	97
Table 15: Summary results	108
Table 16: Optimisation terms of reference	117
Table 17: MPC results	118

1 Introduction

1.1 Energy in Buildings

In both developed and developing countries, buildings are responsible for more than 40% of global energy use and one-third of global greenhouse gas emissions; making buildings the largest energy consumers (United Nations Environment Programme [UNEP], 2009).

According to the U.S Department Of Energy (USDOE, 2008); buildings account for 72% of U.S electricity use and 36% of natural gas use, making up 40% of all energy use in the United States. Both residential and commercial building energy use are growing, and represent an ever increasing share of U.S. energy consumption.

At EU level, the Directive 2010/31/EU (EU, 2010) sets stringent energy standards for buildings in an attempt to rein in Europe's most energy-thirsty sector by 2020. Buildings currently account for around 40% of Europe's energy use and a 36% of its CO₂ emissions. In the UK, building stock is responsible for over 40% of the country's CO₂ emissions (Clarke et al, 2008).

Globally and especially in hotter and more humid climates, air conditioning accounts to around 15% of all electricity consumed worldwide (JRAIA, 2002), and there are evidences to suggest the trend is on the increase due to higher living standards in the developed world (Santamouris, 2006).

The 1970's energy crisis seem to have given an impetus to search for alternative energy sources as well as other energy saving ways that can fulfil the world's energy demand (Salunkhe & Shembekar, 2012). On the building sector this impetus is focused on energy efficiency through careful design and operation of buildings (Ren & Wright, 1997). Moreover, the worldwide understanding of the need for reduced carbon emission via reduced energy consumption, has shifted the priorities research and development efforts towards building energy consumption.

There are a number of well researched methods by which the energy consumption (especially in the Heating Ventilation and Air Conditioning (HVAC) sector) of buildings could be reduced; such as Water side or Air side economizer. But technologies that employ the use of the building mass that is incorporated in the building envelop, although known to be used since ancient times, had not been aggressively & widely employed as much as they should. However, in recent times the use of thermal mass and the active control of it (activation), it seems has been seen as an alternative and has been gaining momentum as a suitable low carbon technology (Warwick, 2010).

Using the building fabric as thermal storage can sufficiently regulate zone thermal environment in buildings with relatively low thermal load. For those buildings with heavy thermal load, the combination of building fabric and mechanical systems can reduce the peak demand as well as increasing operational efficiency of air conditioning plants (Ren & Wright, 1997). Therefore, the thermal inertia of the building is a key parameter to control the unnecessarily fluctuations of the internal temperatures of buildings. The concept is: heat is stored inside the building structure or fabric so as to modulate the heat gains and maintain occupant's comfort. This simple sounding process can considerably reduce the energy consumption of mechanical systems, especially in areas where there is a large diurnal temperature swing (Balaras, 1995).

1.2 Thermal Mass

Thermal mass is defined as the ability of a material to store (charge) heat, and later on release (discharge) it when activated mechanically or naturally through one or a combination of conduction, convection and radiation. For the thermal mass to be useful in building environment, it has to be able to absorb and release heat roughly at the same rate as the building's daily heating and cooling cycles.

Effective use of the 'building fabric' (building envelope, the interior partition, the furnishing, or even the building structure) for modulating the building internal gains passively has been known since antiquity, and since the 1970s, mechanical air activation of Hollow Core Slabs has proved the system can take care of up to 50W/m^2 cooling load at an air flow rate of 50-

100 m³/h for a surface area of 6 m², equating to ~ 70% reduction in chiller load (Andersson et al, 1979).

The effective use of thermal mass for heating or cooling is primarily limited by its slow response to heating or cooling demand, and the need for a preparatory charging / discharging a head of time. Because of these limitation, application of conventional controls to control thermal mass, which are not preparatory in nature, provide insufficient control definition. An ideal control system requires a successful prediction of the duration required to charge and discharge a slab in order to achieve the set point at the onset of occupancy.

1.3 Air Activated Hollow Core Slab

In a hollow core ventilated slab, ventilation air is circulated through the hollow cores of the ceiling and floor slab system. The air path is extended by blocking the core ends and cutting connecting conduit between the cores (figure 1.0). The air having passed through the cores is supplied to the zone being served by overhead diffusers or by an under floor air system (displacement ventilation system).

In this project a hollow core air activated slab system will be modelled in IES-VE whole building simulation tool through geometry to Heating Ventilation and Air Conditioning network system and this will be used further to study demand limiting and peak load shifting as prudent measures to cut energy cost. However, this study would not be complete without the effective control of the charging and discharging of the thermal mass and for this purpose Model Predictive Control is considered and is implemented through the use of the IESVE™ and the IES Optimise™ tools.

The study focused on a building ‘box model’ located in Denver Colorado¹ and has an integrated two hollow core slabs as part of the roof assembly. Building cooling is particularly selected for the study, as it is strongly coupled to Time Of Use (TOU) electric charge structure and the practical challenges of optimal precooling.

¹ Randomly selected to exploit its large diurnal and nocturnal temperature difference

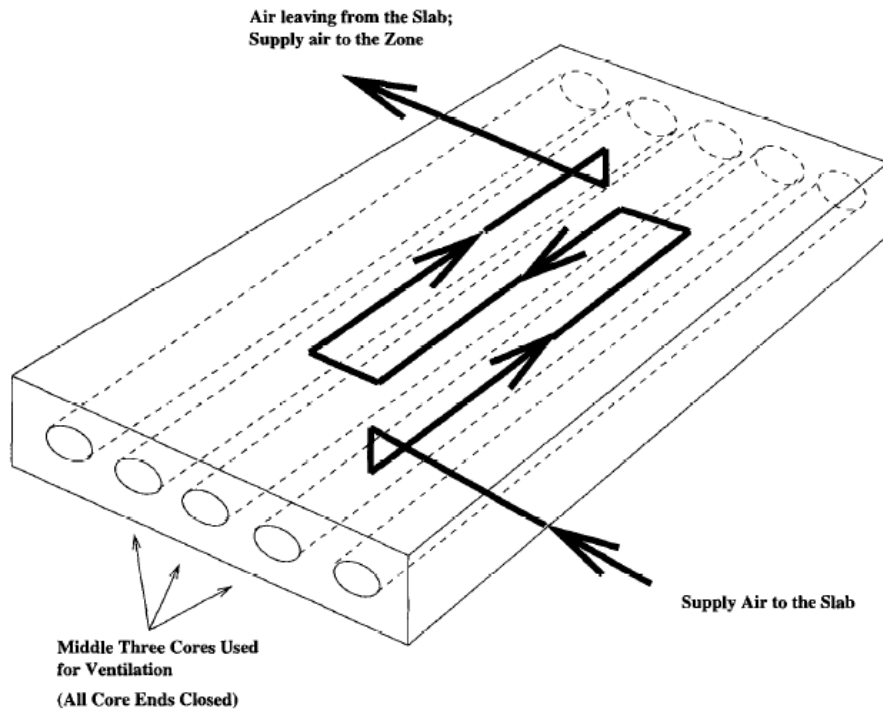


Figure 1.0 Hollow core slab as described by Ren, 1997

1.4 Peak Demand Limiting and Peak Load Shifting

Building thermal mass can be used to reduce peak cooling load through precooling the building mass (in summer for example) during off peak hours in order to reduce the on peak hours' cooling load. Building cooling is stored in the building mass during this off peak hours. By doing this, the cooling load is shifted in time and the peak demand is reduced or kept within a limit (Xu, 2004).

Peak demand limiting is a strategy that controls the discharge of the thermal mass optimally, so that the stored building cooling is discharged in such a way that there are no rebounds before the shed period ends (xu, 2004).

1.5 Model Predictive Control

Model predictive control utilises the thermal response model of the building to predict the future evaluation of the system and to compute control actions by optimising cost, while

maintaining comfort. MPC is a high level control strategy that in tandem with low level controls enables an optimal control of the building system.

1.6 Aims and Objectives

Other researchers' work on ventilated slab systems through the use of a hollow core slab indicates that appreciable energy savings can be achieved when the ventilated slab system is used as a thermal storage element to cool the building. The studies developed various numerical models to characterize the performance of the system, but most of the experimental as well as theoretical model findings are based on simulated or measured energy consumption for a particular space, time and climatic condition. Moreover, the studies do not include the impact of the Air handling Unit, AHU, or primary and secondary systems such as boiler and chillers. Consequently, it is difficult to generalise the findings of separate studies.

Therefore, there are great advantages to be gained by modelling systems using Building Information Modelling (BIM) software, since they are capable of generating results for a wide range of different input parameters, such as climate, location, HVAC configuration and building design. In this work the Virtual Environment whole building simulation tool developed by Integrated Environmental Solutions (IES VE) has been used to perform these models.

The effectiveness of the thermal response of a hollow core slab system is highly dependent on how effectively its interactions with the building zones, the AHU and the secondary systems is managed and controlled. These interactions should be considered whilst optimising the controls for hollow core slabs, for use in peak demand limiting and peak load shifting.

However, as hollow core slab system is a slow response system (*hours as supposed to minutes*), the optimal control of its energy charging and discharging can only be effective if the need or lack of it, could be predicted hours (perhaps a day) a head of the actual use of the system. This prediction is dependent on forecasts of the weather as well as occupancy and other disturbances ahead of time. MPC is as an ideal candidate in order to realise the optimal control.

MPC of other thermal mass types in conjunction with peak demand limiting and peak load shifting has been done by various researchers, through the use of whole building simulation tool or using reduced order thermal response models. However, the optimal control of hollow core air activated slab system has not been previously studied in conjunction with demand limiting and load shifting through the use of a whole building simulation tool.

Considering the above, the aims and objectives of this thesis are:

- to model a hollow core slab system in whole building simulation tool
- to develop an optimal control strategy for cost effective use of the system
- through the use of the model to study the effectiveness or lack of it, of the system, for demand limiting and load shifting

In order to achieve the objectives stated above, I aim to:

1. Develop a working model using whole building simulation tool, IESVE, and validate the model based on previously published data
2. Through the use of the model #1 above, the study of the thermal response of the system to known strategies (for instance precooling through mechanical and/or free night ventilation)
3. Based on #2 above, to develop an optimal control method, Model Predictive Control, through the use of the IES Optimise tool as an aid

This thesis is organised into 7 chapters:

The following two chapters, chapter 2 & chapter 3 present a general background: concepts, knowledge base and facts that has shaped the thesis. In chapter 2, focused literature review will be presented on thermal mass and modelling of a hollow core slab system, where as in

chapter 3 the review will focus on optimal control of the system and the use of thermal mass for demand limiting and load shifting.

Chapter 4 presents modelling and validation of the hollow core slab system in IES-VE, while chapter 5 presents a case study on the use of the developed model in conjunction with conventional control strategies with aim of model & supervisory variables identification for use later in Model Predictive Control (MPC).

Chapter 6 is dedicated to present the MPC implementation and its use for demand limiting and load shifting. Finally, Chapter-7 discusses the results and concludes the work with proposal for further work.

2 Literature survey, Thermal Mass and Modelling

2.1 Thermal Mass

2.1.1 Thermal Mass and Thermal Mass Activation

The term Thermal Mass Activation (TMA) is used to describe the active use of the the building mass to store thermal energy (for heating/cooling purposes) (Aschehoug & Anderesen, 2008).

Night cooling is one of the well-known examples of TMA (Warwick, 2010). In night cooling, the thermal mass of a building is cooled at night by circulating relatively cool outside air through the building. When the thermal mass is activated through circulation of air the next day, the slab absorbs heat, thereby offsetting heat gains and limiting internal temperature fluctuations.

A previous analysis of the dynamic thermal behaviour of buildings in relation to convective nocturnal cooling showed an annual electricity saving of about 100 kWh/m², compared to conventional design. Moreover the study of forced air to activate thermal mass resulted in a 70% decrease on chiller loads (Zmeureanu & Fazio, 1988).

There is ample evidence to support the use of TMA and its contribution to reduction in energy consumption while not compromising occupant's health and comfort. Work carried out by Corgnati et al (2006), Yang & Li (2008), Braun (1990), Zmeureanu & Fazio (1988), Seshadri et al. (2013), Pfafferott et al (2007), Ren & Wright(1997) & Henze et al (2007); shows that the use of thermal mass coupled with night free cooling and/or off-peak mechanical precooling considerably reduces the on-peak (occupied hours) energy consumption.

2.1.2 The Building Fabric as Thermal Storage

The use of building fabric as thermal storage employs two approaches and these are:

1. Exposing as much as possible the internal surface of the building, for instance having no false ceiling; or
2. Passing ventilation air through the hollow cores of the floor and ceiling slabs

The first approach has been proved to be effective in reducing peak summer load, however it lacks effective use of the full thermal capacity of the mass due to weak coupling between the room air and the building mass (Ren & Wright, 1997).

Whereas the second approach improves upon the the first one by increasing the thermal coupling through increased turbulence, thereby increasing the convective heat transfer coefficient between the mass and the air, which is being forced through hollow cores of the floor and ceiling slabs.

The amount of energy stored in the hollow core slab is dependent on the following factors (Ren, 1997):

1. The mass & thermal properties of the slab
2. the area available for the heat exchange between the air and the slab
3. the heat transfer characteristics between the air and the slab

2.1.3 Thermal Mass Characterisation

Reviews of previous studies (computational & experimental) by Balaras (1996), found sixteen parameters that could be used to characterise thermal mass effect in buildings. Thermal mass is primarily characterised by its physical or material properties such as: heat capacity, conductivity, and density; which are believed to have influence on the 'time lag' or 'phase shift' & 'decrement factor' or 'attenuation factor' (Asan & Sancaktar, 1998). Walls that are designed to have very low decrement factors and high time lags could prevent the big temperature swing of the outside air over 24 hour period (see figure-2) from propagating to the inside, there by maintaining almost constant inside temperature (Asan & Sancaktar, 1998) (see figure 3).

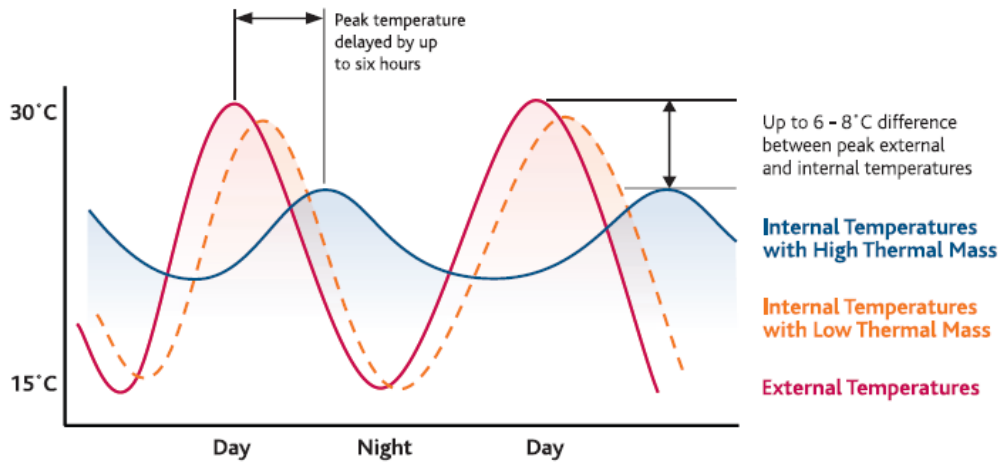
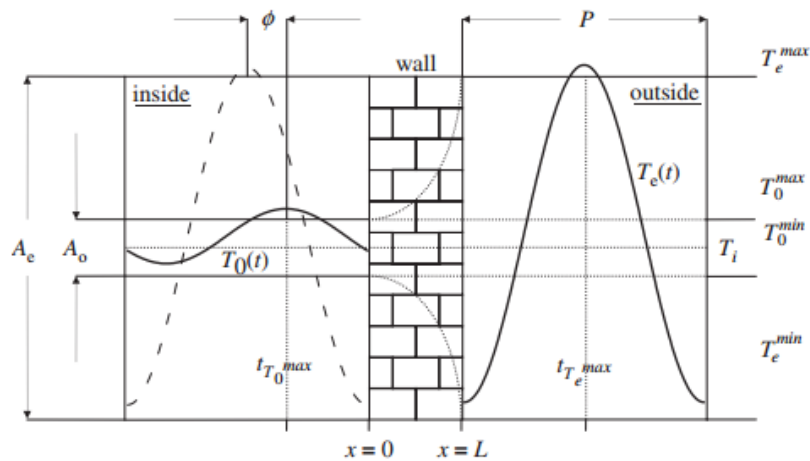


Figure 2.0: Time lag and decrement factor ([the Concrete centre](#))



$$f = \frac{A_o}{A_e} = \frac{T_o^{\max} - T_o^{\min}}{T_e^{\max} - T_e^{\min}}$$

Figure 3.0: Representation of time lag ϕ and decrement factor f (Asan, 2005), f is the ratio of the amplitude of the temperature fluctuation between the maximum and minimum temperature ranges within the 24 hour

Designing buildings with low decrement factor and large time lag, can prevent the large fluctuation of the outside air from propagating to the inside environment.

The thermal capacity of the building characterises the ability of the building to store thermal energy, and is defined by ASHRAE (1999) as the amount of heat that is needed for an increase of the temperature of a given mass by one kelvin. The thermal capacity takes two

forms: apparent and effective (Balaras, 1996). The apparent capacity is a rough indication of the thermal storage capacity of the building elements, whereas the effective capacity is a real indicator of the capacity of the all the elements of the building. Always the effective capacity is less than the apparent one.

For thermal mass to be useful in buildings, it must be able to absorb or release heat at a rate in sync with the as the building's heating and cooling cycle. As shown in table-1 below, concrete and masonry products perform well in this respect, being dense materials, and also can store a lot of heat. Wood absorbs heat too slowly to be effective as thermal mass, and steel conducts heat too rapidly to be in sync with a building's natural heat flows over the day ([the concrete centre](#)).

Material	Density [kg/m ³]	Specific heat [kJ/KgK]	Volumetric heat capacity [kJ/m ³ K]	Conductivity [W/mK]
Water	1000	4.186	4186	0.466
Wood	610	1.420	866	0.130
Concrete	2100	0.840	1764	1.400
Brick	2050	1.000	2050	1.250
Steel	7800	0.480	3744	47
Glass	2500	0.840	2100	1.100

Table 1.0 - Properties of building material

The dynamic thermal storage performance of a thermal mass is measured via a parameter called Thermal Admittance factor (TA). The thermal admittance factor is an indicator of the heat exchange ability of the mass with the environment, given variation of temperature that is cyclic (usually 24 hrs) (Balaras, 1995). Construction materials are compared to each other using their thermal admittance or effectiveness.

The diffusivity of the material determines the depth of penetration of heat via conduction, in a given cycle (Li & Xu, 2006). The 'diurnal heat capacity' or 'the amount of energy per degree swing in temperature stored in the material & returned back to the indoor space during the

diurnal cycle per unit surface area' is one such parameter that measures the effectiveness (Balaras, 1995).

2.1.4 Active Thermal Mass Performance & the key parameters

The performance of thermal mass such as: the amount heat stored, the rate of heat transfer & its effectiveness is affected by the following parameters (Balaras, 1995):

- Material thermal property – such as diffusivity (see above)
- Location of the thermal mass
- Insulation of the thermal storage wall
- Ventilation
- Pattern of occupancy

2.1.5 Classification of Thermal Mass

Thermal mass is characterised based on location and the activation method employed:

2.1.5.1 Thermal mass by location

Based on the location of the thermal mass, there are two types: external (Walls & roofs) or internal (furnishings and internal partitions). External mass is exposed to the direct fluctuation of the ambient temperature whereas internal mass is in contact with indoor air temperature (Li & Xu, 2006).

2.1.5.2 Thermal mass by activation

There are two categories of thermal mass activation based on the 'activation principles: Surface Thermal Mass Activation (SA) and Core Thermal Mass Activation (CA) (Warwick, 2010). As the name suggests in SA, the surface of the element plays a key role where as in the CA, the thermal mass will contain ducts for circulation of air or embedded piping for circulation of water.

2.1.6 Historical use of Thermal Mass for Comfort

The use of thermal mass as heat/cold storage is not something new. There are solid evidences to suggest, it (*called gudeul in Korean, see figure-4*) has been used in ancient times as far

back as 11th century B.C. in what is now Northern China and Korea (Sourbron, 2012). In Europe, under floor heating was used in Greece for heating baths, while the Romans later ingeniously used it for heating their houses (*Roman hypocaust*, see figure-5).

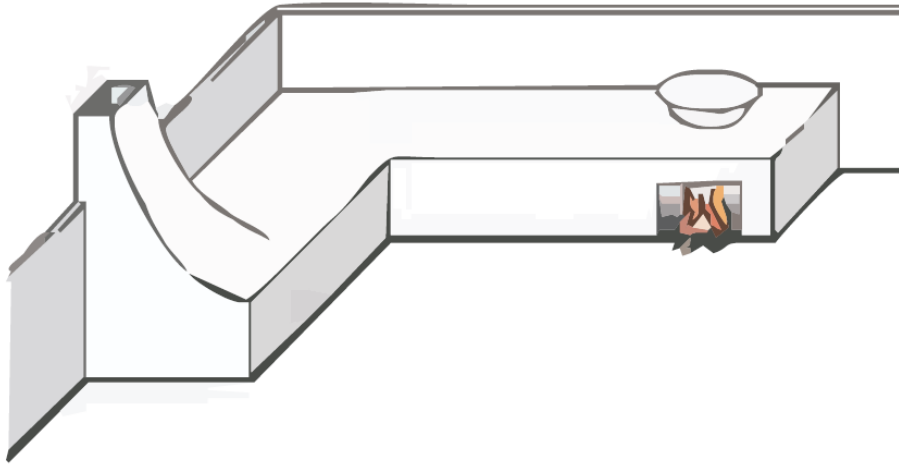


Figure 4: Korean Gudeul or heated stone (Sourbron, 2012)

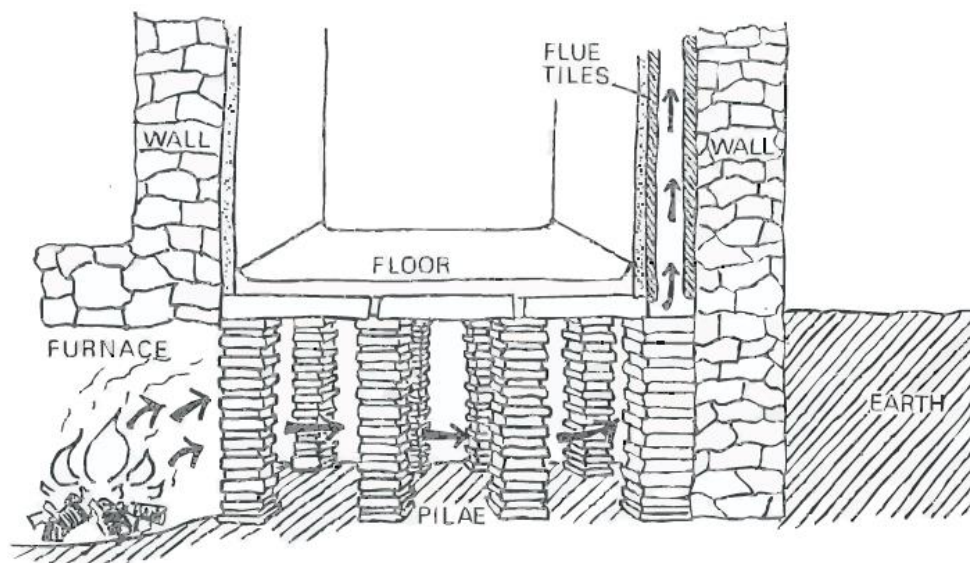


Figure 5: Roman hypocaust, under floor heating (Sourbron, 2012)

In more modern times thermally activated rock beds, Trombe Walls, Phase Change Material and Rammed earth wall (aka Taipa), has been introduced by building designers to enhance comfort.

2.1.7 Passive heating strategies that employ the use of thermal mass

There are many passive heating systems that utilise the thermal capacity of building materials and these are classified into two categories, direct gain and indirect gain systems. In the direct gain system, the thermal mass directly picks up solar radiation and stores it for release later on. Whereas in indirect gain system, the sun's rays are intercepted directly behind the collector glazing, by a massive wall that serves as heat storage (Psarompas, 2000). Some example of the practical use of these strategies are given below.

2.1.7.1 The indirect Gain Systems

2.1.7.1.1 Mass wall

The mass wall consists of an external glazing and a thermal mass with high heat capacity & low thermal diffusivity (24 to 40 cm thickness). This enables the absorption of the solar gain into the mass during the day later to be released into the indoor environment. Usually the thermal mass wall is placed near a south facing glazing, for maximum exposure to sun. Control of the indoor temperature during summer is achieved via two vents at the top and bottom of the glazing. Thermal comfort is achieved through radiation and convection of the stored heat (figure-6).

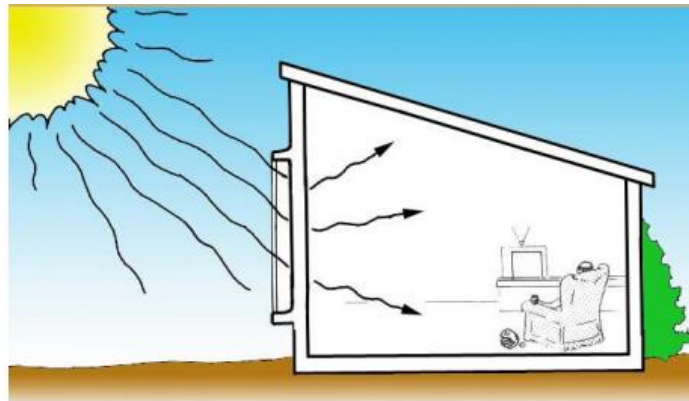


Figure 6: Mass Wall (Psarompas, 2001)

2.1.7.1.2 Trombe-Michel wall

This system is similar to the above mostly, but has two air vents below and above the thermal mass in order to allow movement of heated air or to stop cold air flow during lower outside temperatures or hot air during hot summer time. Some of the variations of this system have over hangs to shade the sun during warm summers (figure-7).

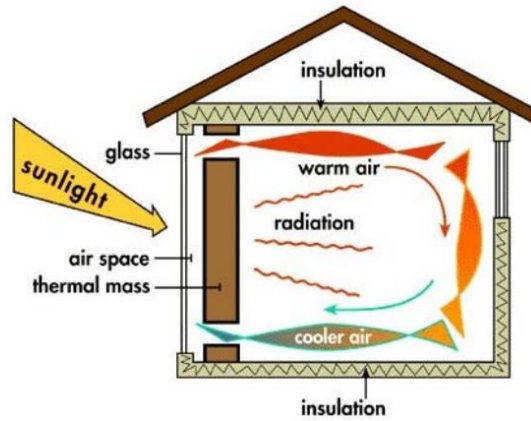


Figure 7.0: Trombe Wall, showing radiation and convection as mechanisms for heat transfer between the mass wall and the indoor environment (Psarompas, 200)

2.1.7.1.3 Water wall

A water wall also known as a “Drumwall” is a variation of the Trombe-Michel wall and uses water as a thermal mass, due to its high heat capacity. This system tends to be more effective than the previous one as it absorbs heat faster & releases heat faster due to the convective currents inside the containers (figure-8).

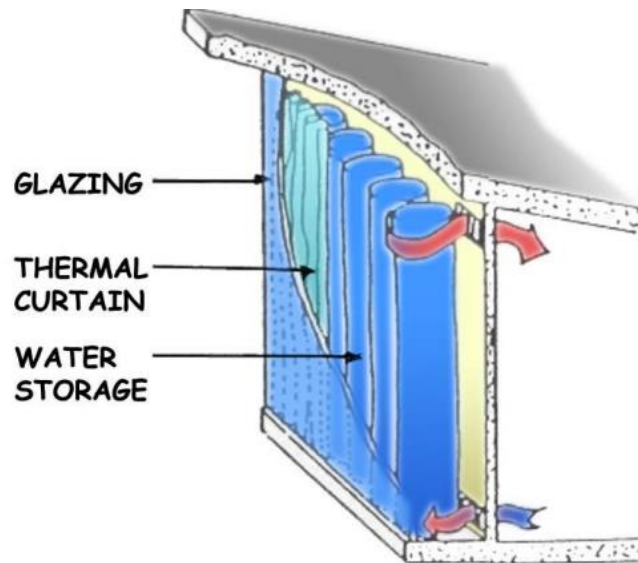


Figure 8: water wall (Psarompas, 2000)

2.1.7.2 Thermosiphonic Panel

This system is similar to the above two systems & consists of a thermal mass, a thermosiphonic panel with black absorber to absorb the solar heat. With the heat absorbed heating the air inside the siphon, the warm air moves through the top vent into the room while a cold air is drawn through the vent below, inducing a natural convection (figure-9).

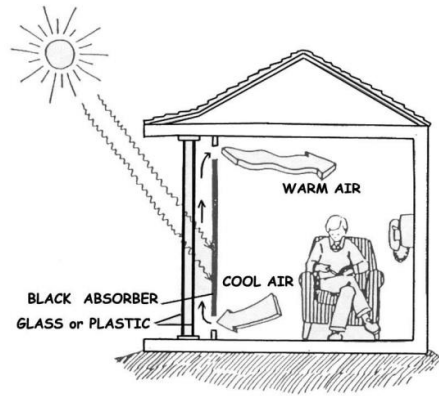


Figure 9: Thermosiphonic panel, heated air moves up the vent inducing stack flow that brings cold room air into the siphone, causing convection in the room .(Psarompas, 200)

2.1.8 Direct Gain System

Direct gain system is the most common passive solar system in architecture. It uses the actual living space as a solar collector, heat absorber and distribution system. Sunlight enters the building through the aperture (south-facing glazing material made of transparent or translucent glass) see figure-10. It then strikes masonry floors and/or walls, which absorb and store the solar heat (Psarompas, 2001). The absorbers usually have dark colour so that they can absorb more heat so that the heat absorbed is used to warm rooms at night via convection and radiation.

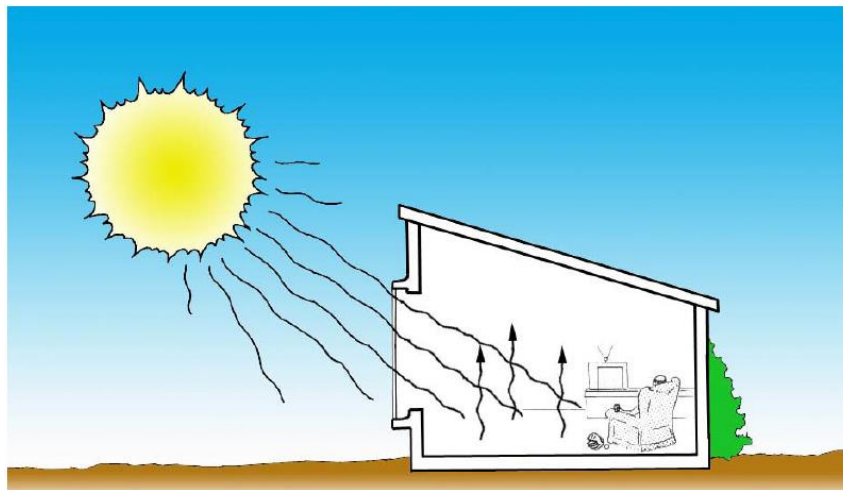


Figure 10:Direct gain (sun room) Psarompas, 2001

2.1.9 Passive cooling strategies that employ the use of thermal mass

Passive cooling systems have been incorporated with HVAC systems to reduce or offset the on-peak load for cooling. Various studies including by Braun (1998) have shown that building components such as floors, ceilings and walls can be utilized as thermal storage and that this approach is effective in damping peak cooling loads.

2.1.9.1 Ventilative cooling

In ventilative cooling, where the outside air is cooler (and where there exists a considerable difference between diurnal and nocturnal temperature difference), natural ventilation is exploited through the design of vents and air passages. The cooler air flowing into the building is used to flush out heat stored as well as to cool the building mass so as to help modulate room temperature for next day.

2.1.9.2 Radiative cooling

Radiative cooling exploits the fact that all material bodies emit thermal energy in the form of electromagnetic radiation. In this strategy, a heavy and highly conductive roof material is exposed to the night sky. The roof then cools down at night via radiation as well as convection and will be insulated externally during the day. Any adjacent rooms can then exchange heat with the roof, cooling the rooms. Further improvement to this strategy is the exploitation of the high heat capacity of water through roof ponds.

2.1.10 Active Heat Storage Strategies Employing Thermal Mass

2.1.10.1 Ice and Chilled Water Storage

The heat storage methods exploit the high heat capacity and large heat of fusion² of water in order to store thermal energy in it. There are differences between the two (ice storage and chilled water storage) energy storage systems and their application varies accordingly too. At a temperature difference of 10 degree C, a 2.2 kg of chilled water can store 19kJ of thermal energy, whereas the same mass of ice can store 178 kJ. Therefore ice storage needs only 12% of that of the chilled water storage tank. Chilled water storage tends to be large-capacity and is used for larger applications whereas ice storage has a small footprint and is ideal for urban applications (Wang, 2001).

This technology is widely used and can be often found in campus-wide air conditioning or chilled water systems of large buildings. In this application, chillers are made to run at night (when electricity is cheap) to produce an ice or chilled water. During the day, water then circulates through the ice to produce a chilled water or the stored chilled water will be

² One metric ton of water or one cubic metre of water can store 334 mega joules (MJ) or 317,000 BTU of energy, which is equivalent to 93 kWh or 26.4 ton-hours

distributed to take care of the load that would normally be the chiller's daytime output (Wang, 2001).

2.1.11 Phase Change Material (PCM) as a Thermal Mass

PCMs are the substances that can absorb, store and release a large amount of thermal energy. Latent heat storage using phase change materials has proved to be efficient means to store thermal energy and has been applied to increase the capacity of different system's thermal energy storage (Ora, et, al, 2012).

The total heat addition/release to/from the PCM consists of sensible heat and latent heat. During sensible heating the thermal energy is stored up to the initiation of the melting process, whereas the thermal energy stored during the phase change process is known as the latent heat. One of the major advantages of the latent heat storage system is an isothermal release or gain of thermal energy. In contrast, the temperature decreases/increases during sensible cooling/heating (Salunkhe and Shembekar, 2012)

Phase change materials' energy charging and discharging takes place at low temperatures ranges varying between 20 °C and 32 °C depending on the material used. Also, phase change materials exhibit higher thermal mass capacity (can store more heat per unit volume) and more isothermal behaviour when charging and discharging, compared to sensible heat storage (Mehling & Cabeza, 2008).

These properties make PCM ideal for space cooling and heating. Telkes(1975), studied the use of PCM in buildings and concluded that given an acceptable melting temperature and high enough thermal (latent heat) storage capacity, controllable conditions can be maintained with 5 to 14 times less equivalent mass than conventional building material in the same temperature range (Salunkhe and Shembekar, 2012).

2.1.11.1 Incorporation of PCM in building material

PCM is incorporated in building materials in one of the following forms (Pasupathy et al, 2006):

- 1 Solar heat storage wall for building ventilation
- 2 Phase change dry wall impregnated with PCMs

- 3 Concrete blocks impregnated with PCMs
- 4 PCM integrated in wood-light weigh concrete
- 5 Thermally enhanced frame wall with PCMs
- 6 Thermally effective windows with moving PCM curtains

An example of PCM in use in solar heat storage wall is shown in Figure 11.0. In the figure; layer(1 & 2) are Transparent Insulation materials (TIM) that prevent the transfer of convective and radiative heat, layer 3 is a PCM in a transparent plastic casing, layer 4 is a channel for heating ventilation air, layer 5 is insulation and layer 6 is plaster .

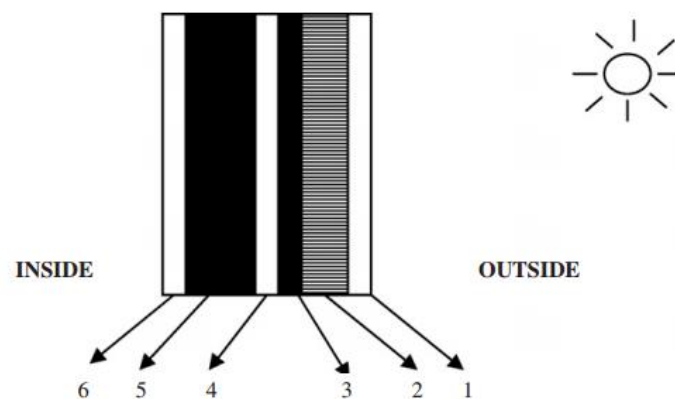


Figure 11.0: Elements of a PCM Solar wall

2.1.11.2 Characterisation of Phase Change Material

When using PCM in the building fabric, like other conventional building materials, the time lag and decrement factor need to be considered. Moreover, it is worth considering the fact that the temperature distribution through walls with PCM and conventional building material differ in that: while for conventional building material the trend is linear, for PCM it is nonlinear as the heat capacity of the PCM varies with temperature (Y. Zhang et al, 2007).

The two characteristic parameters of PCM are the heat of fusion (H_m) and the melting temperature (T_m). The higher the heat of fusion the higher the thermal capacity of the PCM and the higher the melting temperature. However, higher temperatures are not ideal for comfortable conditions for occupants in buildings, making PCM less suitable for building cooling and heating. If the melting temperature is too low, then PCM is less likely to involve latent heat transfer and its use is suboptimal. A satisfactory melting temperature is slightly

higher than the average comfort temperatures range, 22 -25 °C (Peippo, et al, 1991; Neeper,D.A. (2000) & Clarke, J.A., & Heim,D. (2004).

Zhang et al (2007) studied the temperature trend of the PCM wall's inner surface for different heat of fusion and melting temperatures. Given the right material with melting temperature that is within the comfort range, varying the heat of fusion varies duration the zone PCM wall is kept close to the room set point. Varying the melting temperature while keeping the heat of fusion constant demonstrated that the surface temperature is kept close to the melting point of the PCM (see Figure 12.0). The period the surface temperature is kept close to the room set point is called 'PCM lag' and it is used to characterise PCM materials' suitability for use in buildings.

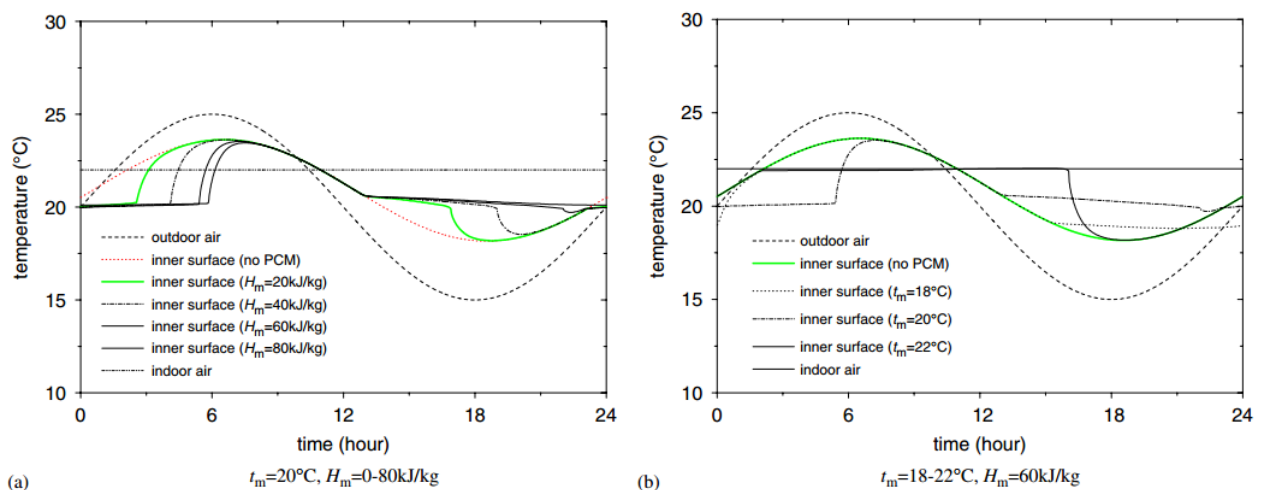


Figure 12.0: Temperature of PCM wall's inner surface with different heat of fusion and melting temperature (Y. Zhang et al, 2007).

See Castell et, al (2010), and Telkes (1975) for further information.

2.1.12 Thermal Mass Modelling

Load calculations of buildings date back to 1911 when Willis Carrier developed Psychrometric charts. However, it wasn't until Mackey and Wright developed Sol-Air temperature method in 1944 where direct thermal mass calculations were possible. Soon after, thermal network method was introduced which could represent thermal mass as a capacitor in an electrical RC network analogue. The heat electricity analogy is still used to model thermal systems.

Computer simulation of thermal mass, first appeared in 1967, when the thermal response factor method was developed by Stephenson & Mitalas (1967). Further development of the algorithms introduced transfer function method, heat balance method & radiant time series method.

Currently there are over 50+ commercial software programs that are able to model the whole building in attempt to quantify the energy use, design efficient buildings and even analyse the merits of the different thermal mass strategies.

2.2 Heat Transfer Modes in Buildings

The transfer of heat to and from the building fabric and the interior occurs by convection, radiation and conduction. The thermal mass exchanges heat with the room by convection and with the occupants and the other materials within the room by radiation. Heat is transferred through the material or to other materials or occupants in contact with the surface via conduction. For hollow core slabs convective heat transfer is the main mode of heat transfer, because it directly affects the charging/discharging process (see section 4.1.2).

2.2.1 Convective heat transfer

Convection occurs from the core air to the slab core surface and then from the slab external surface to the air in the building zone. The convection equation is generally described as:

$$q_c = h_{c,surface} (T_s - T_{air}) = \frac{1}{R_{conv}} (T_s - T_{air}) \text{ ----- (Eq-1)}$$



 (Conduction into or from the air)

where:

k_f (W/mK) is the air thermal conductivity

$h_{c,surface}$ (W/m²K) is the surface convection heat transfer coefficient or film coefficient

T_s (K) is surface temperature

T_{air} (K) is the temperature of the fluid outside the thermal boundary layer

$R_{conv} = \frac{1}{h_c A}$ (K/W) is the convective heat transfer resistance

The heat transfer coefficient h_{air} is calculated from an empirical formula for turbulent flow in circular and non-circular ducts (CIBSE 2007), which is:

$$Nu = 0.023 Re^{0.8} Pr^{0.33} \text{ ----- (Eq-2)}$$

where:

Nu is the Nusselt number

Re is the Reynolds number

Pr is the Prandtl number

However Equation 2 is based on the surface roughness of the air path being smooth. The Reynolds-Colburn analogy (Holman, 1990) relates the fluid friction and the heat transfer equations, leading to equation:

$$St \cdot Pr^{2/3} = \frac{f}{2} \text{ ----- (Eq.3)}$$

where:

$$St = \frac{h_c}{\rho \cdot v \cdot c_p} \text{ ----- (Eq.4)}$$

leading to:

$$h_c = \frac{\rho \cdot v \cdot c_p \cdot f}{2 \cdot Pr^{2/3}} \text{ ----- (Eq.5)}$$

where:

f is the friction coefficient , $f = k_s / d_e$;

k_s is the Surface roughness (m), and

d_e is the effective tube diameter (m)

The correct determination of h_c is important, because the quantity of heat transferred to/from the slab core and the slab core air is directly proportional to h_c .

2.3 Hollow Core Ventilated Slab System

In a hollow core ventilated slab, ventilation air is circulated through the hollow cores of the ceiling and floor slab system. The air path is extended by blocking the core ends and cutting connecting conduit between the cores (figure-14). The air having passed through the cores is supplied to the zone being served by overhead diffusers or by an under floor air system (displacement ventilation system). In some configurations the air passing through the core does not get supplied to the zone (see figure-13), instead the slab surface in contact with the zone provides the necessary comfort through radiation and convection.

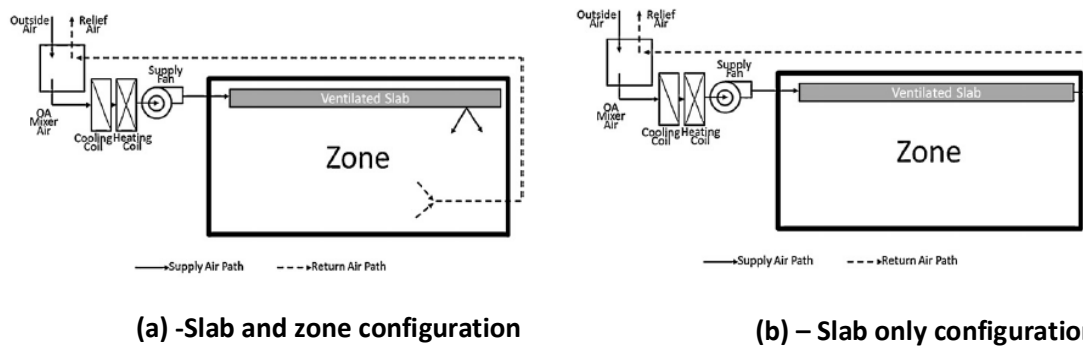


Figure 13.0: Possible configurations of ventilated slab (Chae & Strand, 2013) (in slab and zone configuration, the slab core air is supplied to the zone, whereas in slab only configuration, the core air does not get supplied to the zone)

Most ventilated slab systems are not intended to directly meet the heating or cooling loads during a given time. Many are configured to operate at night when outside temperatures are lower and thus more conducive to pre-cooling the thermal mass in the slab (Chae & Strand, 2013).

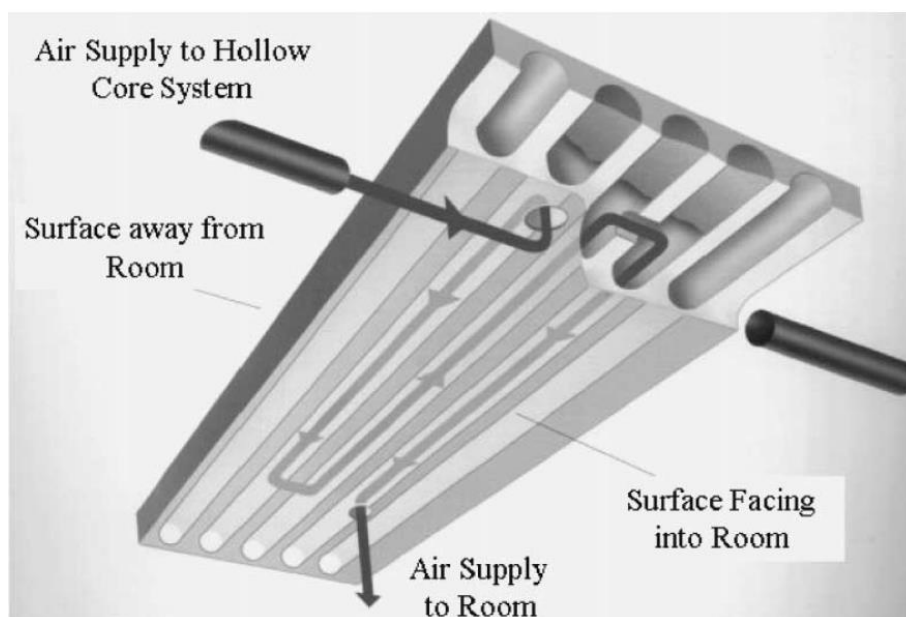


Figure 14.0: Hollow core concrete system (supply air makes three passes through three cores, there by exchanging heat with slab core, before being supplied to the room) Barton et al, 2002

The concrete slab acts as a heat exchanger (figure-14) and for example during summer times, it gets cooled at night and during the day becomes a heat sink that reduces the cooling load

(Chae & Strand, 2013). This system is known to achieve a cooling effect of up to 50 W/m^2 at an air flow of $50\text{-}100 \text{ m}^3/\text{h}$ for an area of 6 m^2 (Zmeureanu & Fazio, 1988). Chae & Strand, 2013, indicated that the hollow core concrete slabs can store about 1200 kJ/m^2 of floor area, while asserting the potential energy storage for a heavy mass (reinforced concrete) amounts to 500 kJ/m^2 floor area. However both authors did indicate the variation in room temperature, the slab temperature & comfort index.

Early use of a hollow core slab dates back to 1970s in Sweden, and utilised hollow cores within pre-cast concrete floor slabs or Termodeck system. This system taken care of cooling load of upto 50W/m^2 at an air flowrate of $50\text{-}100 \text{ m}^3/\text{h}$ for a surface area of 6 m^2 . This amounted to a reduction in chiller load by as much as 70% (Chae & Strand, 2013).

2.4 Active Thermal Mass, Hollow Core Slab, Modelling

Ren & Wright (1998) developed a simplified dynamic (transient) model of a hollow core thermal storage and a served room, based on a thermal network approach (lumped parameter method). The network addresses the heat exchange between the slab cores and the ventilation air, the heat storage and the effect on the room of the different heat disturbances. The model results were validated with measured data replicating the dampening of the oscillation of the outdoor air, after passage through the hollow core slabs. It was found that the heat transfer coefficient around the bends is 50 times that of the straight section of the core, due to increased turbulence, which in turn increases the air film heat transfer coefficient. This last assertion showed acceptable accuracy when compared to measured data.

Zmeureanu & Fazio (1988) developed a two dimensional discretized model, in which the slab cores were approximated as two parallel plates with air passing through them. The heat transfer coefficient along the length of the slab was assumed to be constant. This model was used in the study of the the performance of a hollow core floor system with respect to passive cooling (night ventilation). The model tested using weather data for Montreal, showed that an office that has been night ventilated with only outside air maintained thermal comfort without the need for any mechanical cooling the next day. The model incorporated an estimation of Predicted Mean Vote (PMV) to measure comfort. The study concluded that the use of night time ventilation with a hollow core slab design provides an estimated saving of 28.4 to 44.2

W/m² which is a reduction of 35% compared to mechanical cooling, as well as a PVM that is acceptable under standard cooling conditions. However authors did not quantify the fan energy for the night cooling and whether the saving quoted included the fan energy used for night ventilation.

Winwood et al (1994) modelled a hollow core slab using a Computational Fluid Dynamics (CFD) package, CFD 2000 and validated their model against the Building Research Establishment (BRE) commissioned experimental data. This data (see Figure 16 below), had become the basis of most of the studies conducted on hollow core slabs in later years. This modelling approach, approximated the circular cores with a rectangular ones with the same surface area (perimeter) as shown in figure 15 below.

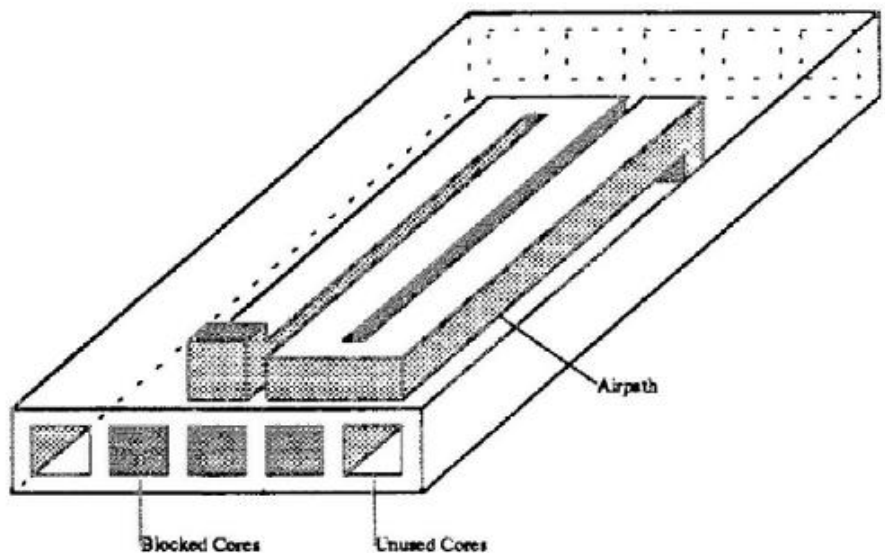


Figure 15: Four sided hollow core slab model (Winwood et al,1994)

However, Winwood et al (1994)'s noted that the model does not take into account the external temperature variations, nor the fact that the slab fabrication process makes the corner of the cores much rougher than the straight sections, giving a higher heat transfer coefficient. For these reasons, Winwood et al (1994) did not reproduce the BRE experiment, it over predicted the heat exchange. Nevertheless, this work has noted that there is twice more heat exchange around the corners of the core than the straight section and when modelling hollow core slab, circular cores could be safely approximated by rectangular duct of the same "area of interface" as the slab cores, rather than the rectangular ducts of same cross section.

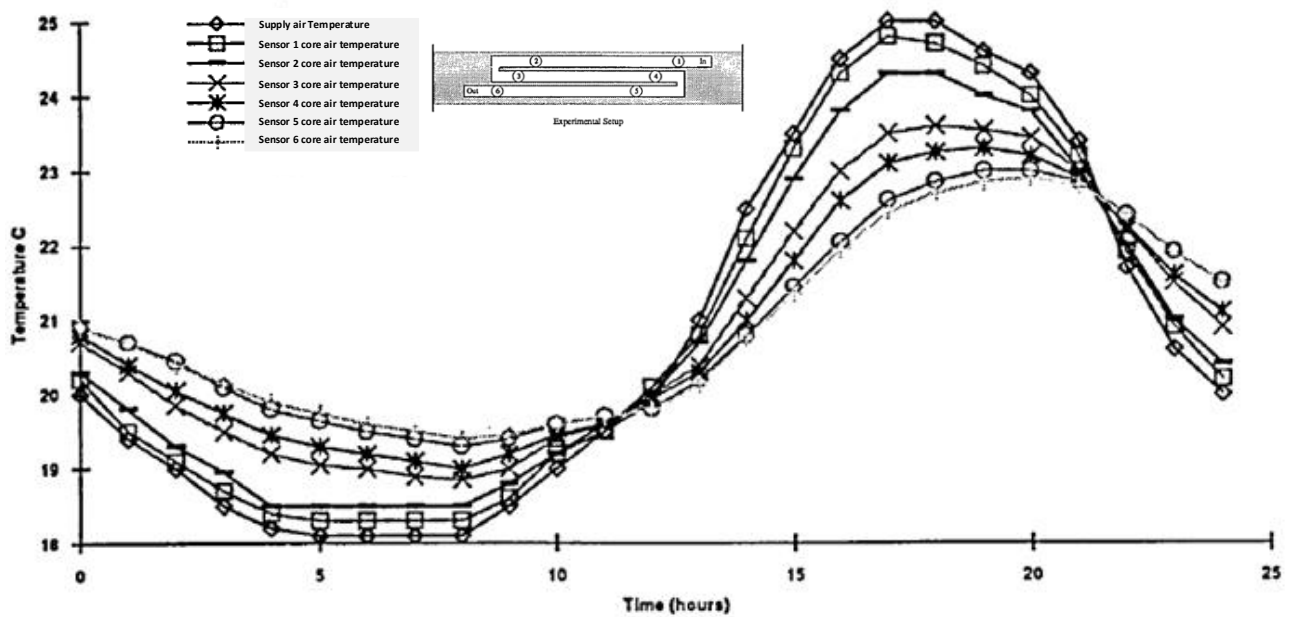


Figure 16.0: Experimental response to diurnal range (Winwood et al, 1994)

Willis & Wilkins (1993) in BRE studied the ThermoDeck™ system and made three observations: most of the heat transfer in the slab cores is attributed to the core connecting bends due to increased turbulence in these regions, the system smooths out fluctuations in the room supply air temperature and maintains comfort; and reducing the number of cores the air passes through, from three to one (switch flow) decreases the influence of the slab on supply air temperature. This work noted a difference of about 1.75 °C in supply air temperature between three and one core utilisation.

Barton et al (2002) did extensive theoretical study of the ThermoDeck system using numerical method (two-dimensional finite difference) with a view of confirming or otherwise of the earlier claims made by earlier studies about the effect of the corner section of the core & utilisation of cores (3 pass vis-à-vis 5 pass). Having validated their model by use of published data (Willis et al., 1993), concluded (based on the theoretical result of the steady state as well as transient conditions) that although there is a large rise in core surface temperature (see figure 17.0) around the bends, the overall air temperature did not change more than 0.2 °C. It was suggested in this study, although the slab temperature increased dramatically as the result of increased heat transfer, at the same time the heat transfer rate drops by an equivalent

amount as the temperature difference between the core air and slab surface decreases (this only applies to cooling mode).

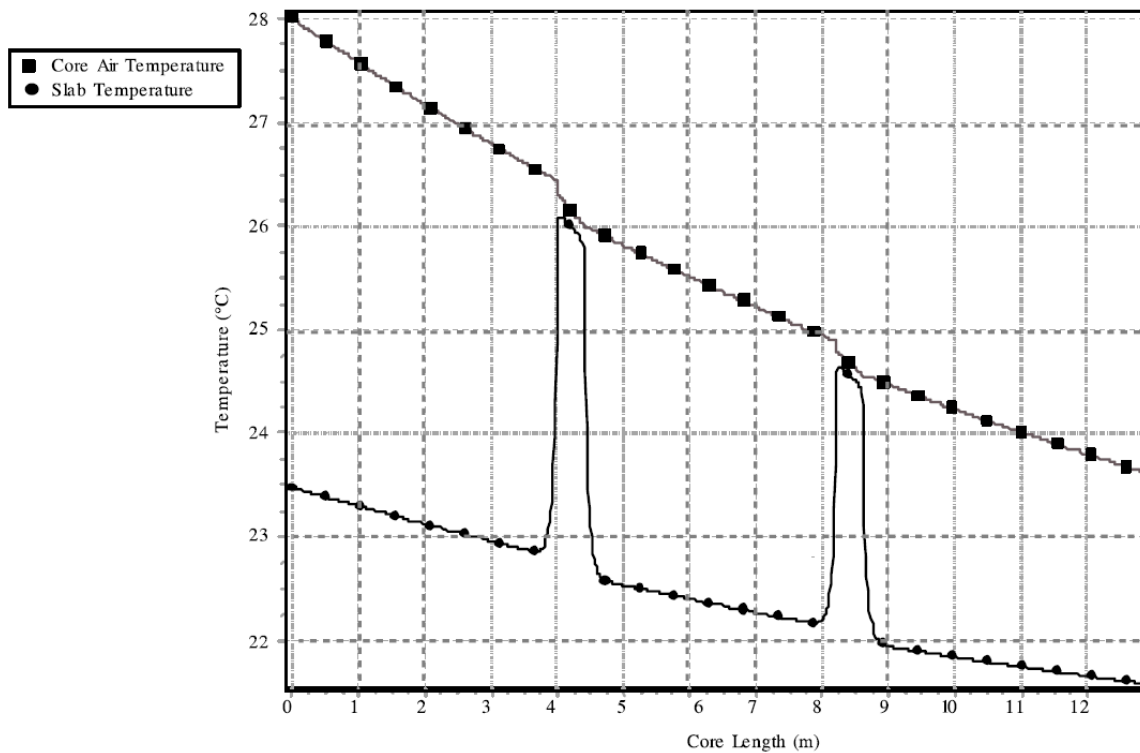


Figure 17.0: Hollow core slab surface temperature and core air temperature at the bend during cooling mode (Barton et al., 2002)

Another interesting observation by Barton et al (2002) is that, core utilisation seem to have effect on time ‘lag or phase shift’ between the core surface temperature, core air temperature and the supply air temperature. In this study it was remarked that the longer the air stays in the core (more passes) the more pronounced the phase shift is.

Yang & Li (2008) looked into detailed theoretical analysis on the relationship of thermal mass and cooling load by using a rather simplified model. The analysis quantified the cooling load as being dependent on the time constant, the outdoor air swing and the convective heat transfer coefficient (both external and internal to the building). This study introduced a concept called the ‘cooling load ratio’, a ratio of the cooling load of a building with thermal mass and that of the same building without thermal mass. Using the cooling load ratio, Yang & Li (2008) demonstrated the effect on cooling load of: outdoor air temperature swing, the difference in temperature (ΔT) between outdoor air and the indoor air & the time constant.

The effect of varying time constant on the cooling load ratio is shown in Figure 18.0 below as an illustration. From the figure it is clear the heavier the building mass the smaller the cooling load as a general trend.

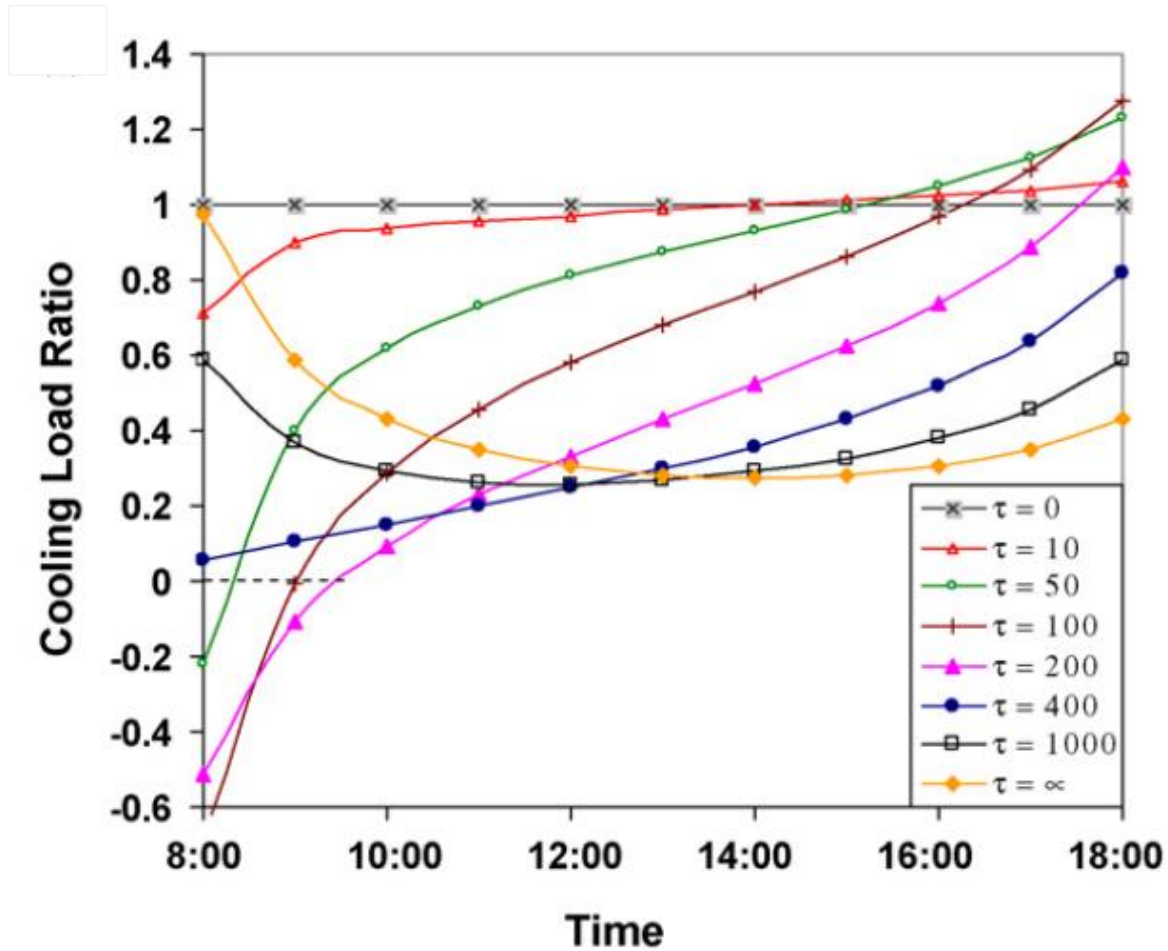


Figure 18.0: The effect of time constant τ on cooling load ratio (Yang and Li, 2008)

Corgnati & Kindinis (2006) studied a hollow core slab (1.3m x .45m x 12m, with core diameter of .25m) coupling with night ventilation using Simulink[®] dynamic mode (finite difference)l in time profile analysis. In this study the hollow core slab was treated as a heat exchanger. The model is based on a room (12m W, 4.8m L & 3m H) in a medium floor of a multi-story building located in Milan, with varying internal gains of 30, 45 & 60 W/m². Using this model, the study simulated, examined and compared 3 ventilation strategies namely: Daily Ventilation (DV), Daily and Night Ventilation (DV & NV); & Daily & Night Ventilation through the Hollowcore Concrete slab (HC& DV & NV). Each ventilation strategy employed control logic to control the air flow and amount based primarily on: outside air, room air and the upper comfort temperature during occupancy; and the surface

temperature of the slab, the outside air temperature and the room temperature during unoccupied hours. *It is worth to note here, during unoccupied hours the main driver of the control logic was not the outside air, but rather it was the slab surface temperature.*

The study by Corgnati & Kindinis (2006), showed the day and night ventilation improved up on the “day only” ventilation (*both with no hollow core use*); and the day and night ventilation with the use of the hollow core improved up on both the former strategies. However, it is worth noting that this simplified modelling approach disregards the contribution of the corners altogether as well as over estimating the overall heat transfer coefficient by assuming the Prandtl (Pr) number to be 1.0.

Chae & Strand (2013) developed a ventilated slab model based on an existing hydronic radiant system model of EnergyPlus and integrated it with EnergyPlus. Since the radiant system models have been through validation studies, the ventilated slab implementation simply adopted the existing framework and treated the ventilated slab as a heat exchanger (*using the effectiveness (ϵ)-NTU model*) with a “stationary fluid” at a single temperature (*at the point of contact with the slab*) on one side and an air loop on the other.

The model by Chae & Strand (2013) is by far advanced model than any of the models mentioned earlier in that it implements control systems in order to prevent malfunction (for example cooling while heating is needed or vis versa) through the comparison of the slab surface temperature with inlet air temperature. Moreover, the model implemented a control to prevent surface condensation through the monitor and comparison of the dew point temperature of the space with the slab surface temperature. If it happens that the slab surface temperature is below the dew point temperature of the space, the system shuts down and stops the air flow through the slab cores.

This model was validated against previous work of Zmeureanu & Fazio (1988) using a test room of 450m² of occupied space with windows (*Window-to-wall ratio of 0.5*) and oriented with its long axis east-west; and using Montreal (Canada) as a weather location. The conclusion of the work by Chae & Strand (2013) based on simulation (single day of July, 22nd) of a traditional ventilation strategy and another with the use of hollow core slab coupled

with night ventilation, was that, the use of hollow core with night ventilation has cooling energy saving potential of 23% on a daily total demand and 28% on peak demand.

2.5 Conclusion

Thermal mass has a potential to be used as thermal energy storage and various researchers have shown this through numerical and experimental studies. Moreover the studies shown that ventilated slab could be used to modulate building zone's temperature and to reduce the energy cost via thermal storage through passive and active means.

The challenge lies in the accuracy of the modelling approach and the technique and tools used in the modelling process. Most of the work focused on studying ventilated slab in isolation from the overall practical building elements, such as the Air Handling Unit and the usual disturbances such as occupants. Therefore, careful interpretation of the results of the works is needed.

3 Literature Survey – Optimal Thermal Mass Control, Peak Demand Limiting and Peak Load Shifting

3.1 Optimal Control of Building Thermal Storage System

The optimal control of air handling units and plant's primary goal is to provide an operational strategy that meets a required instant thermal load in the building space. This steady state optimisation's, (as it is usually referred to in the literature because it does not consider time as an important factor in the control optimisation), objective is to minimize plant energy consumption while satisfying a required instant load. This greatly differs from the optimal control of a thermal storage system. The optimal control of central plant cooling systems with storage, is based on a prescribed cooling curve that is used to find the best plant operating schedules through optimisation process (Ren, 1997).

The optimal control of central plant tend to ignore the zone thermal condition as it does not account for the entire system operation and the building thermal response (*as the plant stores the energy in a separate device and the plant's night time operation is decoupled from building zone thermal conditions*). The optimal control of the building fabric thermal storage on the other hand should try and optimise the zone thermal condition with a view of minimising the plant operating cost. Since building fabric energy storage uses the building mass as energy storage, the coupling between the zone thermal condition and the plant operating strategy, is very strong. Therefore, it is implied that the optimal scheduling of the plant operation should take into account the building dynamics (Ren, 1997, Braun, 1990).

However, this does not imply, the optimisation process should take into account the plant operating set point, the energy input to the building and the building zone set points as control variables. As the primary objective of the control optimization is to maintain the building zone thermal conditions within a limit while minimizing the operating cost, the primary supervisory control variable in the building is the zone temperature set point (Ren, 1997, Braun, 1990). In other words, the zone temperature set point control sits at the higher hierarchy of the supervisory control of the building system and governs the control of the air handling unit and it can further be used to control the primary plant operation.

The optimisation of the zone temperature set point control alone can determine the energy input to the building as well as the plant operating set points over a planning period (Braun, 1990). This decoupling of the optimisation of the building thermal storage from the plant operation, while accounting the complex interaction of the building dynamic thermal response and the plant operation, makes the optimisation problem computationally efficient, flexible and accurate (Ren, 1997).

3.1.1 Thermal Mass control Systems

In the context of building services such as Heating Ventilation and Air Conditioning (HVAC), there are two level of controllers that ensure comfort, ventilation and energy economics is achieved. The hierarchical organisation divides the controllers into low level and high level (Building level). The low-level controller typically operates at the zone (room) level and are used to track a specified set point where as a high-level controller overlooks the whole building and determines the set points for the low-level controllers (Privara et al 2011). The high level controllers tend to be strategies rather than physical devices, whereas the low level controllers are actual physical actuators (devices) such as valves, dampers and time switches. Examples of low level controllers are: ON-OFF switch, Proportional Integral Derivative (PID) controller and Weather Compensated Controller (WCC).

3.1.1.1 Rule Based Control of Thermal Mass

In the domain of activated thermal mass, depending on the type of thermal mass activation, i.e. whether it is air or water based, the control of thermal mass system varies accordingly. For air activated systems, the ambient air temperature, internal space (zone) temperature and slab mass (surface temperature) is used to control the charging or discharging of the thermal store (Ren, 1997). Where as in the water activated systems, which are commonly called Thermally Activated Building Systems (TABS), the control is based on heating or cooling water simply temperature ($< 30^{\circ}\text{C}$ for heating and $> 15^{\circ}\text{C}$ for cooling), water flow rate; zone temperature & the ambient air (Sourbron, 2012). This method of control is called rule based method of control.

In both cases, the high thermal inertia of the building mass plays a major role in connecting the building where thermal comfort has to be maintained in and the heating and cooling

production units or the plants. Due to this coupling, the dynamic nature of the thermal mass and the control of it, plays large role both in terms of energy cost as well as occupants comfort (Sourbron, M, 2012).

Example of rule based control of a hollow core slab is given below (see table-2):

Ventilation logics during occupancy period

Where:

- t_i – indoor temperature
- t_o – outdoor temperature
- t_{comf} – upper comfort limit

Control Logic	Control Action
$t_i \leq t_o$ or $t_i < t_{comf}$	ACH = 2 per hour
$t_i > t_o$ and $t_i \geq t_{comf}$	ACH = 5 per hour
$t_i > t_o$ and $t_i \geq t_{comf, inf}$ and ACH == 5per hour	ACH = 5 per hour

Table 2: Example of rule based control of thermal mass

3.1.2 Air Flow Control in Buildings

Control of air flow in HVAC is achieved through either Constant Air Volume (CAV) or Variable Air Volume (VAV) control. In CAV, the air volume delivered to the zone is constant, but its temperature varies according to the needs of the zone. Whereas, in VAV, the volume of air delivered to the zone varies but its temperature is constant

3.1.3 Thermal Mass Control Strategies

In terms of control strategies, there are two further categories in the building domain: these are: *Conventional* control strategies & *Optimal Control* strategies. The conventional system starts by analysing the different possible settings and the response of the building to these settings, so that the right combination is achieved. On other hand the optimal control strategy starts with the perceived dynamics of the building and its interaction with disturbances, with

the aim of minimising energy use while attempting to achieve maximum comfort (Ren,1997 ; Bauran, 1994; Sourbron, 2012).

3.1.3.1 Conventional Strategies

The conventional strategies are divided into further two categories:

3.1.3.1.1 Night Ventilation / Pre-Cooling / Load Shifting

There are three distinct ways of implementing pre-cooling and these are (Armstrong et al, 2006):

- a short period of reduced set point before chiller curtailment
- an extended period of reduced set point before expected curtailment
- Night cooling

Night cooling is a strategy employed in locations where cool nights and day time larger cooling load concedes throughout the year. Night cooling, uses ambient conditions (cool night air) or mechanical means that tend to be more efficient under night cooling (low lift, small load) to remove heat from the building structure & fabrics. The arithmetic difference between the normal zone set point and the thermal-capacitance-weighted-average of contents and structure temperatures at the start of an occupancy, is directly proportional to the maximum usable cooling capacity to be stored on a given day (Armstrong et al, 2006).

However, the thermal storage capacity of building mass is primarily a function of total thermal capacitance, rate of charge /discharge, night time ambient temperature and comfort constraints. Within the confines of these limiting factors, night cooling is implemented in a number of strategies, these are (Armstrong et al, 2006):

1. Constant Air Volume (CAV) Pre-Cooling, where outdoor air which is at lower temperature than return air is brought into the building and is used to modulate the cooling rate in order to bring the zone temperature to the minimum comfortable temperature (MCT).

2. Delayed Start CAV Precooling, where the outdoor air is brought in only for long enough time to bring the zone to MCT.
3. CAV Pre-Cooling / Tempering, where the building mass is cooled below MCT but the tempering time is tightly controlled so that it is only long enough (optimal) so that the zone can returned back to MCT without additional heating or cooling prior to occupancy.
4. CAV Objective Function, where an objective function that minimises energy cost and plant demand is used to work out the exact length of the pre cooling time.
5. Variable Air Volume (VAV) Pre-Cooling, where fan speed is modulated to reduce daily fan energy.

The 2nd strategy is more optimal than the first one because it reduces the time the fan runs, whereas the 3rd one is more optimal than the 2nd one, because it exploits cooling the building mass below MCT. All the strategies from 1 to 3 are defined based on the state of the building thermal mass at the start of occupancy. This state cannot be observed and is only indirectly related to the objective of minimising plant demand and energy cost. The 4th strategy is by far optimal than the previous three, as it tries to directly exploits the objective of minimising plant demand and energy cost. The objective function represents daily electricity cost and daily cost is minimised by enumerating all all tempering and start times so as to find the combinations that minimises daily cost.

3.1.3.1.2 Curtailment or Demand Limiting

Curtailment is a reduction of load at the electrical service entrance as response to utility contractual incentive. This strategy involves reduction of lighting load and other dispatchable loads that contribute to cooling load. The most aggressive of this strategy involves reduction in cooling capacity through either direct chiller control or raising zone set points, and it could potentially reduce occupants comfort.

3.1.3.2 Optimal Control Strategies

3.1.3.2.1 Optimal Start / Recovery

Optimal start controls the recovery of the building temperature prior to the start of occupancy. For instance in heating mode, maximum energy saving is achieved by starting recovery at the last possible moment (Armstrong et al, 2006).

3.1.3.2.2 Model Based Control

Through the use of thermal response model, model based control strategies estimate the effect of important disturbances on the thermal response of the zone. Zonal temperature is not determined only by the actions of a thermostat and a terminal unit, but it is also dependent on other variable conditions such as weather, internal gains and adjacent zone temperatures. Model based control could be further improved by the addition of prediction of disturbance and the corresponding response, through model predictive control.

3.1.4 Optimal Control of Hollow Core Slab

The primary goal of the optimum control of the building thermal system involves minimizing the total energy cost from the primary plant and AHU over a specified period of 24 hours, while maintaining the zone thermal comfort requirements. The optimum solution to this problem is a schedule of control operation throughout the 24 hours optimization period. The problem can be solved using an optimization algorithm to search for the feasible solution with the minimum total energy cost over the planning period.

The focus of this thesis is the optimal control of an air activated hollow core slab that is structurally used as an air supply route as well as thermal energy storage. The slab bridges the coupling of the zone thermal conditions and the plant operation & therefore the optimal control of it, is crucial as well being very complex business.

Generally, the air entering the slab has paramount influence on the thermal storage of the slab and through that considerable influence on the entire zone thermal conditions. Therefore, the condition of the supply air to the ventilated slab forms the independent variables in the supervisory control of the ventilated slab system. The thermal state of the zone the slab is

supply air temperature, is uniquely determined through two control variables: the supply air flow rate and supply air temperature in conjunction with the ambient boundary conditions and zone thermal disturbances (Ren, 1991).

In this thesis, the system under study is a Constant Air Volume (CV) system and hence the air flow rate is predetermined. Therefore the optimisation of the hollow core slab system only focuses on the supply air temperature.

3.1.5 Building Level or Supervisory Controls

The Building Automation System (BAS) is primarily aimed at controlling heating, cooling, ventilation, positioning of blinds & electric lighting, of a building such that zone temperature, CO₂ and luminance levels are maintained within the desired comfort ranges. In BAS, the control hierarchy is usually divided into two levels: the low-level controller which typically operates at the zone (room)-level and is used to track a specified setpoint, and a high-level controller which overlooks the whole building and determines the set-points for the low-level controllers (Privara et al 2011).

The use of cost actuators such as chillers, boilers, cooling coils and radiators (high cost actuators); as well as low cost actuators such as blinds operation, evaporative cooling & window' opening actuation are crucial for the integrated building automation (Oldewurtel et al, 2012) as it tries to manage cost & maintain comfort. The building automation system needs to work with both the low level controllers and a high level control method that relates them to the building dynamics (Cigler, 2013).

The low level controllers such as ON-OFF, Weather Compensated Control (WCC) and Proportional Integral Derivative (PID) control, lack information about the dynamics of the building. For instance the ON-OFF control for cooling system turns ON or OFF (state S) a cooling coil, according to some room temperature error ($\epsilon_t = T_{\text{setpoint}} - T_{\text{room}}$) threshold, which customarily is implemented as hysteresis curve $S = f_{\text{on-off}}(\epsilon_t)$. This is simple to implement but its drawback is that it does not take into consideration the building dynamics (Privara et al 2011)..

Similarly, the PID controller works based on the same error threshold and it has added advantage of looking back in history, $T_{\text{supplyair}} = f_{\text{PID}}(\varepsilon_t, \text{history})$, however it has no mechanism to take into account the outside weather. On the other hand the weather compensated control air is a feedforward control that controls the controlled variable (for example chilled water supply temperature) by the use of a predetermined cooling curve & the outside temperature. This control system lacks, like the other two, connection to the building dynamics & the feedforward only takes into account the current weather, however it is well used and has proven track record for robustness and simplicity of tuning (Privara et al 2011).

Combining the good traits of the all the above with an ability to predict and optimally work with disturbances so that the building dynamics is used for its optimal control (energy efficient and comfortable), required a change of paradigm and the building sector had embraced the Model Predictive Control (MPC) technique for sometimes now (Cigler, 2013). For instance, as the outside temperature is one of the most influential quantities for the building heating/cooling system, weather forecast can be employed in a predictive controller. This enables to predict inside temperature trends according to the selected control strategy. (Privara et al 2011).

Generally the building dynamics is slow and it is subject to intermittent disturbances such as weather, equipment and occupants, therefore, for example, the appropriate use of the building thermal mass capacity is dependent on prediction of these disturbances. Model Predictive Control lends itself as an ideal platform for tackling this problem, and handles well the interaction of the slow reacting mass to fast acting air handling units (AHU) (Sourbron, 2012).

3.1.6 Model Predictive Control

MPC is not a single strategy, rather it is a toolbox of control methods with the model of the process explicitly expressed in order to obtain a control signal by minimizing an objective function subject to some constraints (Cigler, 2012). The basic premises (see figure 18) of Model Predictive Control is to utilise the model of the process to predict the future evaluation of the system and to compute control actions by optimising a cost function depending on these predictions (Oldewurtel et al, 2012). In building control, one would aim at optimizing the energy delivered (or cost of the energy) subject to comfort constraints (Cigler, 2012).

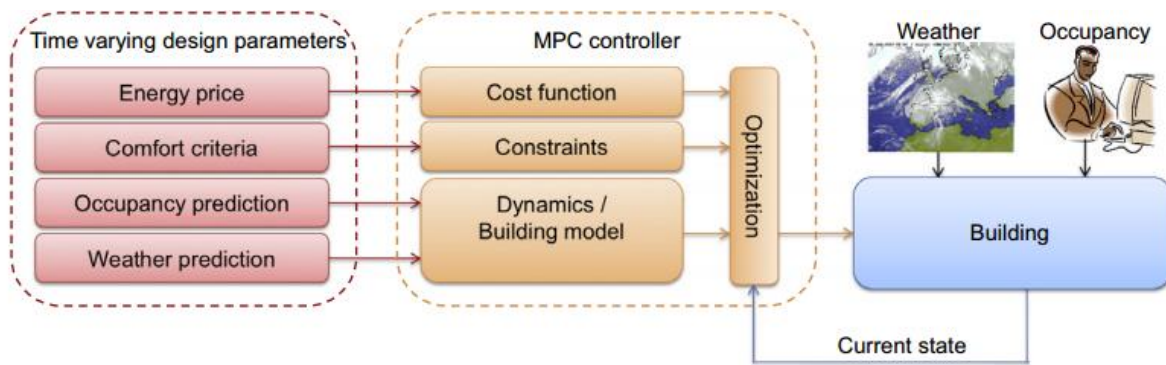


Figure 18: Basic principle of model predictive control for buildings (adopted from Privara et al, 2011)

The inputs to the MPC controller are time-varying design parameters, the energy price, the comfort criteria, as well as predictions of the weather and occupancy. It is obvious from figure 12 that the modelling and design effort of the MPC controller consist of: specifying a dynamic model of the building, constraints of the control problem and a cost function that encapsulates the desired objective. These components are combined in each sampling interval and converted into an optimization problem depending on the MPC framework chosen (Privara et al, 2011).

The generic MPC framework is given by the following finite horizon optimisation problem:

$$J(x_0) = \min_{u_0, \dots, u_{N-1}} \sum_{k=0}^{N-1} p(x_k) + l_k(x_k, u_k) \quad \text{Cost function} \quad \text{-----} \quad \text{(Eq-6)}$$

subject to:

- $(x_k, u_k) \in X_k \times U_k$ Constraints in state and control respectively
- $x_0 = X$ Current state
- $x_{k+1} = f(x_k, u_k)$ Dynamics

where:

- N is the prediction horizon
- X_k & U_k are constraints for state x_k and inputs u_k respectively at time step k.
- l expresses the objective function p, penalizes undesired system state

While cost function and the constraints are the crucial parts of the MPC design, the current state is used as the initial state for control prediction of the next horizon, and the precise modelling of the dynamics of the system ensures good control performance is achieved (Khalid, 2014; Oldewurtel et al, 2012; Smith, 2012).

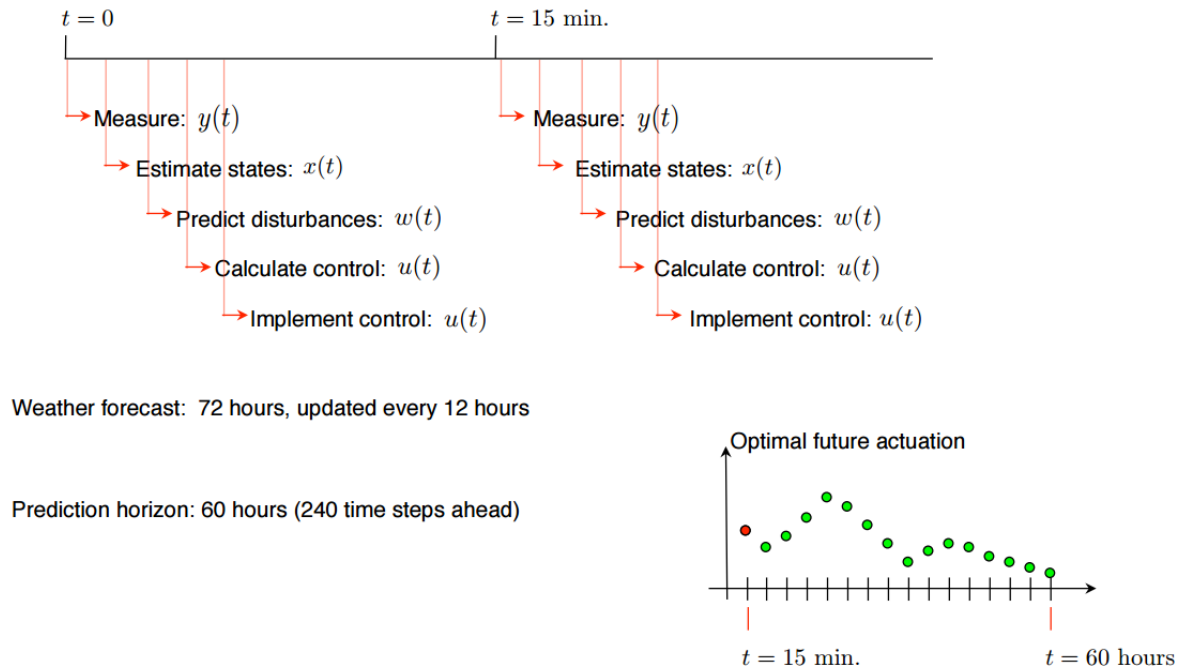


Figure 19: MPC controller operation (adopted from Smith, 2012)

During each sampling time frame, a precise horizon optimal control problem is formulated and solved over a precise future window. The outcome of this is a trajectory of inputs and states into the future, honoring the dynamics and constraints of the building while optimizing some given objectives. In the context of building control, this means that at the current control step, a heating/cooling etc. schedule (profile) is obtained for the next several hours or days, based on a weather forecast.

The optimization could include, predictions of any other disturbances (e.g. internal gains), time-dependencies of the control costs (e.g. dynamic electricity prices), or of the constraints (e.g. thermal comfort range). The building elements such as heating, cooling and ventilation are set based on the first step of the control schedule and then the optimisation process moves forward in step and the the procedure is repeated at the next time instant. Feedback into the

system is introduced via this receding horizon approach, as the new optimal control problem solved at the beginning of the next time interval will be a function of the new state at that point in time and therefore of any disturbances that have acted on the building (Siroky, 2013).

3.1.7 MPC in Building Sector

MPC for buildings has recently been studied intensively. It has been shown that energy savings potential of this technique reaches almost 40 % compared to conventional control strategies depending on the particular building type.

Numerous studies on the theory and application of model based (simulation based) building control, has been done on the last 2 to 3 decades owing to new development of simulation tools and control technologies (Zhao et al, 2013).

In this context there are two dominating model development approaches. These are: first principle and linear identification methods. Most of the works used first principle models and early works focused on attempting to control HVAC at system level. However, several studies so far used linear identification models to optimise the building and system “black-box” models and used real time experimental data or simulation data to train the model and identify the parameters of the linear model (Zhao et al, 2013).

Various researchers suggested MPC as being an effective method to improve building system and energy performance, but there are others who consider the two modelling approaches have their limitations when it comes to practicality, such as (Zhao et al, 2013 & May-Ostendorp et al, 2012):

- The first principle based modelling could not be applied to real buildings,
- Linearly identified models require lots of measured data to be trained (making them time and cost intensive) and;
- Both of them require high level mathematical skills (which is not viable for a day to day building operation).

However, a whole building simulation tools such as the IESVE or EnergyPlus or ESP-r can be used for MPC development. The high-order detailed geometry and system modelling capability in these tools makes them an ideal aid for ‘integrated thermal response model’ development.

3.1.7.1 The Use of Whole Building Simulation Tool

Although some practical difficulties (data operability and time synchronisation with other tools and the challenge of black-box model optimisation) prevented the wider use of these tools for this purpose previously, it seems as shown by the work of Zhao et al, 2013; May-Ostendorp et al, 2012; & Kummert et al, 2011, the difficulty seems could be overcome.

Zhao et al, 2013 implemented MPC with EnergyPlus, Kummert et al, 2011 developed MPC with TRANSYS and Kummert et al, 2011 showed it can be done with ESP-r; all using co-simulation with Matlab/Simulink. The MPC development showed a potential saving of about 18% - 20% in energy while maintaining comfort within the acceptable ranges.

In general, detailed models offer a more accurate representation of the physical phenomena while simpler models have other advantages such as the ease of implementation and computational efficiency. A hybrid approach where the detailed building model is used in conjunction with the simpler models could be a promising proposition.

3.1.8 Previous Work on Optimal Control in Buildings:

Siroky et al, 2013 applied MPC to building heating systems, with predicted weather and analysed energy saving that can be achieved over two months on real building at the Czech Technical University (CTU) in Prague. The findings of this exercise is that the energy saving potential was between 15 and 28% as the result of the use of MPC.

Gayeski, 2010 studied Predictive pre-cooling for Low lift Radiant Cooling using building thermal mass. The MPC designed and developed for this purpose; showed a potential saving of about 25% in energy cost.

Braun et al (1988; 1989a; 1989b) investigated the optimal control of a chiller plant by using system-based models & detailed component models. The power consumption of the system

as whole (as supposed to individual components) was used in the determination of the “near-optimal” control strategy, that was simple and very close to the detailed model. The determination of the near optimal strategy required minimisation of energy cost in quadratic form using the Lagrange multiplier optimisation method. The system-based method determines a "near-optimal" control strategy based on the power consumption of the system as a whole, rather than that of each component. The near optimal strategy is simpler and can provide a strategy very close to the detailed component model approach.

Adaptive control optimisation algorithm was used to control chiller plants and were able to control chiller sequencing as well as control chilled water and condenser water temperatures (Ren, 1997, citing Cascia, 1988).

Ma et al, 2011; presents the effectiveness of an economic model predictive control in reducing energy and demand cost for a building HVAC system. The study used an EnergyPlus model to simulate multi-zone commercial building equipped with of variable air volume (VAV) cooling system. Through the Building Controls Virtual Test Bed (BCVTB) as middleware, co-simulation between Energyplus and a Matlab was possible; and zone temperature and power models were used for system identification for the MPC use. The MPC economic objective function took into account the daily electricity costs, which included time-of-use (TOU) energy charge and demand charge. The Cost savings due to the use of MPC are estimated by comparing the cost of energy with MPC against the baseline (night setup strategy) and it was shown that the use of MPC with time-of-use electrical pricing structure brings about substantial cost saving amounting to 28% and energy saving of 25%.

3.2 Peak Demand Limiting and Peak Load Shifting

Building thermal mass can be used to reduce the peak cooling load, by pre-cooling it during non-peak hours, storing cooling in the building thermal mass, so that peak hours cooling load is reduced. As the result the cooling load is shifted in time and the peak demand is reduced (Xu, 2004, Braun, 1990)). As the comfort constraints during unoccupied hours could be relaxed, the precooling of the building mass can be done effectively at these hours (Xu, 2004). Saving is achieved by reducing on peak energy and demand charges.

Different thermal mass discharge strategies result in different cooling load reductions and savings. The goal of an optimal discharge strategy is to maximise the thermal mass discharge while minimising the possibility of rebounds before the shed period ends (Xu, 2004).

3.2.1 Demand Response

Demand Response (DR) is an approach that encourages the end users to change their regular electricity usage pattern in response to the time-varying price of electricity. The basic strategy to shifting peak demand takes the form of pre-cooling or pre-heating, by taking in to account an electricity market that applies time varying rate or Time of Use Cost (TUC). Whereas in basic demand limiting strategy, the zone temperature trajectories are obtained by solving an optimisation problem during on-peak hours under pre-determined target demand (Braun, 1990). However, this strategy does not respond well to the impact of disturbances, such as the weather and building internal loads (Xu, Peng, et al, 2011).

3.2.1.1 Demand or Load Shifting

Load shifting control uses precooling (PC) with set point temperatures put at the lower end of the comfort zone before the onset of occupancy and off-peak period; and then resets the set point to near the upper comfort limit during the occupancy and on-peak period.

This way, the stored thermal energy is utilised to the maximum and the on-peak electrical charge is minimised. But, it is important to balance the increase in total cooling requirements, as the result of precooling vis-à-vis the benefits; and hence the demand reduction and load shifting savings are directly proportional both to the method of control and the specific application (Braun, 2003).

In most buildings (especially large commercial or public buildings) most of internal gains (about 70%) are in a form of electromagnetic radiation and are absorbed directly by the building fabric before getting convected to the air space. In other words, the cooling load in a building is a result of internal gains (light, equipment and people) & internal surfaces convection; as the state of the building thermal mass and its tight convective coupling dictates the cooling load (Xu, .

Considering the thermal capacity of a typical concrete building mass is in the order of 2 - 4 W-h/°F per square foot of floor area, it had been indicated by previous work (Braun & Lee, 2007) that the energy required to maintain the air space condition within the thermal conform region can be shifted considerably via the management of the thermal mass energy storage with relatively small temperature swing.

3.2.1.2 Demand Limiting

With demand limiting, the building is precooled prior to occupancy and on-pick or critical pick-pricing period (Braun & Lee, 2007) and then set points are adjusted in an optimal fashion, so that the stored energy is controlled and the peak cooling load is minimised. This strategy limits the on-peak demand charges and is most suited for scenarios where the utility take active role on end-user at times of critical demand (Braun & Lee, 2007).

3.2.2 Zone Temperature Adjustments and Zone Temperature Optimal Trajectories

Thermal fabric energy storage has been recognised for some times now as a crucial passive asset to manage demand shifting and many researches have studied the reduction of peak demand through the adjustment of zone temperature set points of HVAC systems (Xu, Peng, et al, 2011; Braun,1990).

Zone temperature set point has a profound impact on zone load variation and controls the interior surfaces' heat emission to the zone (gains) (Lee and Braun, 2007). The reduction & cooling load shifting has been shown to be further enhanced via the adjustment of zone temperature set points within the bounds of thermal comfort (Braun and Lee, 2007). The adjustment could be done in such a way that, instead of a fixed set point that is always aligned with upper region of the comfort zone, if zone set points were made to vary between the upper end and lower end of the comfort zone, it is believed that considerable amount of energy and hence operating cost could be saved.

As an example, for cooling applications the zone temperature set point could vary in this way: starting at the lower end of the comfort zone at the start of occupancy and gradually increasing to the top end of the comfort zone, eventually free floating above the upper end, up until such time (*dependent on outside conditions, plant characteristics and utility rate*

structure) that is enough for the equipment to precool the building to the lower end of the comfort zone, just before occupancy

Braun, 2003 applied non-linear optimisation techniques on daily basis to determine the minimum daily energy costs with Time Of Use (TOU) electricity rates & minimum peak demand, through the determination of zone temperature set points. This shows, the energy storage of the building thermal mass can be controlled via variations of the zone set point (temperature) over time while not compromising thermal comfort region (see figure 20).

The varying of zone set points provides opportunities for shifting cooling loads from daytime to night-time so that (Braun, 2001):

1. Peak electrical demands are reduced,
2. Low night time electrical rates are taken advantage of
3. Mechanical cooling is offset with "free" cooling at night, &
4. Equipment's operation is enhanced by operating them at more favourable part-load conditions

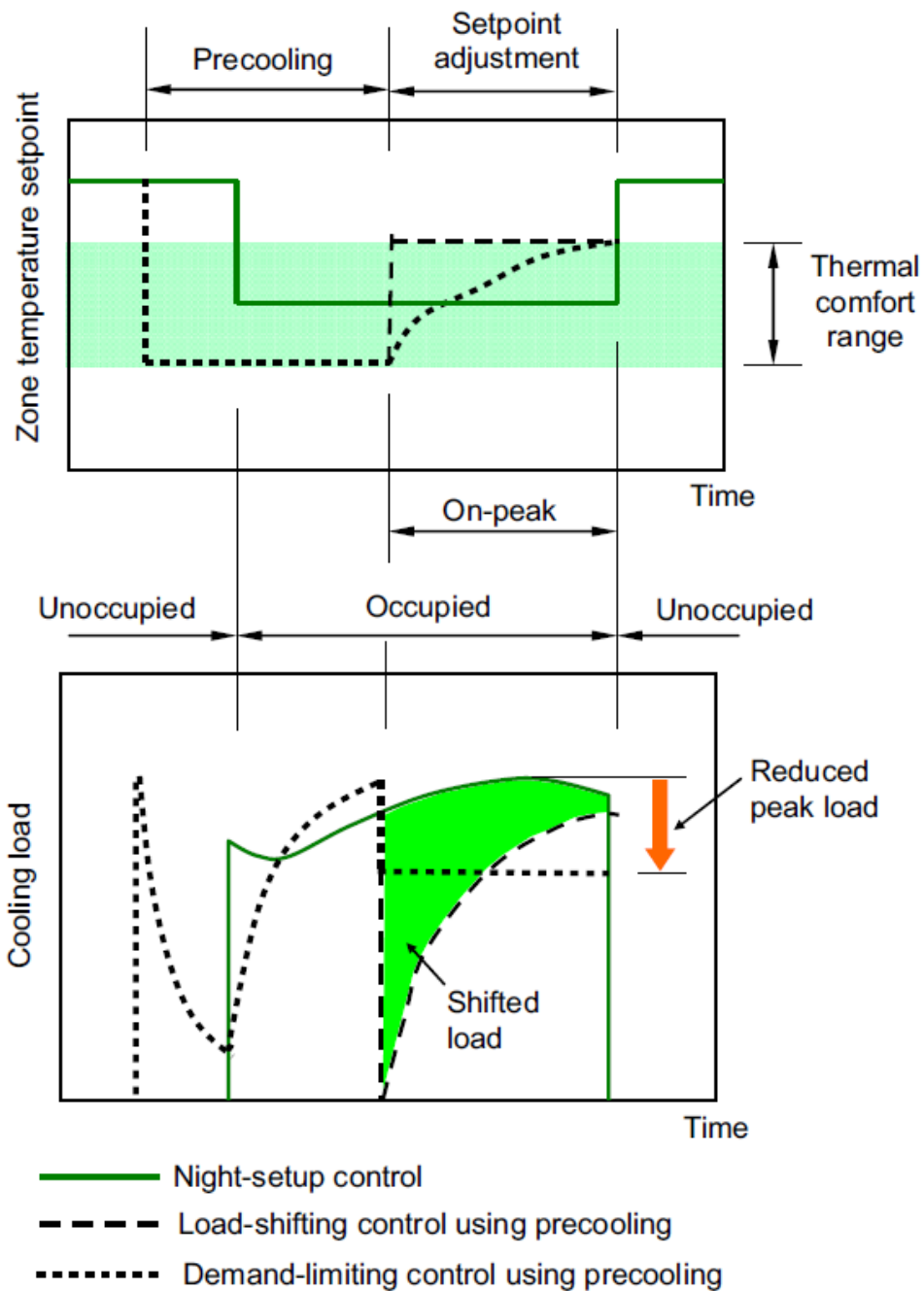


Figure 20- Comparison of night setup, load shifting and demand-limiting control (Braun and Lee, 2007)

Among the above four, the first two help towards reduced energy use whereas the second two change the time of use of electrical energy, but in the process could increase the overall energy use due to lower average zone temperature set points (Braun and Lee, 2007). But, it is worth noting here that, the increased energy usage at the building, could actually results in

primary energy usage reduction at the power plants (as the energy at the building is being used at the times of lower capacity at the plant and when efficient equipment's are employed) and hence prompting the utility companies to introduce incentives for energy use at times of off-peak.

3.3 Previous work on Zone temperature adjustment, Demand limiting and Load Shifting

A number of previous studies did look into the optimal adjustment of zone temperature set point and its impact on load shifting and peak load reduction (Braun & Lee, 2007; Braun, a; Braun et al., b; Xu, et al., 2012) and demonstrated the significant potential it possesses.

Braun and Lee, 2007; studied demand limiting by determining an optimal set point trajectory of the zone temperature set points in conjunction with precooling, using the inverse model of the Energy Resource Station (ERS) building in Iowa, as a case study. A test data that was collected from the building over 17 days in August was used to train the inverse model. The model was further validated using the data and was able predict cooling loads within 5%. Later on the demand limiting strategy from the study was implemented at the ERS site and a reduction of 30% on peak cooling load was achieved, compared to the conventional night time set up strategy.

Braun, 2003 attempted to define the problem of optimising the zone temperature set point and presented specific results that have been obtained through simulations, controlled laboratory testing & field studies. This study demonstrated the potential of the building thermal mass in saving energy cost, and also showed how the savings are sensitive to factors such as: utility rates, type of equipment, occupancy schedule, building construction, climate conditions and control strategies.

Morris et al (1994) used the National Institute of Technology (NIT) building as a case study and performed various tests on the potential of the building for load shifting and load levelling. Optimisation routines that were constrained to thermal comfort being maintained during occupancy were employed on the simulation in order to determine the control strategies that have been used in actual experiment. Comparison of Night Setback (NS) strategy to minimum cooling system energy and minimum peak cooling system electrical

demand were conducted, and the optimal control strategy showed significant load shifting potential over the NS with about 40% less cooling requirements.

Peng Xu, 2007, studied the potential of precooling on load shifting & peak demand reduction utilising building thermal mass on two commercial buildings, which are made up of light and heavy mass and are located in the Bay Area of California. The work consists of simulations, laboratory and field studies and concluded that precooling has the potential to affect for better the demand responsiveness of commercial buildings while maintaining comfort for the occupants. Moreover, the study concluded that precooling and demand shed strategies are equally applicable to both light mass and heavy mass buildings & gave figures of 25-35% and 50% reduction in peak HVAC load, respectively.

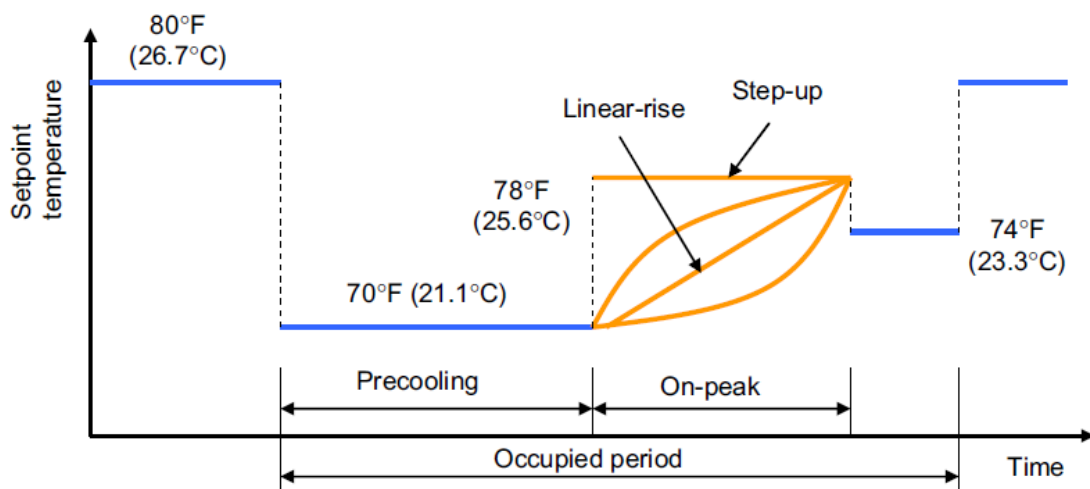


Figure 21 - Example of demand-limiting building set point temperature control (adopted from Braun & Lee, 2007)

In this study, Peng Xu, 2007, devised test setups made up of control strategies (see figure-21) in addition to the conventional night set up and compared the performance of these additional strategies against the night setup that was taken as a bench mark. The additional strategies studied are: precooling and linear zonal set up, precooling and aggressive linear set up (*this is the same as liner zonal setup except that temperatures set points were raised more aggressively in the afternoon*), precooling and exponential set up and no-precooling and liner set up. The conclusion of this study in terms of the performance of the different strategies is that:

- Exponential temperature reset strategy, if properly controlled, could discharge thermal mass smoothly, it could avoid rebound and it creates a float load curve during peak hours in both light and heavy buildings
- Night pre-cooling works better in reducing peak demand and energy consumption with heavy mass building than light mass

Lee & Braun (2007) demonstrated a simplified approach for estimation of variations of zone temperature set points that minimises the peak cooling demand during critical demand periods, using short-term measurements for training. Three differing methods: Semi-analytical (SA), exponential set point equation-based semi-analytical (ESA) & load weighted-averaging (WA), were used. The first two methods employed an inverse building model trained with short term data and a use of analytical solution to determine set point trajectories using the same model. The weighted-averaging method is purely data based and it aimed to find the optimal weighting factor that minimises the weighted average of two loads in order to weight averaging two initial bound set point trajectory, using the minimised weighted average (see figure 20 below). The set point trajectory found this way is adjusted so that the shape of the load is improved on daily basis.

On the companion paper, Lee and Braun, 2008 evaluated the applicability of the three methods and concluded the weighted average is recommended as it is simple to implement, performs well and can be directly applied to building aggregates. This conclusion seems based on test findings of the simulation of sample buildings, that produced peak cooling load reduction of 22-32W/m².

The use of weighted-average method by Lee & Braun, 2008, is based on the premise that the two set point trajectories produce load variations that intersect at some point during the demand limiting period (see figure 22 below), and that the cooling load is a linear function of zone temperature. With this assumptions, the optimisation problem was the minimisation of the cost function, equation (Eq-7) below with respect to weighting factor, w .

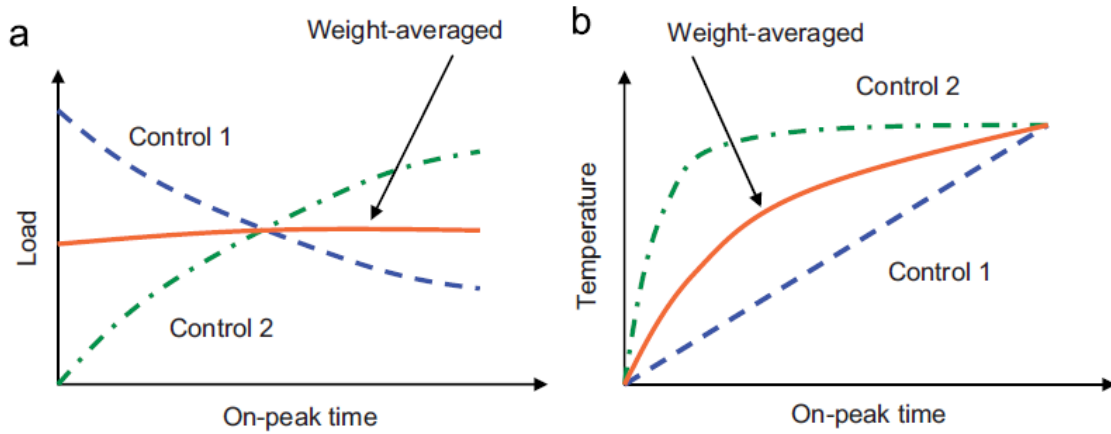


Figure 22: Illustration of the weighted average method (a) Load & (b) zone temperature (adapted from Lee & Braun, 2007)

$$J = \max_w [wQ_{1,k} + (1 - w)Q_{2,k}] = \max_w [Q_{w,k}] \text{ for } 0 < t \leq t_{\text{demand limiting}(dl)} \text{ ----- (Eq-7)}$$

Where:

- $Q_{1,k}$ is the cooling load for time interval k under control 1
- $Q_{2,k}$ is the cooling load for time interval k under control 2
- $Q_{w,k}$ is the weighted-average cooling load for time k

And the zone temperature trajectory that minimises the zone load is given as:

$$T_{z,w,k} = w^*T_{z,1,k} + (1-w^*)T_{z,2,k} \text{ for } 0 < t \leq t_{dl} \text{ ----- (Eq-8)}$$

where:

$T_{z,1,k}$ is the zone setpoint temperature for time interval k with control 1

$T_{z,2,k}$ is the zone setpoint temperature for time interval k with control 2

$T_{z,w,k}$ is the optimally weighted average zone set point temperature at time k

w^* is the optimal weighting factor obtained by minimising the cost function in equation (x above)

3.4 Thermal Comfort models

There are two main categories when it comes to thermal comfort criteria in a built environment: these are standard models such as Fanger's model and adaptive thermal models such as the prescribed method by ASHRAE-55 (Sourbron, M, 2012). In the standard model, where buildings are expected to be kept within a fixed temperature limits, a heat balance between the human body and its surrounds is calculated and parameters such as Predicted

Mean Vote (PVM) and Percentage of People Dissatisfied (PPD) are used to assess the thermal comfort.

Where as in the adaptive thermal comfort model, it is assumed that the occupants of the building will attempt to adopt their behaviours to achieve comfortable state. In fact, when occupants' expectation toward thermal comfort are not narrowly specified, they tend to tolerate temperature swings. The implication of this is that, for instance, cooling cost could be reduced by adjusting the zone set point slightly higher than that of normally done. (Barton, 2012, Sourbron,2012).

In adaptive comfort model the basic idea is, when indoor climate expectations are less stringent, the occupants will be more tolerant towards a wider range of temperatures (Sourbron, 2012).

3.5 Conclusion

The challenge of the determination of the zone temperature set point optimal trajectories is important because it gives us a bench mark for the maximum cost saving associated with simpler near-optimal control approaches (Braun, 2003).

As shown by previous works, control of the zone temperature trajectory could be used to indirectly control other elements of the building, such as plant energy consumption as well as directly playing a significant role in peak demand reduction. The effectiveness or lack of it, of peak cost reduction of a particular strategy is dependent on number of variables that are in play in the building environment, however optimisation of all of the variables at the same time is time and resource intensive.

It seems the challenge lies on deciding which details can be neglected without jeopardizing the validity of conclusions [Gyalistras, 2010]; i.e. the challenge lies on identifying a couple or more of the key or supervisory variables for the optimisation use.

4 Model Development and Validation

4.1 Model development

As discussed in chapter 2, different people attempted to model hollow core slabs using different approaches ranging from Capacity Transfer Model (CTM) to numerical analysis involving a Finite Difference Method (FDM).

Ren, 1997 used the work of Winwood, et al, 1994, which was based on CFD software, as inspiration and developed a lumped parameter model (figure-23) of the hollow core slab. For the purpose of this thesis, Winwood's modelling approach will be used for representation of the geometry of the hollow core slab and Ren's modelling approach will be the basis for thermal modelling.

4.1.1 Previous Modelling detail of Hollow core slab, by Ren, 1997 and Winwood, et al, 1994

A typical concrete slab will have five cores but only three are generally used for ventilation. This as well as the air path taken inside the slab makes the determination of the effective thermal capacitance of the slab a very challenging job (Ren, 1997). For modelling purposes, the slab thermal capacitance is best determined first by simplifying the representation of the air path, followed by determination of the width and length of the slab that produces the same thermal response as a commercial slab, based on measured performance data (Winwood, et al, 1994).

Although, it was believed that the temperature of the slab core is assumed to remain constant along the path of the air flow, due to temperature differences from one zone to another (for instance the zone above and below) the mass temperature is not evenly distributed about the centre of of the slab (Ren, 1997 citing Augenbroe & Vedder, 1985).

In order to account for this effect, Ren, 1997, in his lumped parameter model (figure-23), divided the slab into two halves, with one half coupled to the zone or environment above and the other half coupled to the zone or environment below. In other words, the modelled hollow core is simplified into two flat plates containing the effective thermal capacity of the slab but cut in the middle with a thickness, δ . Given The effective storage area, A , of the slab, the

model effective thickness of the slab above and below the slab air gap is given by $\delta = \frac{A}{Z}$ (figure-24). This modelling approach ensures that the zones below & above the slab see a flat plate of cross-sectional area equalling the real slab's effective storage area.

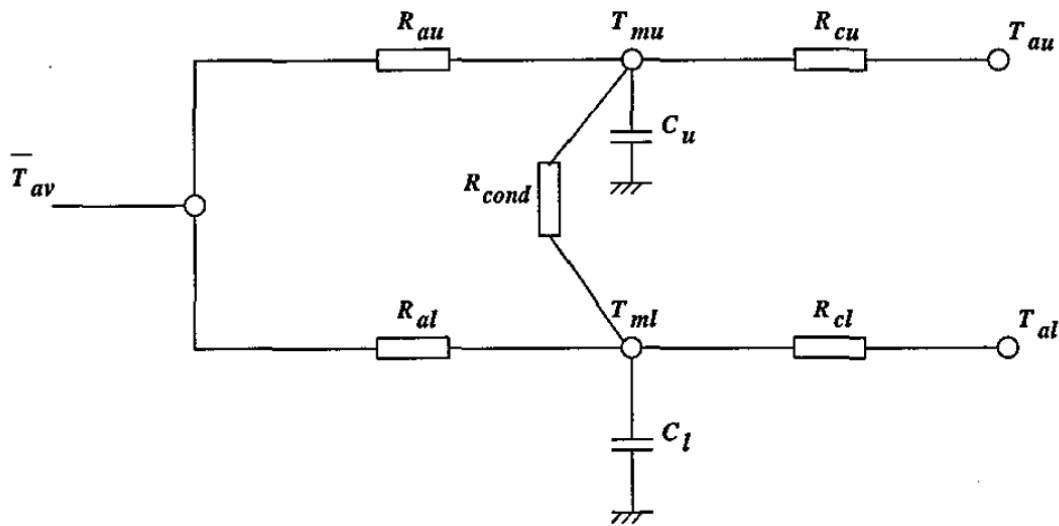


Figure 23: Ventilated hollow core slab, R-C model

In the above modelling approached, as done by Ren, 1997, the total air path length in the model was made to be equal to that of the real system, the width of the area relating to the effective thermal capacitance was made to be equal to the span, W , of the hollow core section of the slab as shown in the figure below.

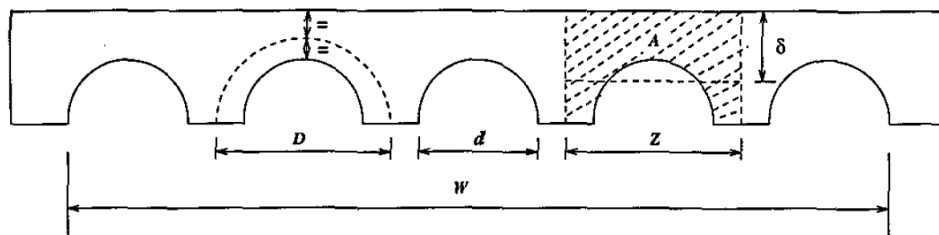


Figure 24: Illustration of the approximation process

In order to calculate thermal resistance of half of the core, the mass node is considered to be located close to a perimeter of a circle, with diameter of D , positioned half way between the edge of the core and the external surface of the slab. Assuming an isothermal cylinder, the thermal resistance R_c was given by:

$$R_c = \frac{\ln(\frac{D}{d})}{\pi k L} \text{----- (Eq-9)}$$

where:

D and d, are as shown in figure x above

K is the thermal conductivity of the concrete slab

L is the total length of the air path in the hollow core slab

From this it is obvious that a hollow core could be modelled as two separate halves of the core and the crucial bit of the modelling is the determination of an equivalent effective surface, as that of the actual core.

4.1.2 Air film resistance calculation

The air film resistance or the heat transfer coefficient, h is a function of the Nusselt number, Nu, thermal conductivity, k_{air} , and the core diameter, d_{core} ;

$$h = \frac{k_{air} Nu}{d_{core}} \text{----- (Eq-10)}$$

The air film resistance of the inside surfaces of air core is a function of both the air flow and the nature (roughness or smoothness) of the surface of the cores. The Nusselt number in turbulent flow is related to the friction factor, f , (to account for the roughness of the core inside surface) using Chilton-Colburn analogy expressed as:

$$Nu = 0.125 f Re Pr^{1/3} \text{----- (Eq-11)}$$

In previous modelling, the heat transfer coefficient for the straight section is calculated from an empirical correlation (Ren, 1997, citing Holman, 1986 & CIBSE, 1986) as formulated by Dittus-Boelter:

$$Nu = 0.023 Re^{0.8} Pr^{0.4} \text{----- (Eq-12)}$$

where:

Nu is the Nusselt number

Re is the Reynolds number

Pr is the Prandtl number

However, because this equation is valid for smooth tube and a large temperature difference across the air, this equation is prone to large percentages of error, as high as 25% (Cengle, 2004). To reduce this error and take the surface roughness of the concrete core into account a more complex equation, by Gnielinski is considered as an alternative. The equation takes into account the friction factor, f , which can be worked out from Colebrook equation.

$$Nu = \frac{\left(\frac{f}{8}\right)(Re-1000)Pr}{1+12.7\left(\frac{f}{8}\right)^{1/2}\left(\frac{1}{Pr}-1\right)^{2/3}} \text{----- (Eq-13)}$$

where:

Nu is the Nusselt number

f is the friction factor

Re is the Reynolds number

Pr is the Prandtl number

The friction factor in fully developed turbulent flow depends on Reynolds number and the relative roughness ε/D (Cengle, 2004). The Colebrook equation, relates the friction factor with Reynolds number for turbulent flow via the equation:

$$\frac{1}{\sqrt{f}} = -2.0 \log\left(\frac{\varepsilon}{3.7D} + \frac{2.51}{Re\sqrt{f}}\right) \text{----- (Eq-14)}$$

where:

f is the friction factor

ε is the surface roughness

D is the hydraulic diameter

Re is the Reynolds number

Previous work by Winwood, et al, 1994; & Willis and Wilkins, 1993, asserts that the heat transfer around the bends of the hollow core is by far higher than the straight section, due to turbulence and hence due to the increased convective heat transfer coefficient. Therefore, a

Correction factor (x20) based on commercially available slab and air temperature measurements, was used to account for the bend heat transfer coefficient.

Based on experimental data from Winwood & Benstead, 1994; the impact of the bend and the enhanced heat transfer coefficient on the core air and core surface temperature was investigated.

4.1.3 Modelling of the hollow core slab in Virtual Environment, the VE™

The model used in IESVE is shown in figure-25, which approximates the actual slab (see figure-26).

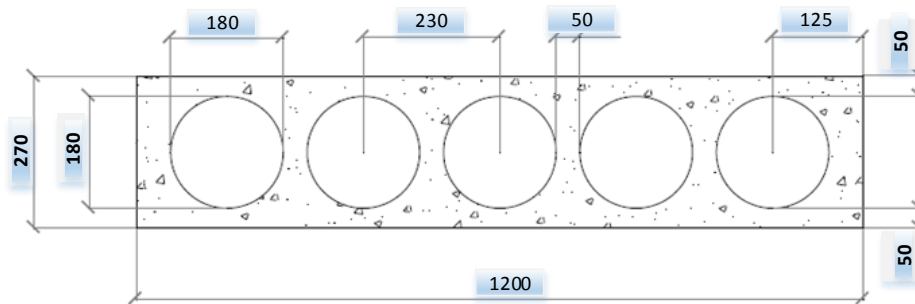


Figure 25.0: Actual Dimensions (mm) of hollow core slab modelled in VE

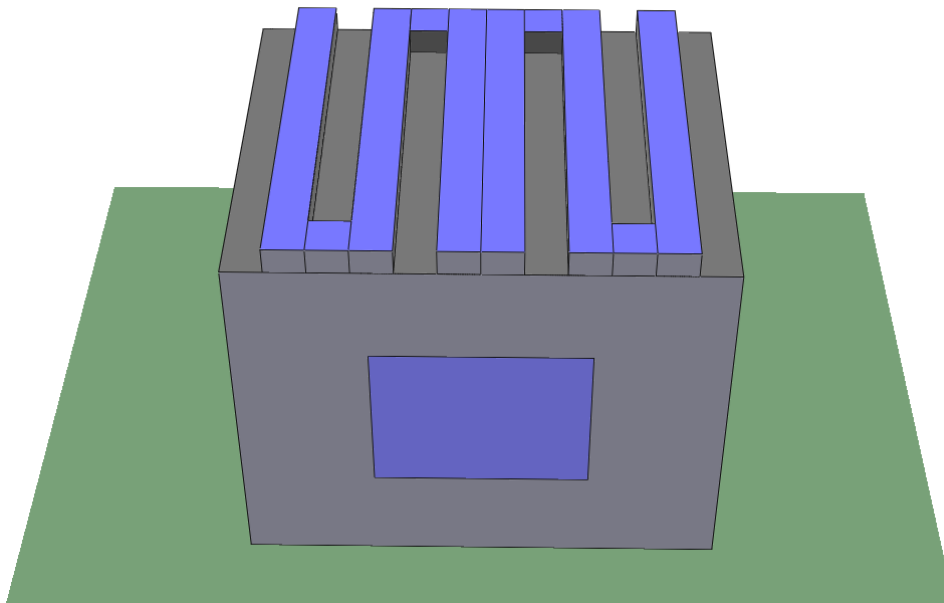


Figure 26: Cross-section of the VE model showing the hollow core slab

The following calculations were made to achieve equivalence:

$$\text{Cross sectional area of concrete} = (1.2 \times 0.270) - (5 \times \pi \times 0.09^2) = 0.197 \text{ m}^2$$

Splitting this between two plates there is 0.098m^2 of concrete in contact with the room above and 0.098m^2 in contact with the room below. Splitting this between the 5 cores there is 0.0196m^2 in contact with each core.

The internal surface area of the hollow core slab is used to determine the width and depth of concrete for each core:

$$\text{Circumference} = \pi d = 3.142 \times 0.180 = 0.5654 \text{ m}$$

Therefore 0.28m is in contact with the room above and 0.28m in contact with the room below.

$$\text{Depth} = 0.0196 / 0.28 = 0.07\text{m}$$

To keep the cross sectional area of the air path through the slab the same the depth of the air void is determined by:

$$\text{Cross section of 1 core} = \pi \times 0.09252 = 0.02688\text{m}^2$$

The depth of the air void between the parallel plates is therefore:

$$\text{Depth of air void} = 0.02688 / 0.28 = 0.097\text{m}$$

4.1.4 Bend Geometry

In order to work out the bend geometry, first it was required to determine separation of the cores, while preserving the volume of concrete between the cores. Using the equivalence shown in the figure below, core separation comes to about 9.7 cm. Based on assertion by Winwood, et al, 1994, the cross sectional area of the bend is only 60% of the total air path, however this seems to be a large figure and it is not specified how this number is calculated based on the dimensions (see figure-27). Barton et al, 2002, did a theoretical study of a

hollow core on the basis of Winwood’s model and took the equivalent bend length at the same core diameter to be 415mm. This number is used in this work.

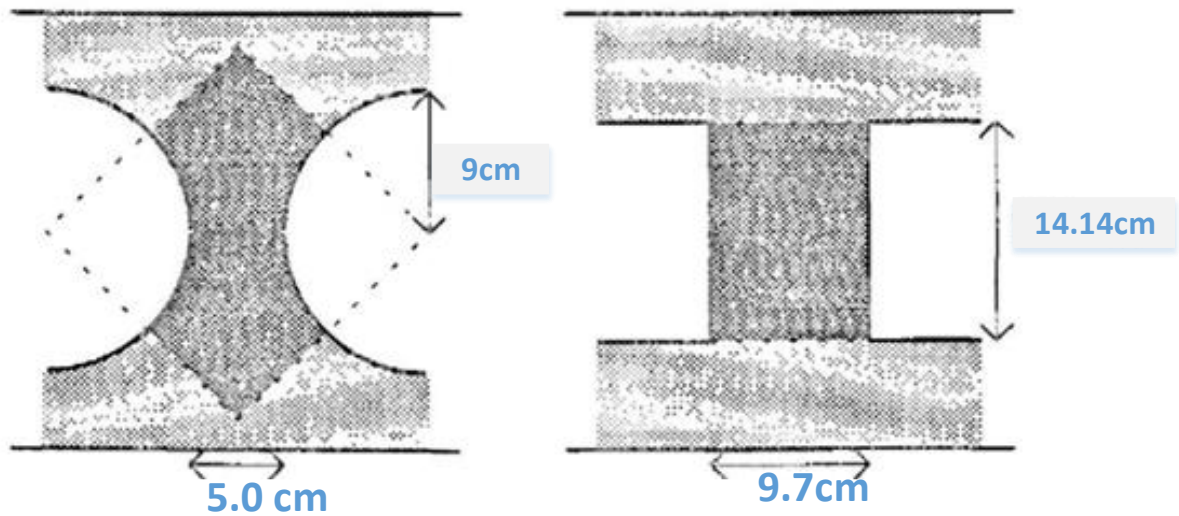


Figure 27: Bend Geometry

4.1.5 Model Parameters

The model has the parameters shown in table-3 and table-4.

	Thickness (mm)	Conductivity (W/m.k)	Density (kg/m ³)	Specific Heat Capacity (J/kg.K)	Resistance m ² .K/W
Top of Hollow Core Slab					
Insulation	60	0.0300	40	1450	100
Membrane	1.0	1.0	1100	1000	0.0001
Hollow Core	80.4	1.8591	2432	985.1	0.0432
Bottom of Hollow Core Slab					
Hollow Core	80.4	1.8591	2432	985.1	0.0432

Table 3: Model parameters

<u>Hollow Core Section</u>		<u>Surface resistance, m²K/W</u>
Upper Section	Outside	0.0400

	Inside*	0.0301
Lower Section	Outside*	0.0301
	Inside	0.1000

Table 4: Model inner and outer surfaces

<u>Room condition description</u>	<u>Value</u>	<u>Schedule</u>
<i>Lighting gain</i>	<i>0.15 kW</i>	<i>09:00 – 17:00</i>
<i>Peoples gain</i>	<i>0.18 kW</i>	<i>3 people, 09:00 – 17:00</i>
<i>Equipment gain</i>	<i>0.22 kW</i>	<i>09:00 – 17:00</i>

Table 5: Room Conditions (these make the hollow core inside and hence will be in contact with the forced air with properties of: density of 1.2 kg/m³, specific heat capacity of 1008 J/Kg.K, laminar viscosity of 1.58 x 10⁻⁵ m² S⁻¹ and thermal conductivity of 0.0255W/mK)

4.2 Model Validation

The model above is validated by comparing qualitatively with experimental and simulated data from Winwood, et al, 1994. The experimental data, suggests the test room has boundary conditions of 18⁰C at the top and 22⁰C at the bottom respectively. Apart from this information, there is no indication of whether the test room is exposed to outside elements or if it is a laboratory room at standard temperature and pressure.

Nevertheless, to re-create the experimental environment, a room with dimensions of 4m by 4.8m floor area and 3.5m high, and window to surface ratio of 9.3%, was created in VE ModelIT in the middle floor of a three story building. This allows the right boundary conditions to be put in place. The room above the test room is kept at constant 18⁰C, as well as the rooms on the right and left. The room below the test room is kept at constant 22⁰C. The hollow core sits as a ceiling at the top of the test room.

In the setup used by Winwood et al, 1994, there are 4 hollow core slabs used as the ceiling; but only two of them were thermally activated. Moreover, although the slabs each have 5 cores each, only 3 cores each (of the two which are thermally active) were thermally active.

Based on this information a HVAC network was assembled as shown in the figure-28 below and the thermal labyrinth (4) was put together in ApHVAC. A flow of 4 ACH was considered and hence the total air volume delivered to the room amounts to approximately 80 l/s and each slab will have 40 l/s of air delivering to the zone via the flow controller (3), which is set to deliver this.

With the HVAC network assembled, in order to perform validation, the input experimental data inlet air temperature from Winwood et al, 1994’s experiment was used as an input into the hollow core assembly, via the heating coil (#1) and temperature controller (#3) profile as shown in the figure-28 below.

The simulation with the setup above produced a very close air temperature through the different points in the the thermal labyrinth which compares very close to the experimental air temperatures measures at the same points. Figure-29 below shows the result of the injection of of the experimental air inlet temperatures and the response of the hollow core assembly.

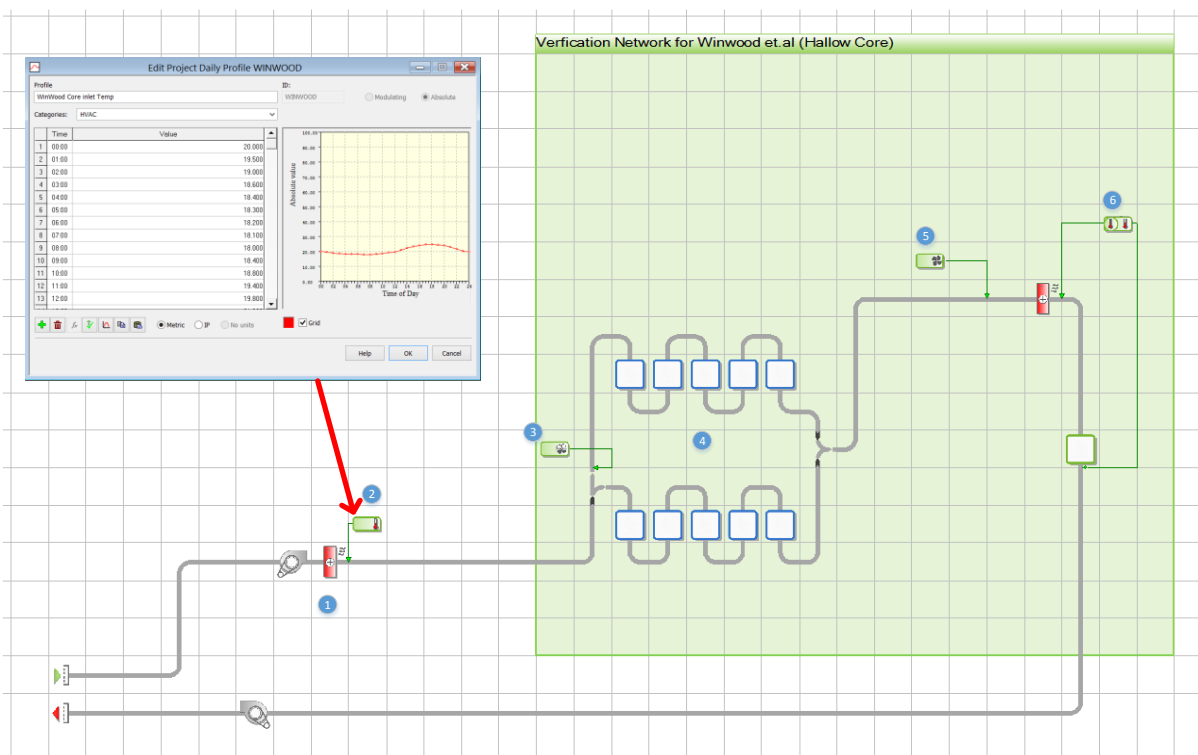


Figure 28: Model validation HVAC network assembly

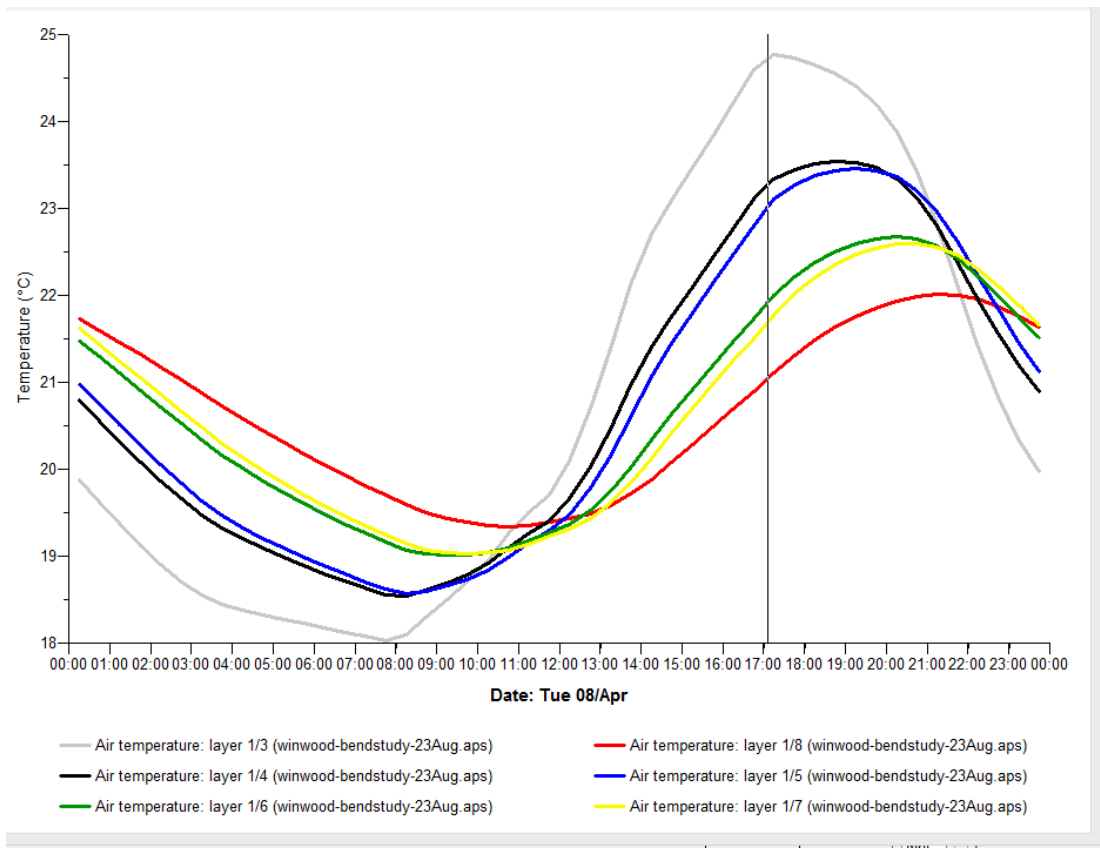


Figure 29: Air temperatures results of the model simulation

4.2.1 Step Input Test

As part of the validation, a step input test was conducted based on an experimental set up by Willis and Wilkins (1993); to ascertain the response of a pre-cooled hollow core slab to the introduction of air with a temperature of 40 °C. In the original experiment, a temperature difference of about 15-16 °C was recorded between the inlet and outlet of a three core slab. The IESVE model developed produced a similar response as shown below (figure-30) and from qualitative analysis, it can be concluded that the model developed in this thesis is valid and can be used to model hollow core slab with acceptable accuracy.

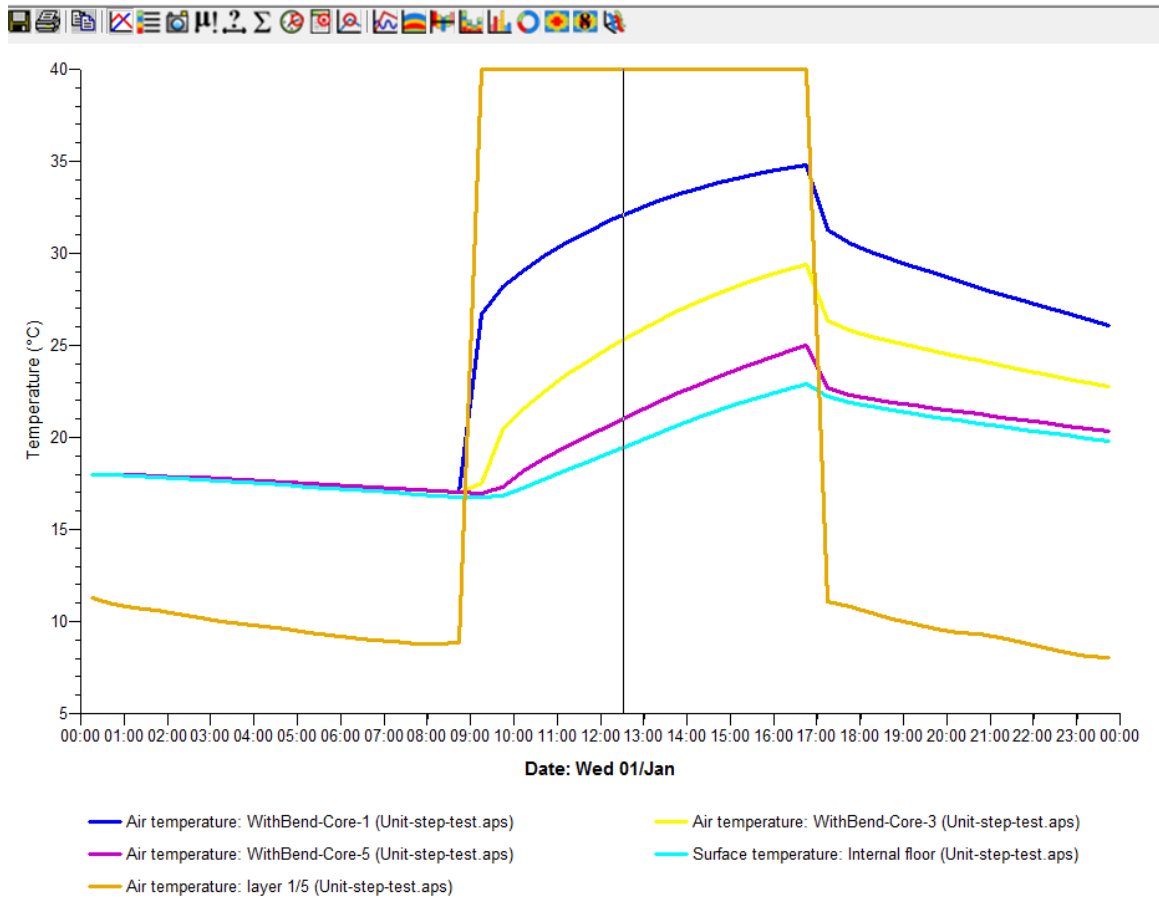


Figure 30: Unit step test based on Willis and Wilkins (1993)

4.3 Refinement of the model

4.3.1 The use of THERMTM to determine effective conductivity

The THERM tool by the LBNL enables steady state two dimensional (2D) thermal analysis on structures of buildings, primarily to analyse thermal bridging on windows and building frames. As conduction plays a major role in the capability of the hollow core for storing heat, the right determination of the effective thermal conductivity is important.

The heat transfer in a hollow core is 2D, but most whole building thermal modelling tools treat the problem as one dimensional and through this underestimate its capacity. However, in this work it is believed that, by identifying the effective thermal conductivity that takes into consideration the 2D nature of the heat transfer process in the slab, one can increase the accuracy of the modelling.

For this reason, the conduction heat transfer in the slab has been modelled in THERM. The boundary conditions and the dimensions of the model are shown below in the figure-31 and table-6. Also in figure-31, an electrical analogy of the thermal resistance is given. The sides of the slab are considered to be adiabatic, whereas all other surfaces can exchange heat to the air by convection.

<u>Boundary Condition</u>	<u>T, °C</u>	<u>h, W/m²K</u>	<u>Remark</u>
Core air film	40	18	Calculated for 40 l/s air flow
Lower outer surface of slab (in contact with room air)	22	9	From ASHRAE fundamentals
Adiabatic	0	0	Default values from the THERM™
<u>Material</u>	<u>k, W/m.K</u>	<u>Emissivity</u>	
Concrete	1.4	0.92	Concrete hollow core

Table 6: Boundary conditions of the THERM modelling

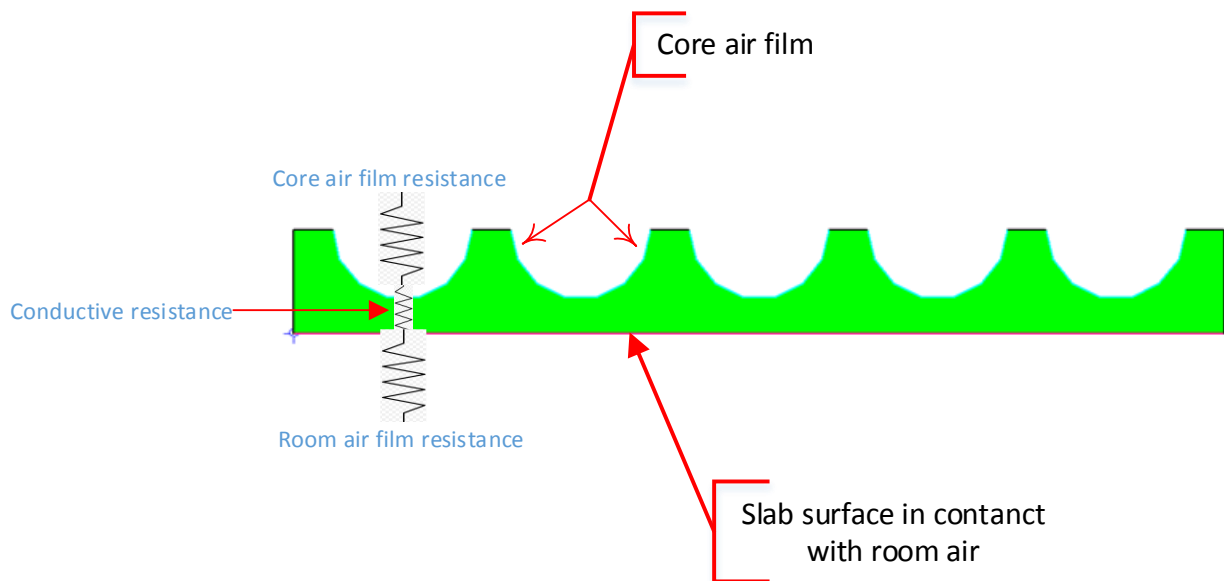


Figure 31: Illustration of the THERM modelling

The result of this modelling is as shown in figure-32. By subtracting the air film resistances (in the core as well as the room side) from the Overall resistance ($1/U$), an effective conductivity of 1.9W/mK is obtained which basically suggests, there is more heat being stored or lost from the concrete than normally thought with default conductivity of 1.4W/mK .

Therefore in the VE model, an adjustment has been made to the conductivity and the results show a closer match to the validation data set.

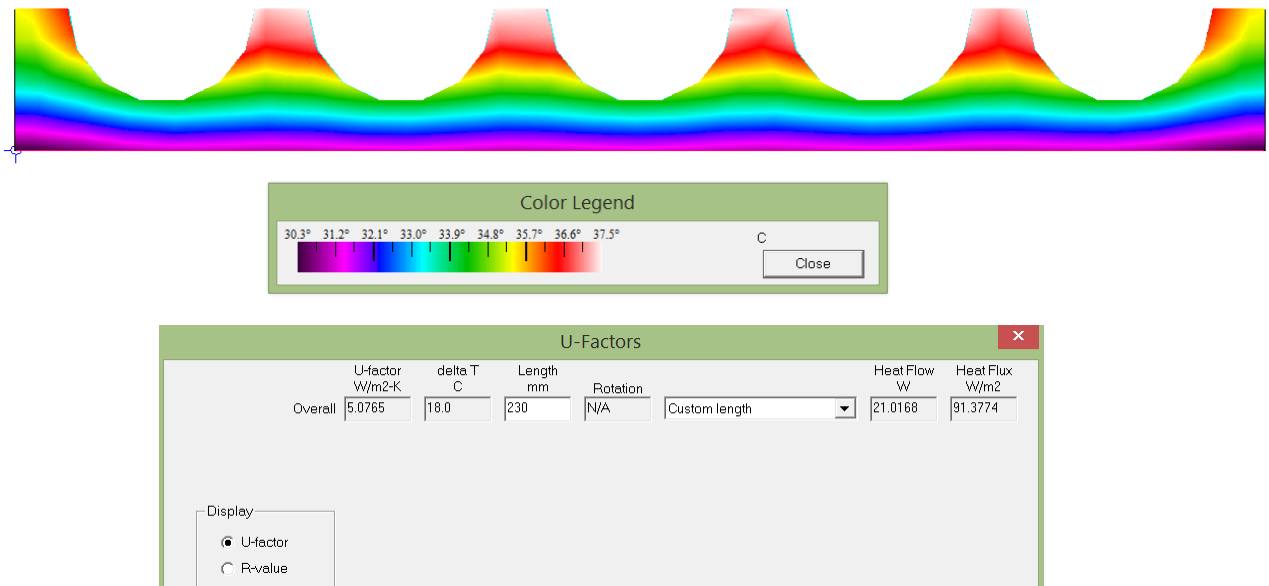


Figure 32: Results showing the THERM modelling

4.3.2 Bend Study

There have been different claims regarding the contribution of the bend element to the overall heat transfer in the hollow core, ranging from an increased heat transfer coefficient in the range of 2 to 50 times compared to the straight section, as discussed in in chapter 2.

Simulation runs have been done with heat transfer coefficients of the straight section adjusted to 2, 10, 20, 30, 40 and 50 times that of the straight section in order to investigate enhanced heat transfer at the bends.

Table 7: Heat transfer coefficient multiples

Multiplication factor, X	Resistance, $\frac{1}{h}$ (m.K/W)	Remark
1	0.0155	<i>This is the straight section resistance adjusted for bend length</i>
2	0.00775	
10	0.00155	

20	0.000775	
30	0.000520	
40	0.000390	
50	0.00031	

Distance along the core length (m)	Heat flux to the concrete , kW			
	x2	x10	x20	x50
4	0.2164	0.216	0.2164	0.2164
4.42	0.0214	0.0207	0.0204	0.0188
8.42	0.1482	0.1488	0.1489	0.1489
8.84	0.0147	0.0139	0.0135	0.0123
12.84	0.0853	0.0857	0.0855	0.0855

Table 8: Heat flux along the length of the path of the core air

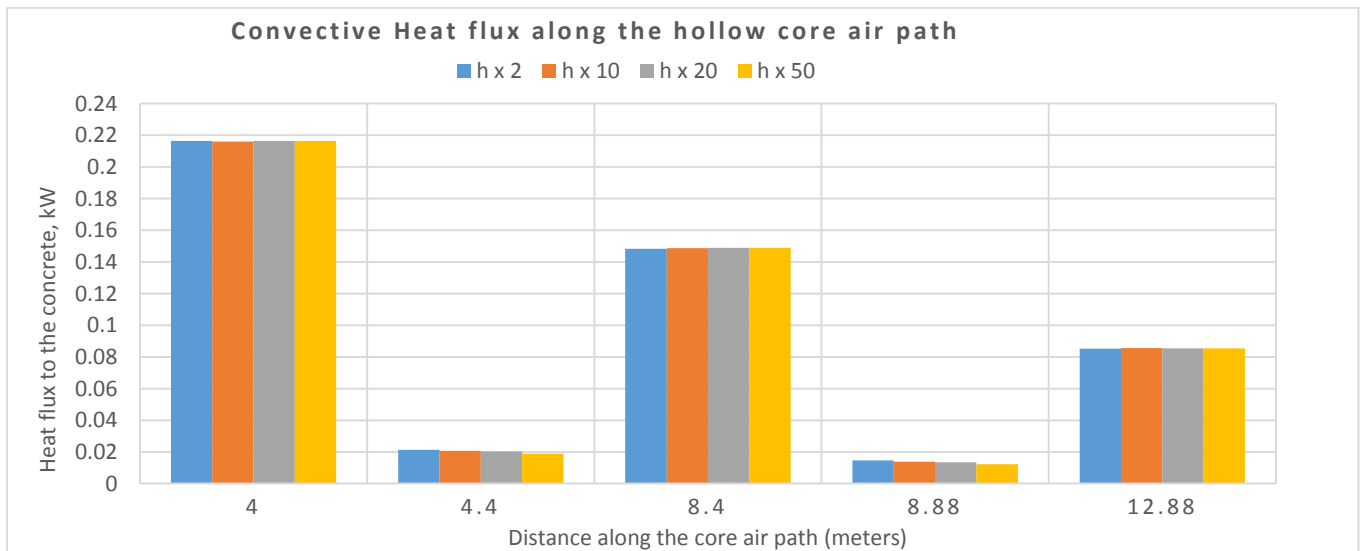


Figure 33: Bend and straight section heat transfer comparison (the bends are located at 4.4 m and 8.88 m)

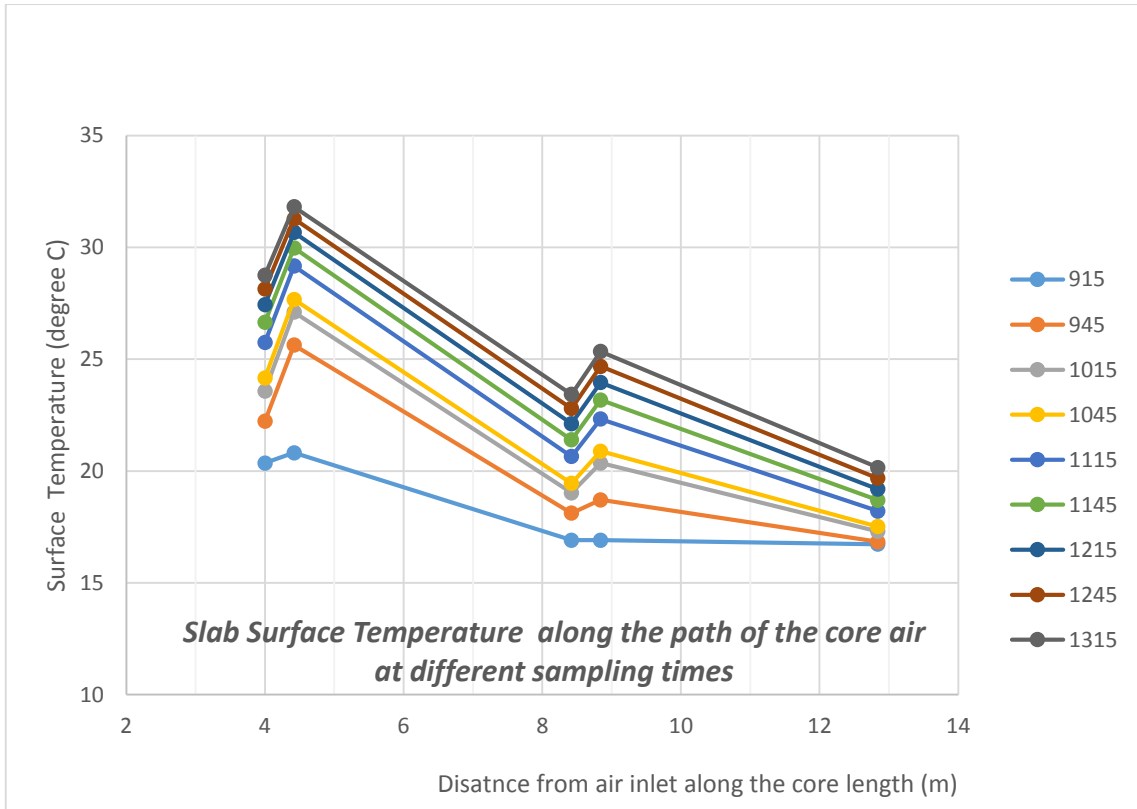


Figure 34: Temperatures profiles along the core path (at the bends, 4.4 and 8.8 m the increase in slab surface temperature is pronounced)

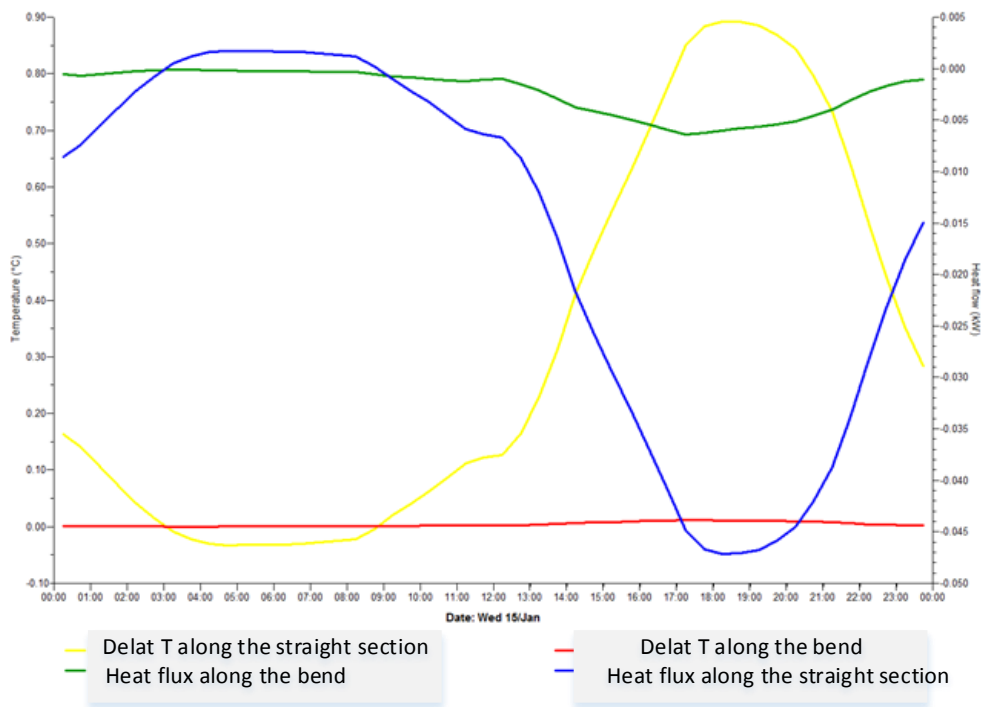


Figure 35: Bend and straight section heat flux and delta T between zone surface and room temperature (the heat flux axis is

The results shown in figure 33, 34 and 35 show that there is negligible impact on heat flux caused by enhanced bend heat transfer. This was also reported by Barton et al, 2012.

The reason being, the slab surface temperature at the bends increases “at the surface” more than the straight section (see figure-35) due to increased turbulence which brings the temperature difference between the core air and surface section right down, thereby preventing further heat transfer.

4.3.3 Number of core utilisation

The impact of core utilisation on the core air was studied for a 3-pass simulation vis-à-vis 6-pass simulation. As shown below in figure-36, the number of cores used have a large impact on time lag and decrement factor. The more cores used the greater the lag and decrement factor. Figure-34 shows air temperatures (blue & red lines) after passing through 3 cores and 6 cores respectively. The result also agrees with what Barton et al, 2012.

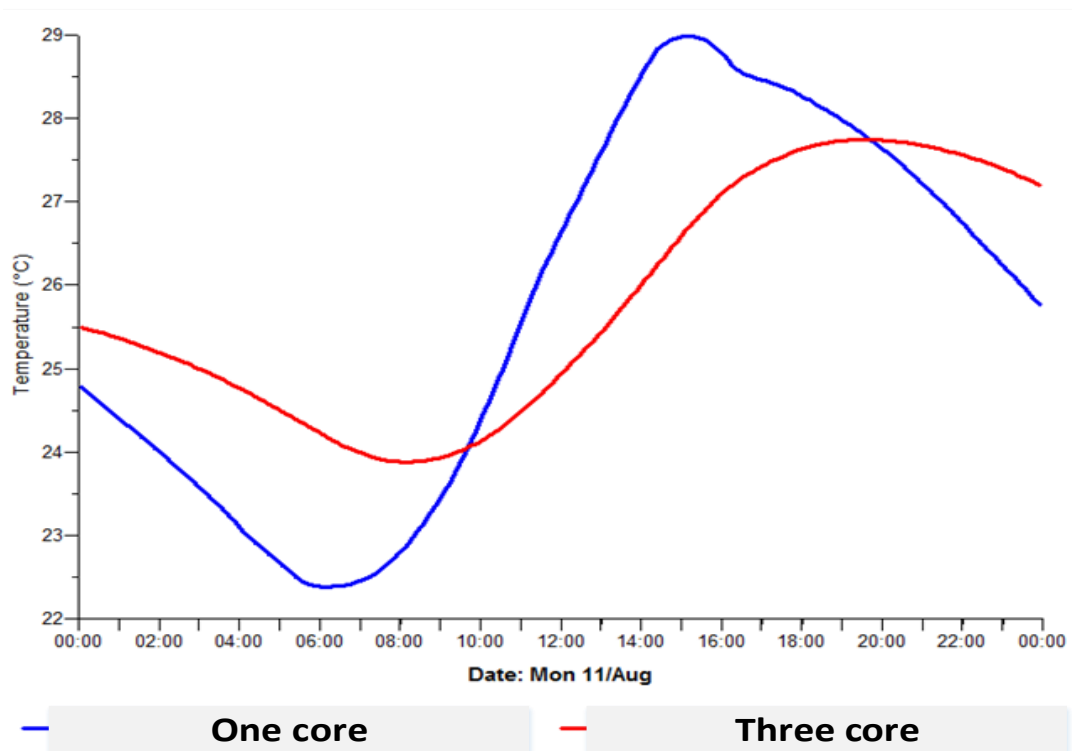


Figure 36: Comparison of 3 core vis-a-vis 6 core pass

4.3.4 Conclusion

A model of a hollow core ventilated slab have been developed and validated. The validation process involved the use of boundary conditions as used by the test environment and experimental test data used by previous researchers. The model developed here is accurate to 1.5 °C, when qualitatively compared to the measured date used by the previous researchers.

The use of THERM tool to calculate effective conductivity provided improvement on the simulated data and on closer look, the value of 1.9 W/m.K gotten out of the THERM simulation agrees exactly with what Winwood et al, 1994 recoded as experimentally achieved conductivity value. The conclusion reached here is that, if used carefully, the THERM tool could be a valuable addition to whole building simulation tool.

The findings on the bend study and core utilisation agrees with the conclusion reached by Barton e al, 2012. The bend has no exaggerated effect on heat transfer inside the core. The simulation result shows that, although the slab surface temperature increases in the bend dramatically, with assumed increased levels of heat transfer coefficient, the overall heat transfer (heat flux from the air to slab) from or to the slab is less, as the ΔT between the air and the slab diminishes (see figure 35), as the surface of the slab equilibrates with air temperature. On the other hand this behaviour could not be observed in the straight section of the core.

And finally, the use of 3 cores as supposed to 6 cores, shows dramatic effect of the number of cores utilisation on the time g (see figure 36) which is in agreement with previous work.

5 Case Study-I Conventional Control Strategies

5.1 Introduction

This chapter refers to consequences of using different conventional HVAC control strategies with model explained in chapter-4. This will facilitate the identification of the control (supervisory) variables and the model for use in Model Predictive Control. The system performance under various control strategies is examined by simulating the thermal response of the zone (to precooling) as a function of the core air inlet temperature, the ventilation rate, the switch flow and the zone's temperature set point trajectories.

A focus on the cooling of the building is made as it is tightly coupled to electricity use and hence is very sensitive to the Time Of Use (TOU) cost. Furthermore, the problem of controlling thermal mass for heating is relatively straight forward, it can effectively be reduced down to an optimal start problem (Braun, 2006 & Armstrong et al, 2006) and heating does not primarily depend on electricity.

The conventional control strategies to be investigated here will be Constant Air Volume (CAV) precooling (with additional free cooling where applicable), delayed start CAV precooling, heat recovery, recirculation, peak demand limiting and peak load shifting.

5.2 Conventional Control Strategy

In order to confirm the conventional strategies yield expected outcomes the following HVAC network shown in figure-37 was assembled and was used to run simulations under various scenarios, table-9. The scenarios were selected based on previous work by Ren, 1997; so that results are compared. The first five strategies in the first five cases are intended to investigate the system response to differing ventilation rate and ventilation precooling, whereas the last one is concerned with the impact of the switch flow operation. Result of the run are as shown in figure 38.

Scenario ID	Strategy Description	Air flow (ACH)	Room Set point
1	24 hour ventilation	4	23 °C
2	24 hour ventilation, with Coil off at night	4	23 °C
3	Day time only (9:00-17:00) ventilation	4	23 °C
4	Day time (9:00-17:00) ventilation with night (05:00-09:00) precooling	4	23 °C & 19 °C at precooling
5	Variable ventilation Air flow	4 during the day, 6 during precooling	23 °C
6	Switch flow (using one core)	4	23 °C

Table 10: Conventional Strategies parameter (controller dead band used is 2 °C, strategy #2 uses free cooling and no mechanical cooling at night)

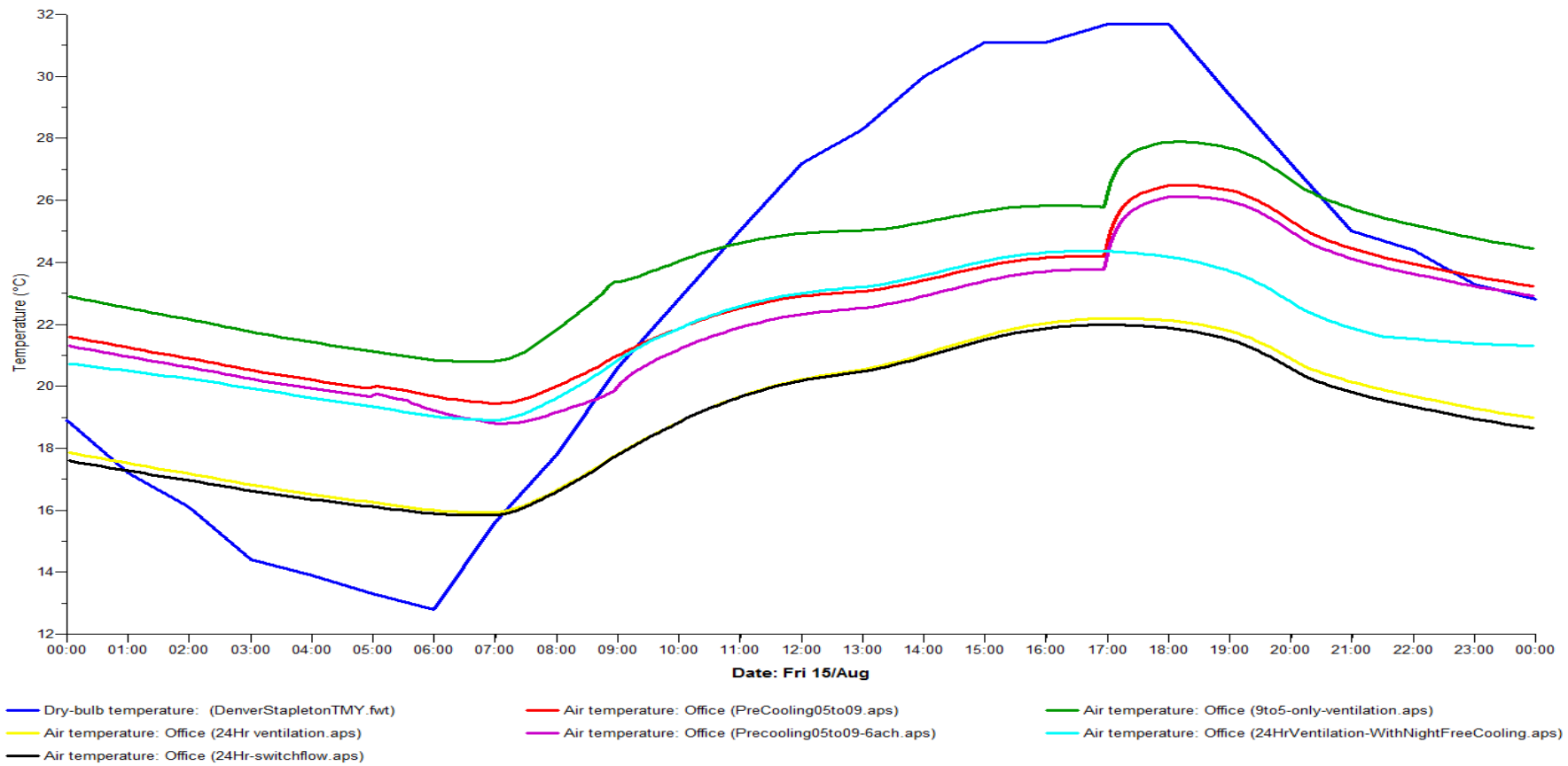


Figure 38: Zone air temperature with different conventional strategies

5.2.1 Discussion of Results

The decrease of the precooling time from the entire night to just between 4 hours (between 05:00 to 09:00) resulted in average room mean radiant temperature during occupancy to rise by 2.47 °C. The higher ventilation rate precooling resulted in reduced radiant mean temperature of the room during occupancy, on average by 0.5 °C than that of lower ventilation rate precooling. Free night cooling and day time only mechanical cooling resulted in increase of the occupied hours' mean radiant temperature on average by 2°C from that of the 24hr ventilation and mechanical cooling.

The switch flow (one core) resulted in slightly lower occupied hours mean radiant temperature than that of the 24hr (3 core) strategy, as well as reaching peak 20 seconds earlier than that of the 24hr strategy. Moreover, switch flow (single core) resulted in lower mean radiant temperature at night than that of 24hr (3 core) ventilation, due to less coupling between the cool ambient air and the mass storage and the lower temperature air being supplied to the room.

In general for those strategies with no mechanical cooling beyond 17:00 till the onset of precooling, the radiant mean temperature increase by 0.95 °C as soon the occupancy period ends.

The night time free cooling resulted in reduction of chiller energy for the day from 0.0472 MWh to 0.0349 MWh, which is a 26% reduction. This is considerable saving considering the mean radiant temperature of the room during the day is still acceptable while the PMV value is only slightly outside the upper comfort range. Generally the room radiant temperature at night with this strategy stayed lower than the early morning precooling strategy's temperature, gradually increasing to match the latter's temperature as soon as the morning sun warms the ambient air and room gains start to increase at the beginning of occupancy.

5.2.2 Conclusion

The results of the simulation of the conventional strategies matches expectation and is in a general terms comparable with previous work by Ren, 1997. However work by Ren, 1997

does not specify the location of the simulation, whereas in this study, the weather for Denver, Colorado, is used. Therefore, although the impact of the strategies in this study resulted in exactly the same trend in terms of room mean radiant temperature, the specific numbers do not exactly match between the studies.

Free night cooling, taking advantage of cooler night outdoor air of about 13 to 18 °C shows potential for saving energy and its use could be maximised by coupling it with early morning precooling so that its short comings on comfort could be overcome. Moreover, the use of switch flow during the day could be exploited so that reduced coupling of the cooling air and the thermal mass is used as an advantage to bring the room conditions to comfortable state quicker.

5.3 Conventional Control Strategies with Recirculation & Heat Recovery

Real HVAC networks include heat recovery, night time free cooling (when possible) & recirculation of return air (possibly fully during the night and partially during the day) in order to economise energy.

These mechanisms were implemented in the HVAC network as shown by figure-39 and a description of the network is given in table-11. Although the overall structure of the network does not change, its low level controllers will be configured from time to time to suit the particular study being conducted.

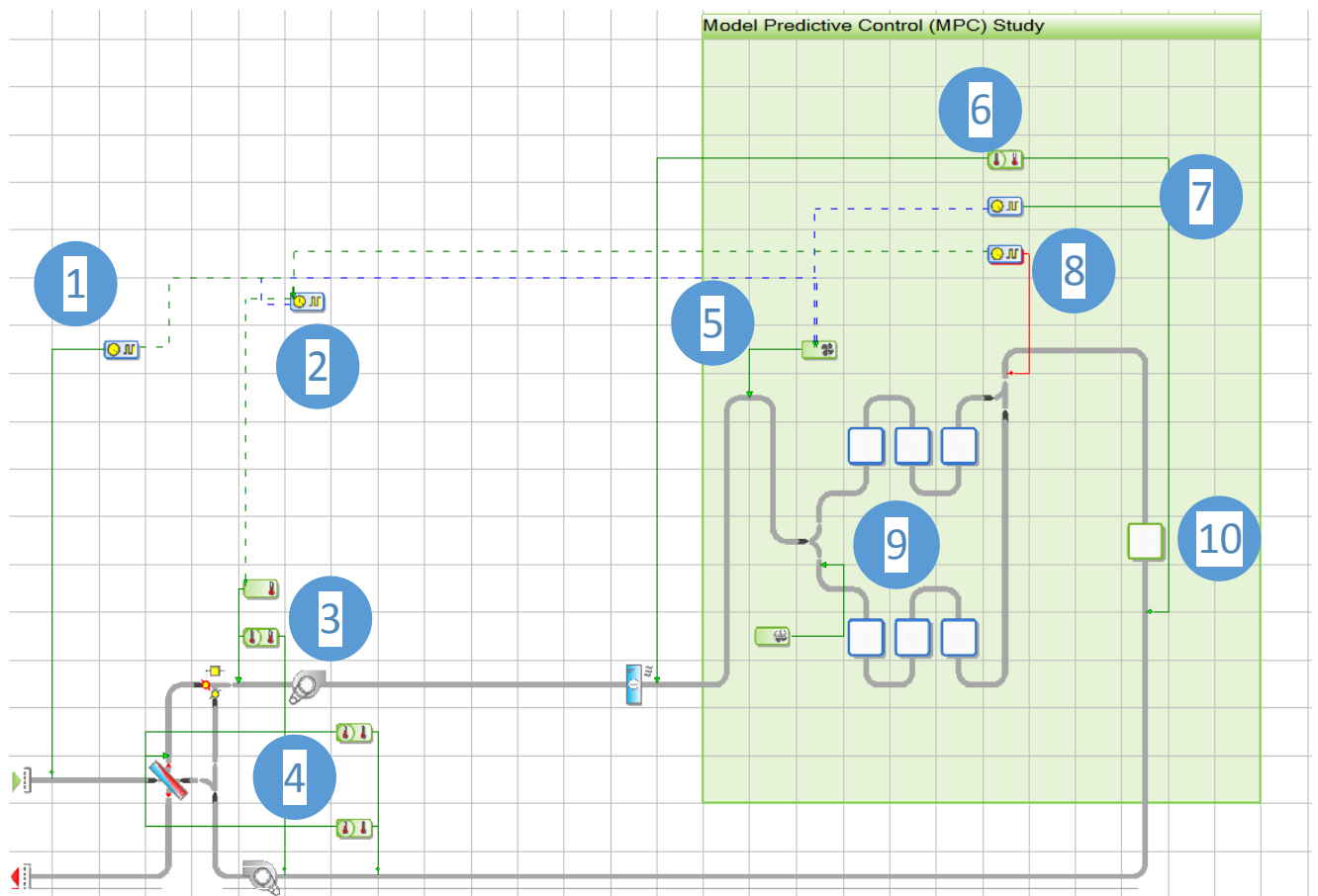


Figure 39: The HVAC network used (air flows clockwise from the green inlet arrow)

The companion HVAC network for this table is given in figure-39.

Network description table:

<u>Identifier</u> <u>Number on the</u> <u>image</u>	<u>Description</u>
1	Night free cooling controller
2	Free cooling and air recirculation supervisory controller
3	Mixing damper controller via target temperature
4	Recirculation controller via target temperature
5	Air flow controller
6	Coil Leaving Air Controller through the zone temperature set point
7	Air flow controller through the zone temperature set point
8	Slab temperature controller
9	Hollow core labyrinth
10	Served zone

Table 11: HVAC network description table

Low Level Control Logic description table

<u>Controlled Parameter</u>	<u>Control Logic</u>	<u>Working</u> <u>Schedule</u>
Outside free ventilation Controller	ACTIVE when Slab Surface T > 18 degree C Outside air T < Zone T Outside air T > 8 degree C	Night time 23:00 – 06:00
HR controller	ACTIVE when Zone air T > 23 degree C Target air T = 15 degrees	On Continuously
Recirculation Controller	ACTIVE when Return T > 23 Target T = 15 degrees	Mon – Fri 09:00 – 17:00
Mixing Damper	32 l/s fresh air during occupancy	Mon – Fri

		09:00 – 17:00
Surface Temperature Controller	ACTIVE when Slab Surface T > 18 degree C	
Air Flow Controller	ACTIVE when Zone setpoint is reached or Night ventilation is required	On Continuously

Table 12: Low level control logic description

5.4 Parameterisation of the Conventional Control Strategies

The impact of the different control strategies on energy cost and comfort can be characterised by the following parameters (see table 13 below): the precooling start and end time, the precooling temperature set point, the proximity of the precooling time to the occupancy (lag or lead), the set point trajectory during occupied hours, and the core air temperature. A subset of these will be identified as the key supervisory variable(s) that will be used as drivers for the MPC system.

<u>Variable Name</u>	<u>Range</u>	<u>Resolution</u>
Precooling start time	00:00 to 12:00	30 minutes
Precooling temperature	18 °C to 20 °C	1 °C
Slab entering core air temperature	8 °C to 12 °C	1 °C
Slab core air flow rate	40 l/s to 90 l/s	10 l/s
Demand limiting start times	12:00 to 15:00	1 hour

Table 13: Problem variables, range and resolution for parametric study

Because a full Monte Carlo sensitivity study of these parameters is beyond the scope of this study, batch runs were performed within a specific range of values for each of the parameters. The batch runs, however, were not performed by hand and were instead initiated using the IES Optimise tool, which, through the use of a Lua script, allowed the parameter space to be defined over a user-specified range and resolution. To cut down on the number of runs, for

each parameter under study, specific choices of the other parameters were made with only the set point trajectory being left as a full open parameter. The results of these runs are shown in figures 47-58, together with a description of the specific parameter choices for those results.

5.4.1 A Brief Introduction to the Optimise™ Tool

IES Optimise is a software tool for building designers to calculate optimised design solutions that aid design decision making. This is coupled with IESVE and its optimisation algorithms have been designed specifically for use with a dynamic building design process (Loughborough University) (see [IESVE](#) for more information).

Optimise has an integrated scripting engine (Lua) that enables defining batch simulation runs and allow post processing the results. It has Genetic Algorithm embedded in it for complex optimisation problems.

5.4.2 Time of Use Cost Structure

In order to parametrise the cost of energy use at different times, a ‘Time Of Use’ TOU cost structure has been devised and the costing schedule is as shown below:

Time	Energy Cost (pence per unit)	Demand Cost (pence per unit)
00:00 to 12:00	0.01	0.5
12:00 to 17:00	0.40	2
17:00 to 24:00	0.01	0.5

Figure 40: Time of Use Energy Cost

5.4.3 Zone Temperature Set Point Trajectory and Demand Limiting

The conventional zone control set point trajectory takes the form of ‘Night Setback’, where temperature is kept at the lowest part of the comfort range during occupancy and is allowed to float freely outside occupancy periods. An improvement to this, is to introduce a

precooling period in the early morning hours before the onset of occupancy. However, a better zone set point trajectory could follow a linear or exponential path.

In order to study the impact of zone trajectories on energy and comfort various set point profiles has been assembled (see figure-41 and 42). In total there are 7 paths a profile could follow during the demand limiting period. The seven paths are: Linear, Exp_1³, Exp_2, Exp_3, Exp_4, Exp_5, and Zonal Reset.

Linear rise is relatively modest & rises slowly, while Zonal Reset is very aggressive with sharp rise; in between there are exponential paths whose rate of rise is determined by their individual curvature. Zonal Reset brings immediate curtailment of cooling plants & hence comfort could suffer as the result, whereas linear rise is slow and could suffer from rebound of chiller power before the shed period ends.

The demand limiting period is between 12:00 and 17:00. The start time of the demand limiting period is between 12:00 and 15:00 inclusive and the finish times are between 16:00 and 17:00 inclusive. This defines demand limiting periods as 12:00 to 17:00, 12:00 to 16:00, 13:00 to 16:00, 13:00 to 17:00, 14:00 to 16:00, 14:00 to 17:00, 15:00 to 16:00 and 15:00 to 17:00.

During the morning, from 09:00 to 12:00 the room set point is set at the bottom of the comfort limit, 20⁰C, and it assumes the value 22 ⁰C at the bottom of the demand limiting trajectory from 12 till the end of the peak period.

³ Exp is short for “Exponential” and the different numbers represent the curvature values of each polynomial, increasing from 1 to 5 in the direction of the arrow in figure-34

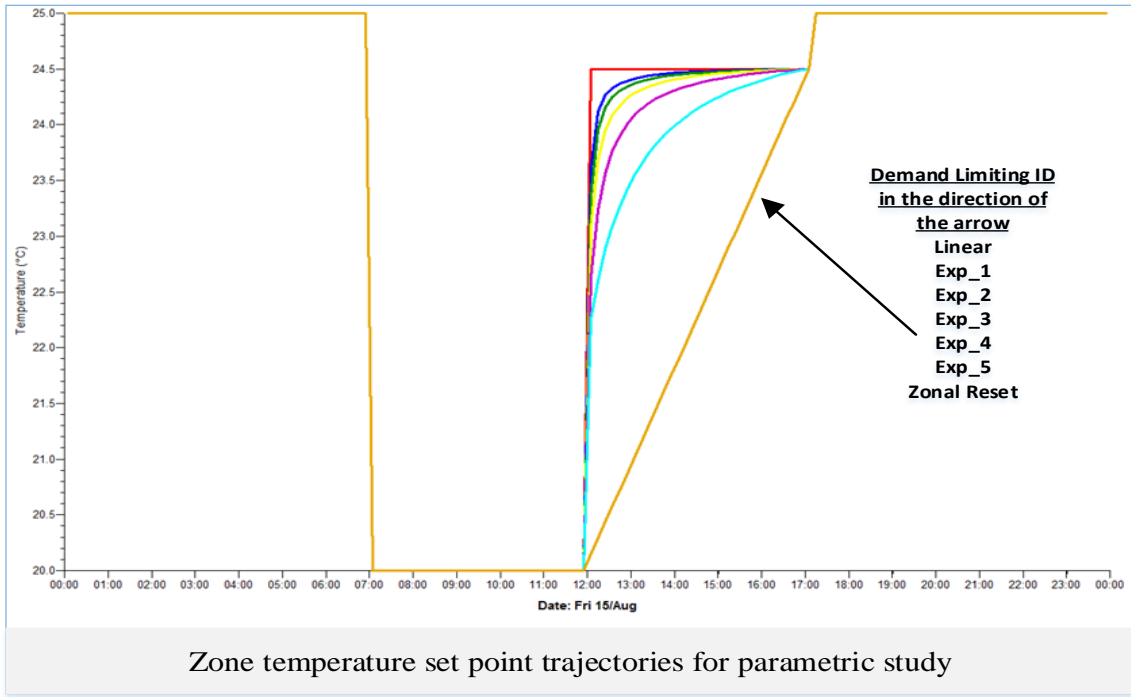


Figure 41: Zone temperature set point trajectory driving profile

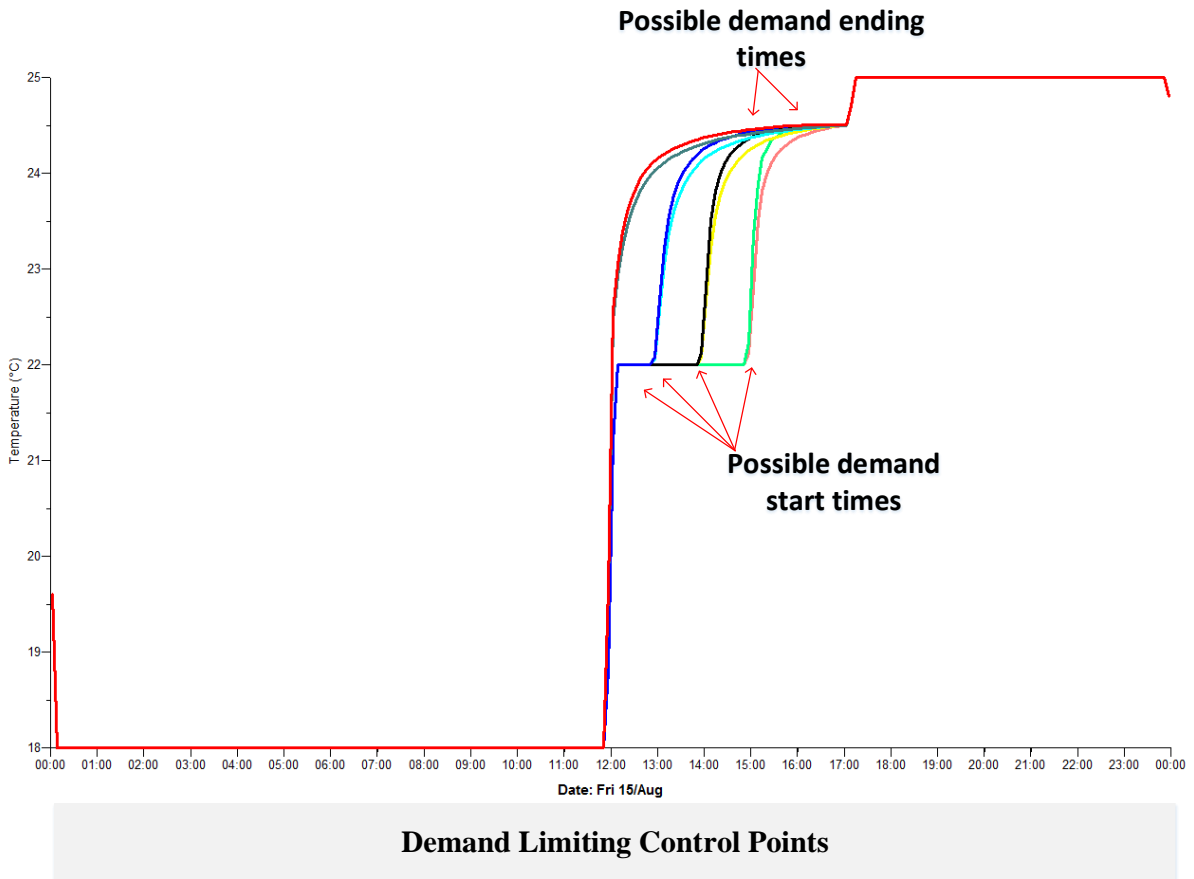


Figure 42: Demand limiting start and end times illustration for polynomial zone temperature set point trajectory as an example (12:00-16:00, 12:00-17:00, 13:00-16:00, 13:00-17:00, 14:00-16:00, 14:00-17:00, 15:00-16:00 & 15:00-17:00)

5.4.4 Precooling start and end times

In buildings where there is a dedicated thermal mass for energy storage, such a hollow core concrete slab, precooling of the slab should be done at night when the electricity tariff is cheap and when relatively cool outdoor air is available. The effect of the duration of the precooling time and its proximity to occupancy start time and the ‘peak-time’ start time is investigated. In order to enumerate the different precooling start times, a profile illustrated below has been put together.

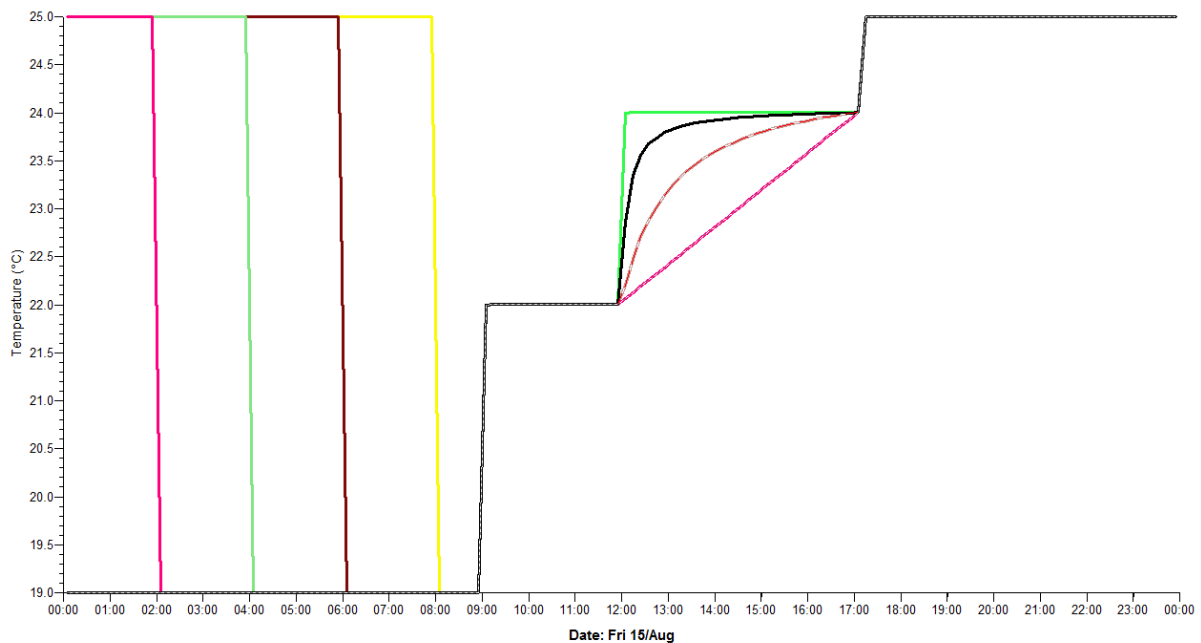


Figure 43: Various precooling start time illustration (the lines at the left show various precooling start times)

5.4.5 Coil Leaving Air Temperature or Slab core Entering Temperature

The CLAT which also is the same as the slab entering temperature, could have a considerable impact on the effectiveness of precooling and the demand limiting. It is expected that the lower this temperature is, the more effective charging is but care has to be taken to ensure the temperature always exceeds the dew point temperature of the ambient air so that to avoid condensation and dampness from forming inside the hollow core slab.

In order to study the impact of the coil leaving air temperature on the performance of the system, values ranging from 8 to 14 will be used.

5.4.6 Core Entering Air Flow Rate

Although this study is focused on CAV, for completeness the impact of variable air flow will be investigated through enumeration of flow rates ranging between 40 and 90 l/s in steps of 10.

5.5 Results

A list of result variables is given in table-10

<u>Result Variables</u>	<u>Definition</u>	<u>Remark</u>
Baseline Peak Cost Ratio	Baseline Peak Cost / Baseline Total Cost	<i>The base line setup, with temperatures set to lower comfort limit during occupancy and free floating at night and any other time. No precooling.</i>
Peak Cost Ratio	Peak Cost / Total Cost	<i>These are non-baseline values and the ratios refer to the values within the same scenario</i>
Number Peak PMV ⁴ violation	Number of times PMV is outside the comfort range of 0.5 to 0.5	
Peak PMV violation ratio	Number Peak PMV violation / Total Peak Period sampling points	
Peak Average PMV	The average PMV during peak periods	
Peak Chiller Off Hours (hr)	The number of hours chillers are off during peak period	
Normalised Peak Cost Ratio	Peak Cost ratio / Baseline Peak Cost Ratio	

Table 14: Result variables

⁴ Predicted Mean Vote comfort ranges are -0.5 to 0.5

Peak Cost Ratio measures the effectiveness of the demand limiting and load shifting control in lowering peak demand and energy use, when measured against its overall power consumption. The lower the ratio, the lower the peak time energy and demand cost. Whereas, normalised Peak Cost Ratio measures the same attribute as Peak Cost Ratio, but compared to the base case peak cost ration

Peak Chiller Off Hours is another measure of the effectiveness of load shifting and limiting when expressed in a number of hours chillers are turned off during peak hours. The higher this ratio, the better the performance of the demand limiting and load shifting.

Number of Peak PMV Violations and Peak PMV Violation Ratio measures the effectiveness of a demand limiting and load shifting strategy in keeping the comfort of the zone within the ranges of -0.5 to 0.5. Number of violations count the number of times the sampled values are outside the comfort range and the violation ratio gives the proportion of the violation during the peak time. The higher this ratio the less comfortable the zone will be.

5.5.1 The Base Line System

The base line system uses the same HVAC network developed in this study (see figure 39) but the mechanical cooling system runs only during occupied hours of 09:00 to 17:00 and no provision is made for precooling or night ventilation. The cooling set point is set at the lowest comfort bound during occupancy and is allowed to float freely outside occupied hours. This way of configuring the system is known as Night Setback (NS). The cooling set point profile is as shown in figure-45 below. NS is not a very efficient strategy and hence it has the highest Peak Cost Ratio of 72.27%, the energy profile of the base line system is shown in figure-44.

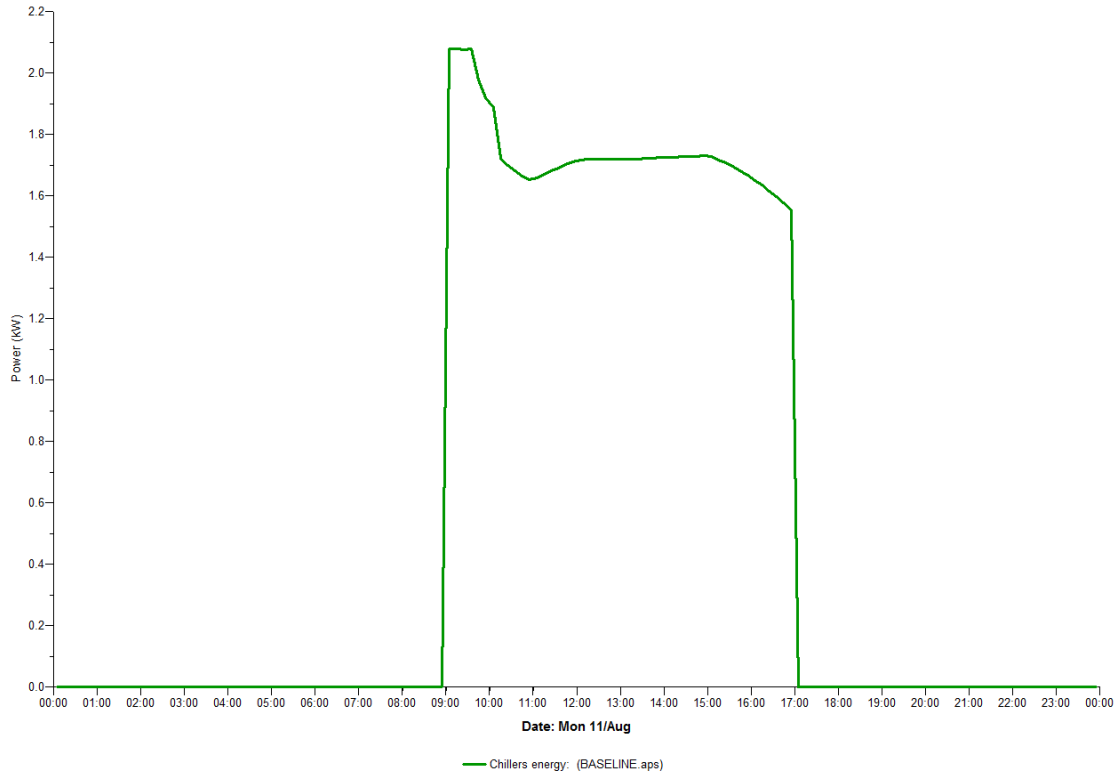


Figure 44: Base line energy profile for conventional studies (not used for MPC)

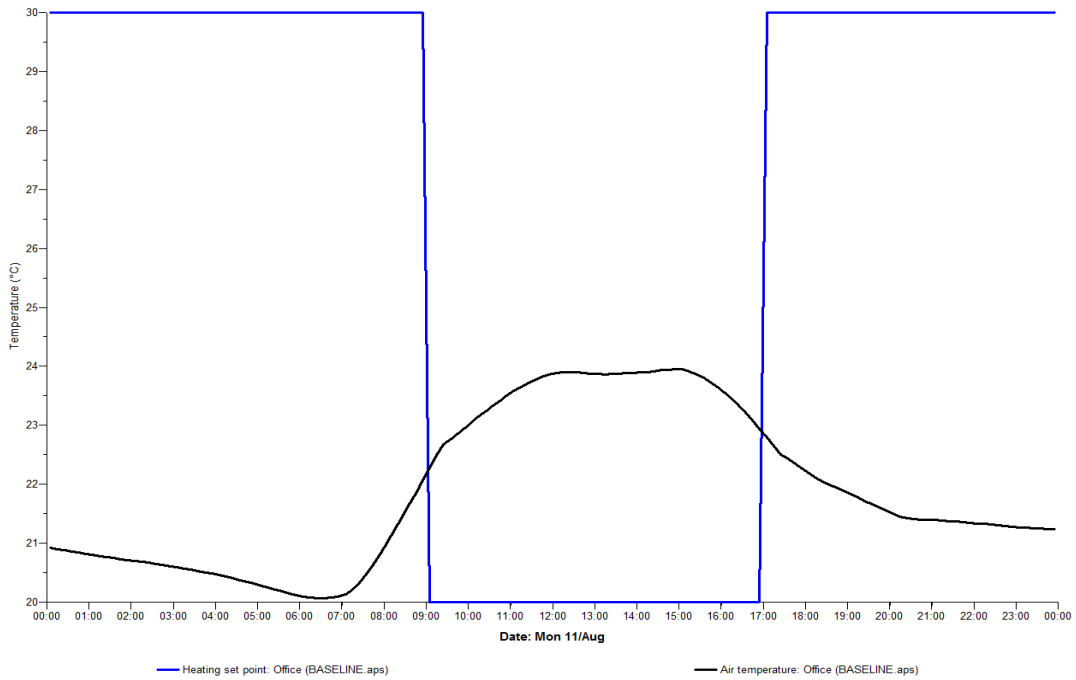


Figure 45: Baseline cooling set point and zoon temperature during occupancy (the black colour is zone temperature, whereas the blue colour is the zone temperature set point)

5.5.2 Precooling Start time

Many time periods are used to discuss the results. For convenience. Figure-46 shows schematic representation of the various time periods referred to in this section.

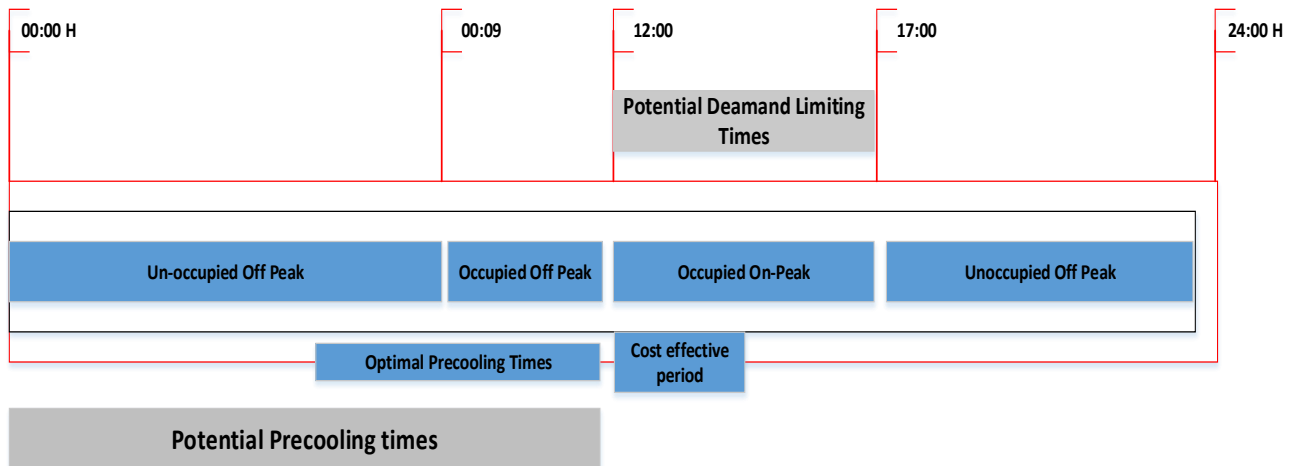


Figure 46: Periods of interest in the study (demand limiting start times are 12:00, 13:00, 14:00 and 15:00; where as demand limiting end times are 16:00 and 17:00; precooling times are from 00:00 to 12:00)

As illustrated in the figure-46, there are 4 time periods of interest but in this work the first three (from left) are the focus. Off peak hours include occupancy period (09:00 to 12:00) and hence precooling could run from mid night to 12:00. Demand limiting could potentially start from 12:00. The optimal demand limiting period lies in the first half of the peak period.

The impact of the precooling start time is investigated for precooling times starting from midnight to noon the following day, with intervals of 30 mins, by running batch simulations. The results show that (see figure-47), the optimal precooling start time is 3am with the lowest peak cost ratio of 24% within the PMV comfort range of -0.5 and 0.5, for demand limiting period of 1200 to 1700.

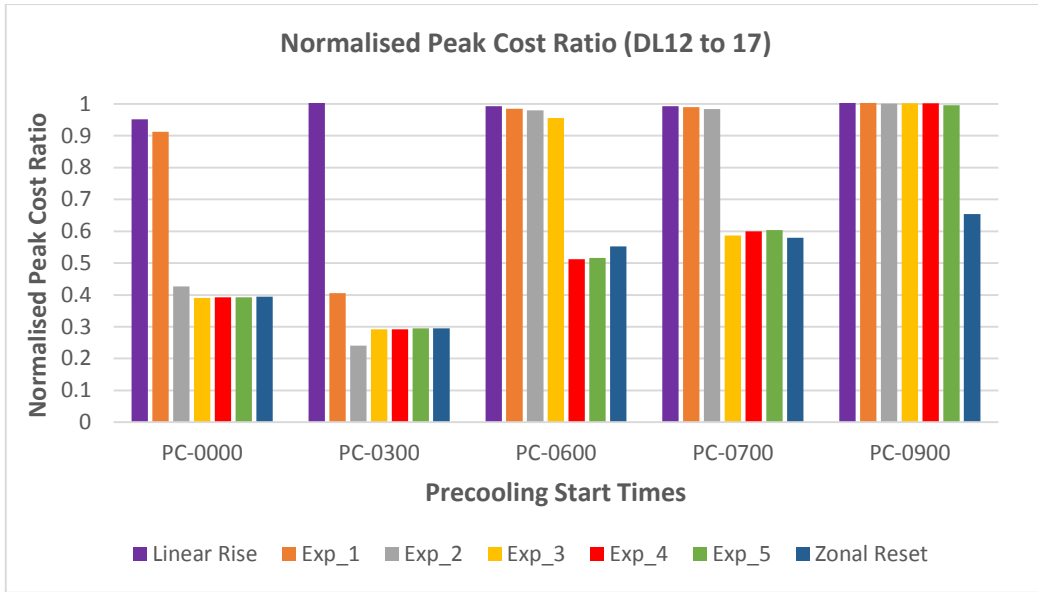


Figure 47: Normalised Peak Cost ratio as a function of precooling times for demand limiting period of 12:00 to 17:00 (the different colours represent the different discharge control trajectories. Precooling start time of 03:00 is optimal when discharged through exponential path of Exp_2)

Figure-47 (above) shows how the different precooling strategies compare to the worst case scenario (the base line). Whereas, the chart below (figure-48) shows, how the different precooling start times perform in peak shifting and limiting, when compared to their daily total chiller energy consumption.

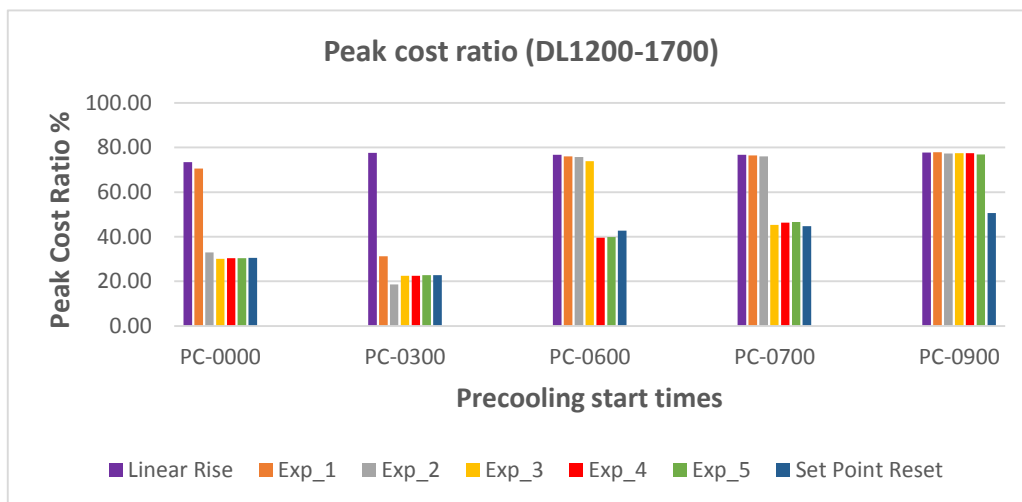


Figure 48: Peak cost ratio as a function of precooling time (DL 12:00-17:00), precooling start time of 03:00 is optimal with trajectory Exp_2

The chart below (figure-49) shows the number of hours chillers are 'off' during peak hours for the start time of 03:00, shows almost the entire peak period did not need chillers to take care of the loads, as the thermal charge stored in the slabs provides comfort.

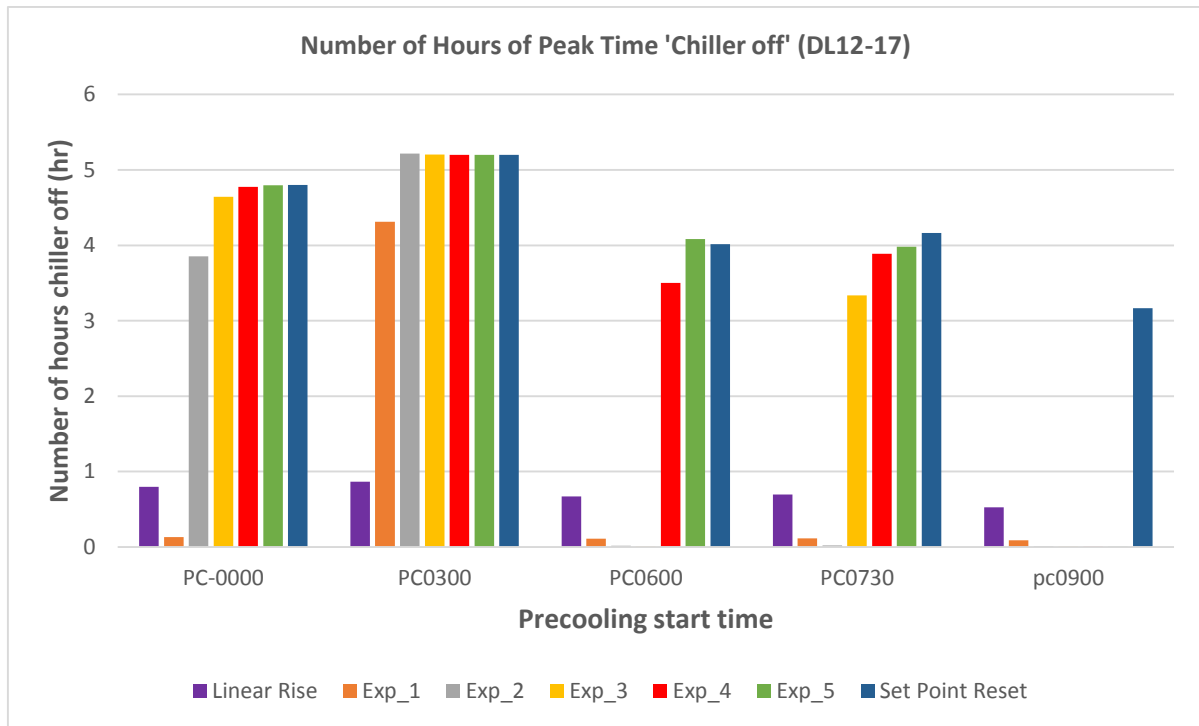


Figure 49: Number of peak time "Chiller off" hours as a function of precooling time (for demand limiting period of 12:00 to 17:00)

However, it is worth noting that the performance of a precooling scenario is dependent on which demand limiting time span is used, and as shown below in figure-50, the second half of the demand limiting time span (1500 to 1700) shows higher peak cost ratio than the first half.

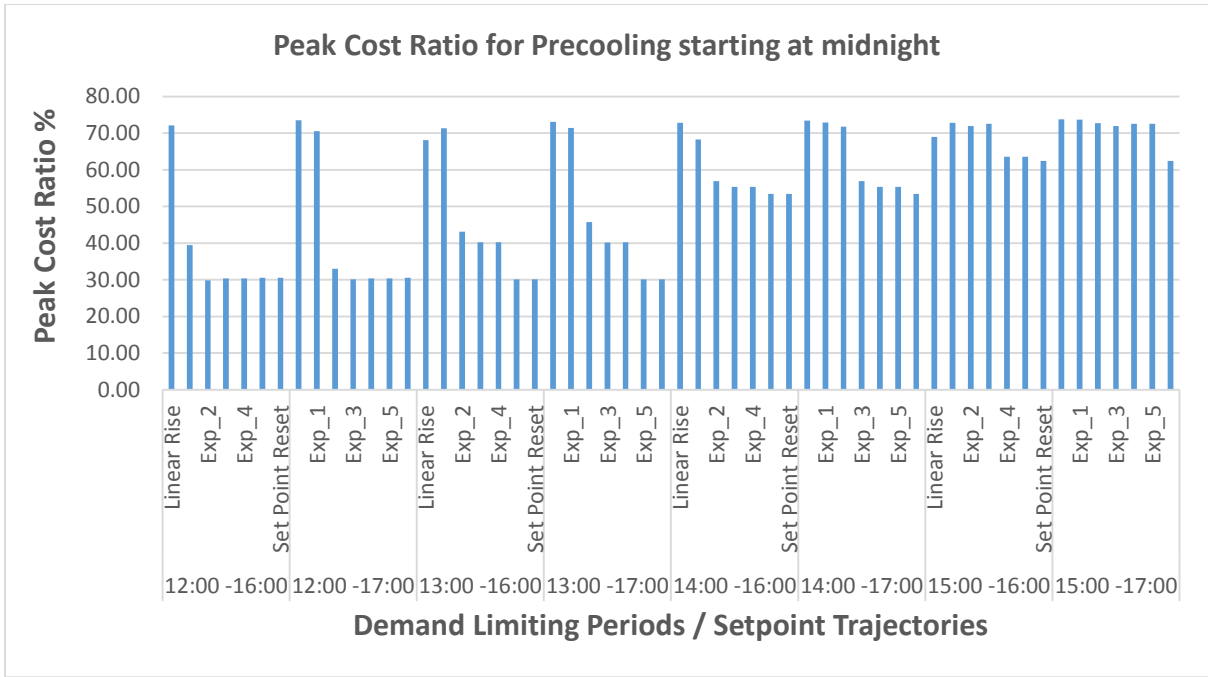


Figure 50: The effect of demand limiting start times on peak cost ratio; the first half (12:00 & 13:00) of the demand limiting start time span shows better performance than the second half (14:00 & 15:00)

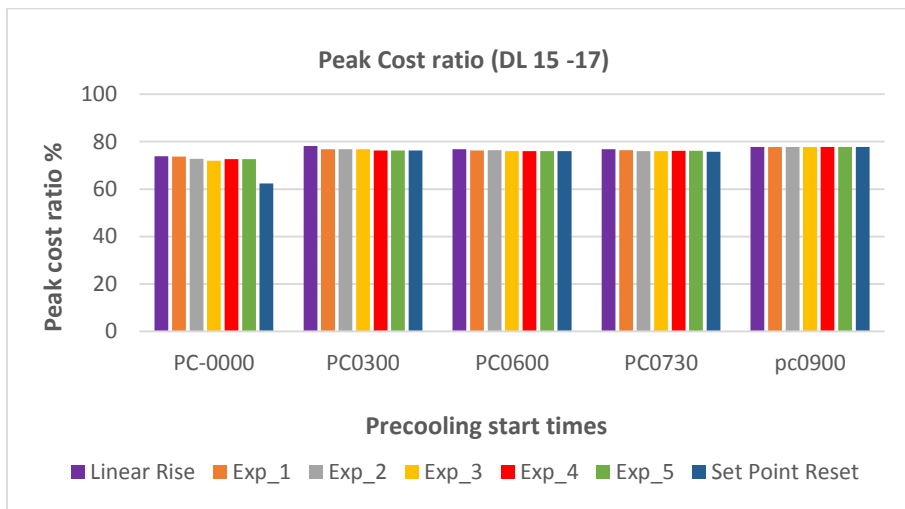


Figure 51: Peak cost ratio as a function of precooling (demand limiting running between 15:00-17) showing sub-optimal performance

The figure-51 above shows all precooling start times have higher peak cost ratio, when demand limiting is in the second half of the demand limiting start time span.

Therefore it can be concluded that, the effectiveness of a precooling regime is dependent on the demand limiting period's relative position in the overall demand limiting time span. The first half of the demand limiting time span seems to deliver cost effective operation but at the expense of comfort towards the end of the day. Whereas, the second half of the demand limiting time span shows maintenance of comfort, at the expense of increased peak cost ratio, as more load has to be handled by the chillers.

5.5.3 Pre Cooling Temperature Set point

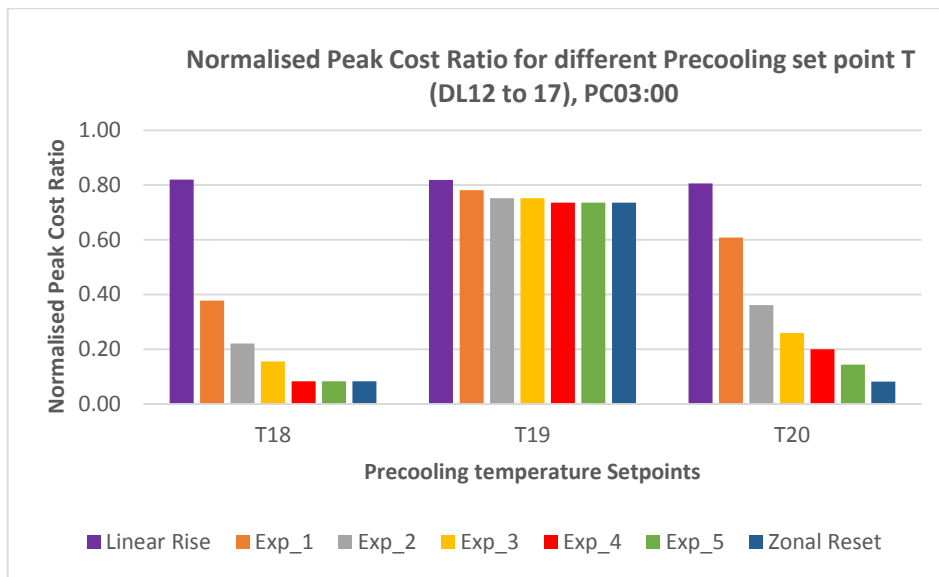


Figure 52: Normalised Cost Ratio as a function of Precooling Temperature set point check

The chart above (figure-52) shows, the normalised peak cost ratio is lower for precooling set point of 18 °C in the demand limiting span of 12:00 to 17:00. As can be seen in the following figure-53, figure-54 and figure-55, the demand limiting time span of 15:00 to 17:00 performs worse than earlier time span in terms of cost but seems to outperform the earlier time span when it comes to comfort.

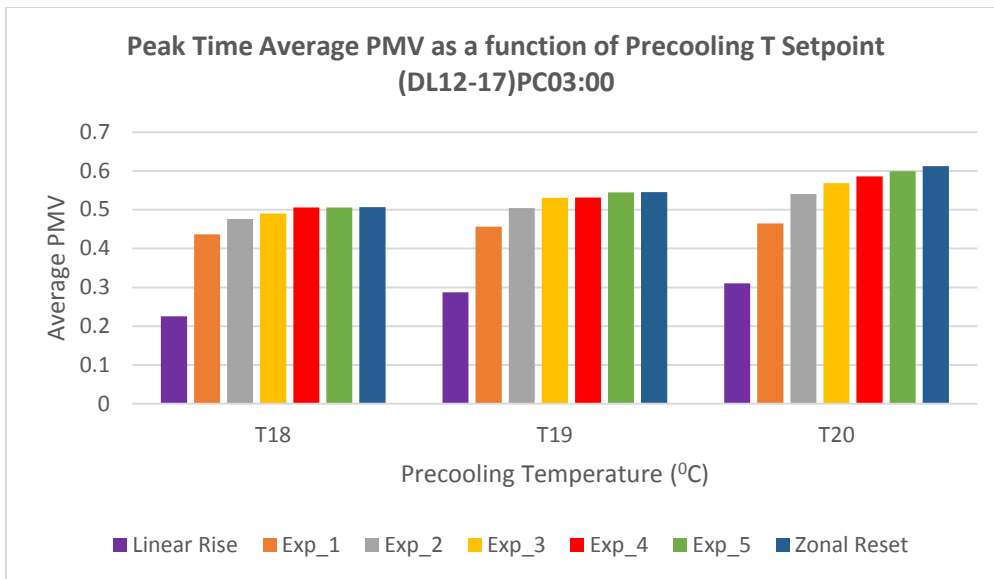


Figure 53: Average Peak Time PMV as a function of Precooling Temperature set point

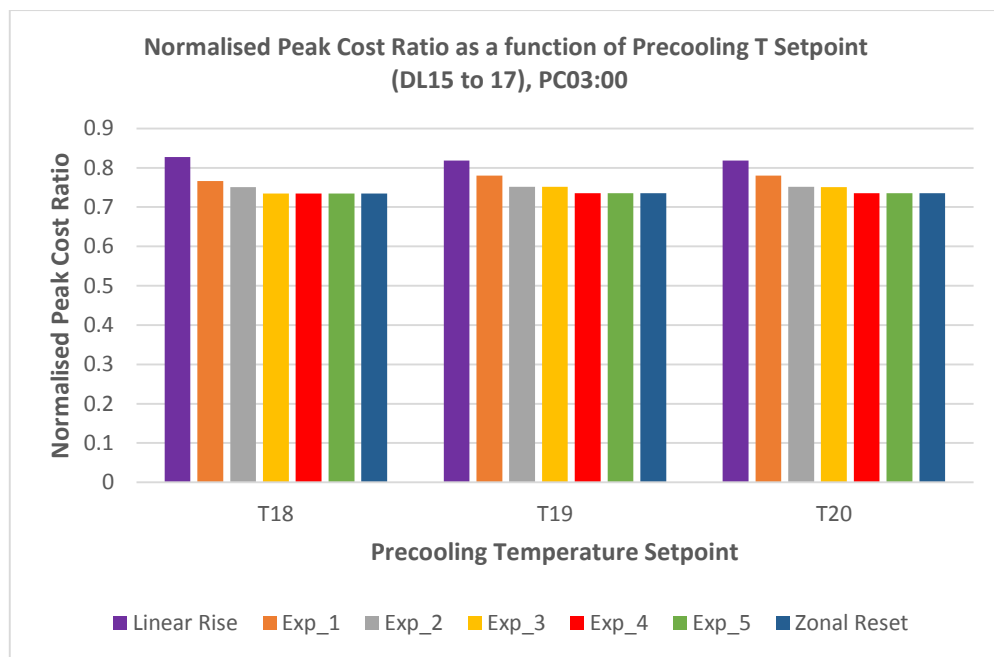


Figure 54: Normalised Peak Cost Ratio as a function of Precooling Temperature set point (it appears the precooling temperature does not seem to make huge difference between the different temperatures used)

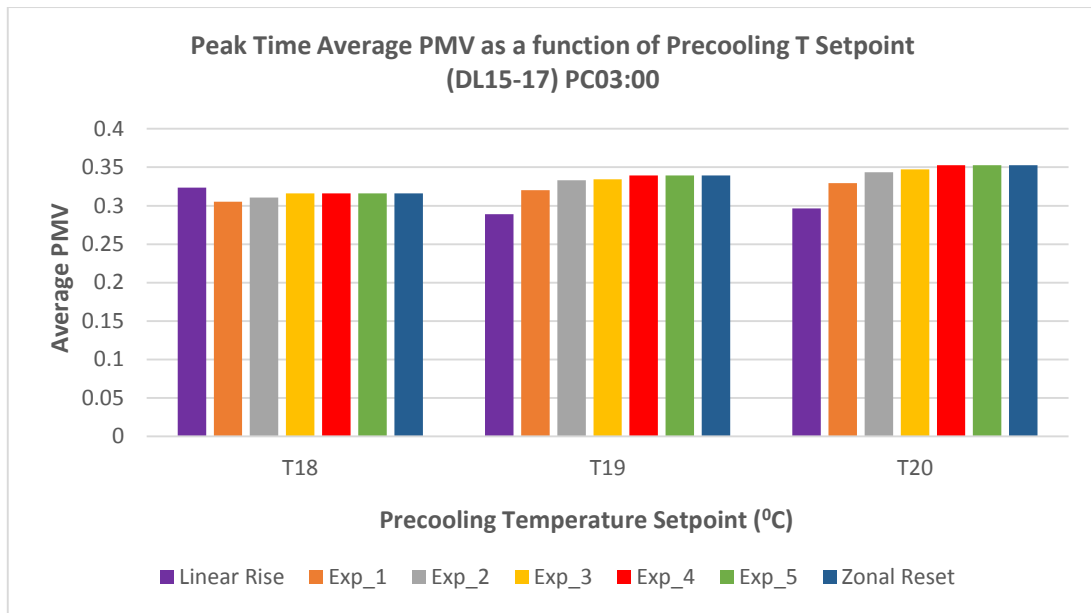


Figure 55: Average Peak Time PMV as a function of Precooling Temperature set point

5.5.4 Slab Core Air Volume Flow

The effect of lower flow rates is dramatic. For flow less than 70 l/s, the chillers seem to be working around the clock (see figure 56 and 57)

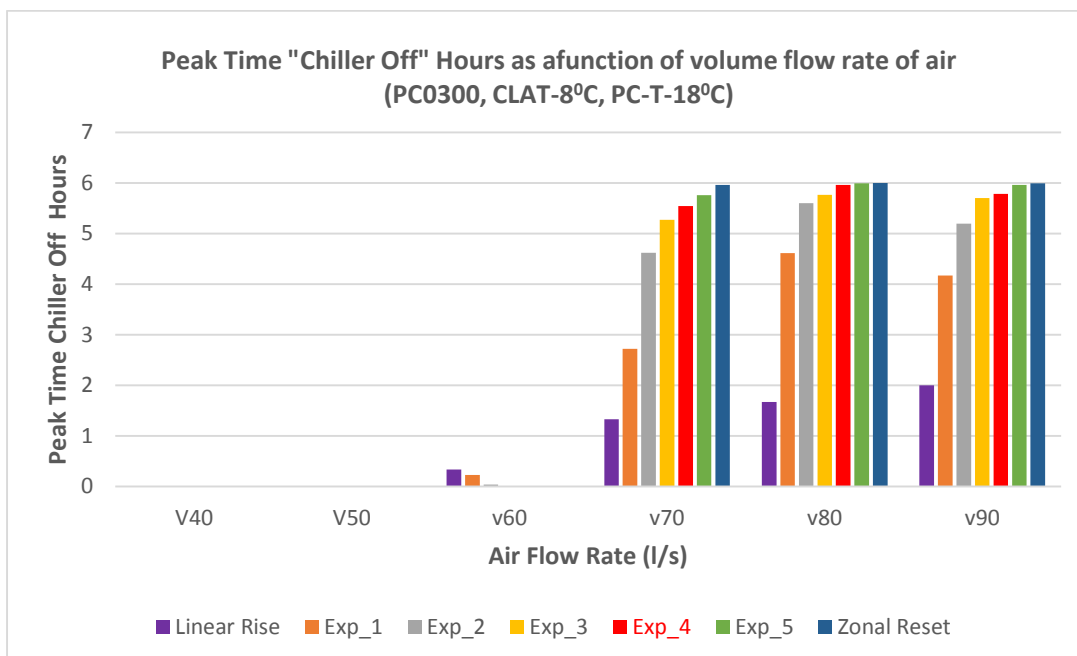


Figure 56: Peak time chiller off time as a function of air flowrate (please note that for lower flow rates, the chillers are on during the entire peak time)

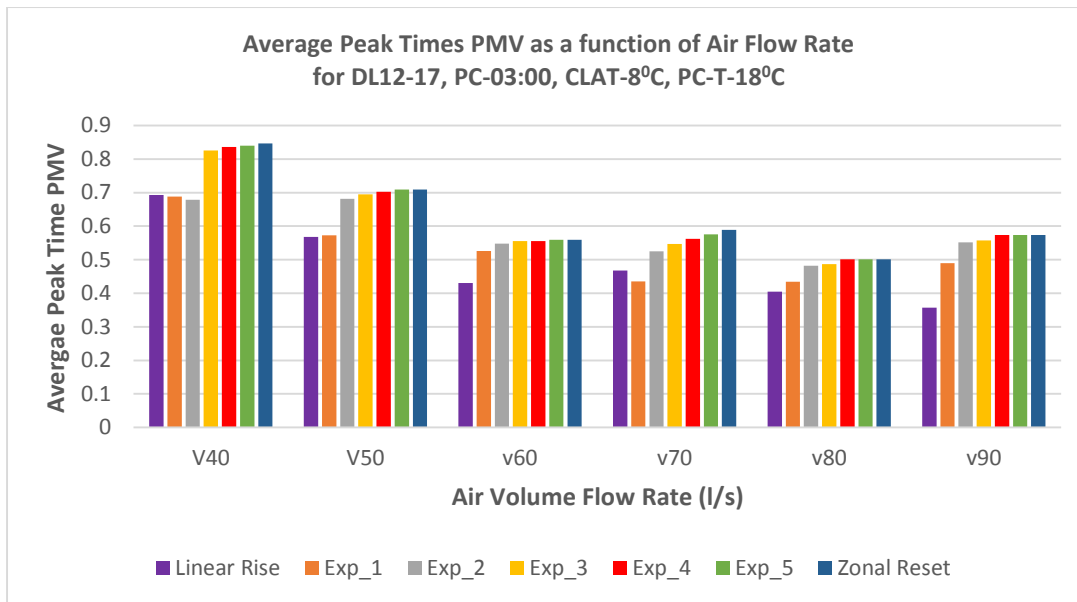


Figure 57: Average Peak Time PMV as a function of Air Flow (lower air flow rates seem to exhibit higher percentage of PMV outside the range -0.5 to 0.5)

At the lower flow rate the coupling between the slab core and the core air is less than at higher flow rates. Therefore, effective storage of cooling is less probable and hence why the chillers have to work harder.

5.5.5 Slab Core Entering Temperature

Batch simulations have been run with values of slab core entering temperature ranging from 8 to 12 °C. The results show that a lower entering temperature of 7 °C performs better than the others in terms of peak cost ratio as well as overall cost (see figure-58). However as 7 °C is very close to the dew point of the outdoor air, in order to avoid condensation and dampness in the slab core, 8 °C is a preferred choice with comparable performance.

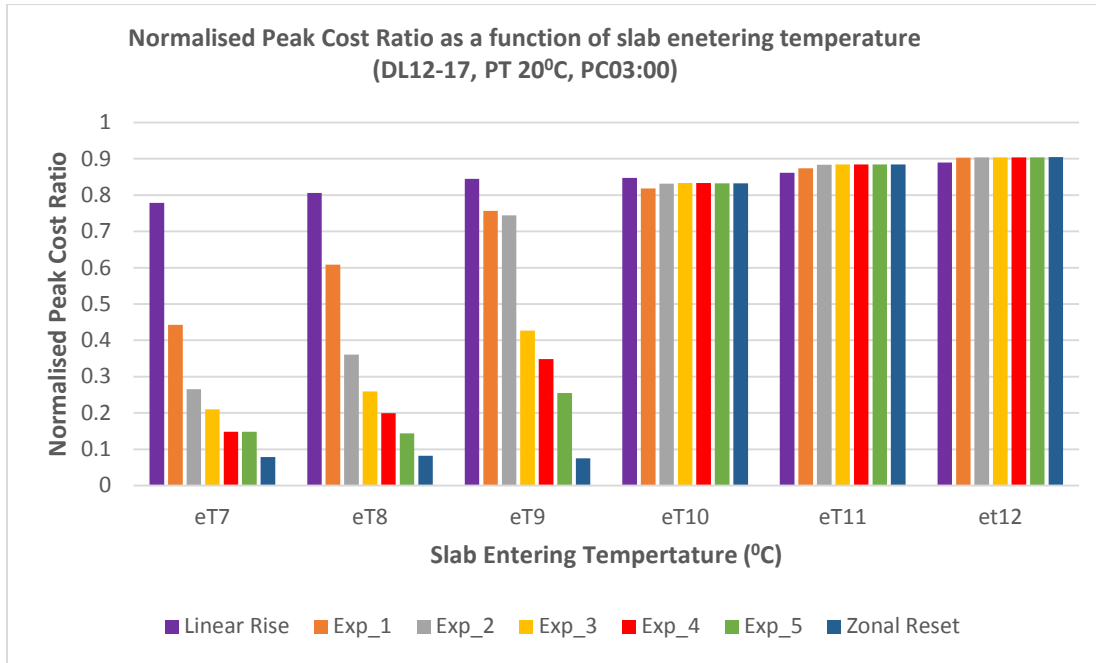


Figure 58: Peak cost ratio as a function of slab core entering air temperature

5.6 Results Summary

<u>Strategy Name</u>	<u>Performance summary</u>	<u>Demand Limiting Trajectory</u>
Precooling start time	Precooling start time of 03:00 shows optimal performance with the lowest normalised peak cost ratio of 24%.	Exp_4
Precooling temperature set point	18 ⁰ C shows optimal performance, although 20 ⁰ C has similar profile. The normalised cost ratio is 12% for demand limiting time of 12:00 to 17:00.	Exp_4
Slab core entering temperature	7 ⁰ C shows the best performance but it is very close to the dew point temperature, therefore, 8 ⁰ C is optimal with peak cost ratio of 5%	Zonal Reset
Slab core air flow rate	80 l/s appears to be optimal at 18% peak cost ratio.	Zonal reset and Exp_5

Table 15: Summary results

5.7 Conclusion

The parametric study results show that there are 3 key parameters at play, these are: the slab entering air temperature, the precooling start time, the precooling temperature set point, demand limiting set point trajectory and the start of the demand limiting period in relation to the whole demand limiting time span, with the latter three being part of the room set point trajectory.

Based on the observation so far, it seems a precooling start time of 03:00, precooling set point temperature of 18°C, core air entering temperature of 8°C, core air flow rate of 80l/s and demand limiting regime starting at 12 noon and ending at 1700, following exponential trajectories appear to be optimal.

However, these variables are very sensitive to disturbances such as change in the room cooling load through gains or the outdoor environment. Ideally, based on these disturbances on each day, each day could have different combination of these variables to suit the day.

Moreover, it is clear that the room set point trajectory (controlling the precooling start time, the precooling temperature, the demand limiting trajectory and the onset of demand limiting) is a supervisory variable.

In conclusion, it can be stated that, the energy consumption and comfort criteria are functions of the room temperature set point trajectory, precooling start time, precooling set point (part of the room set point trajectory) and the slab air entering temperature.

$$E_k = f(\overrightarrow{Setpoint}_k, PCStartTime_k, SlabEnteringAirTemp_k) \text{ ----- (Eq-14)}$$

where:

E_k is the energy consumption at time k

$\overrightarrow{Setpoint}_k$ is a vector of zone temperature set points for time interval k

$PCStartTime_k$ is the precooling start time

$SlabEnteringAirTemp_k$ is the slab core air entering temperature or the the Coil Leaving Air Temperature (CLAT)

k is the sampling time period

N is 24 for a days of simulation

6 Case Study-II Model Predictive Control (MPC)

6.1 Introduction

This section presents the work on Model Predictive Control that has been undertaken using a whole building simulation tool, the IESVE. As presented in the literature survey (Chapter-3, section-3.1.6) the majority of the work on MPC in buildings relies on first principle or linear identification (reduced order model) based building and system models; as supposed to whole building simulation tools' high order models, in their implementation of MPC. As presented in chapter 3, there are some challenges of data operability and time synchronisation that other researchers overcome with other tools that remain a challenge in IESVE, at this time IESVE does not support co-simulation techniques.

The approach taken in this thesis is the exploitation of the IESVE's interoperability with IESVE's 'Free Form Profiles' & the dynamic update of free form profile can be used as a work around for the time step synchronisation challenges. Ideally, one can have two simulations running: primary and secondary; the primary one being the one that generates the control signals and the secondary one representing the building model. Both will have the building model in them, albeit a simplified one in the primary one. The second model could of course be the actual building being controlled.

However, there is a challenge to overcome when it comes to 'initialisation' or 'preconditioning' of simulations. Normally in MPC implementations, the controlling (primary) model and the controlled (secondary) model shake hands in such a way that, the controlled model needs to reinitialise itself at the state sensed by the controlling model, every time the optimisation horizon updates. However, the IESVE would need to do its own preconditioning when it initialises, which means there will not be synchronisation between states.

Without the ability to update state dynamically within the IESVE an alternative to the two simulation approach has been adopted for this work. Only one single simulation acting as both the thermal response model and the controlled model is used, with a caveat that, at the end of an optimisation horizon when an update is needed, the simulation always start from

the same initial point. The simulation horizon however progresses on to the next step in receding horizon fashion.

6.2 Simulation Framework Concept description

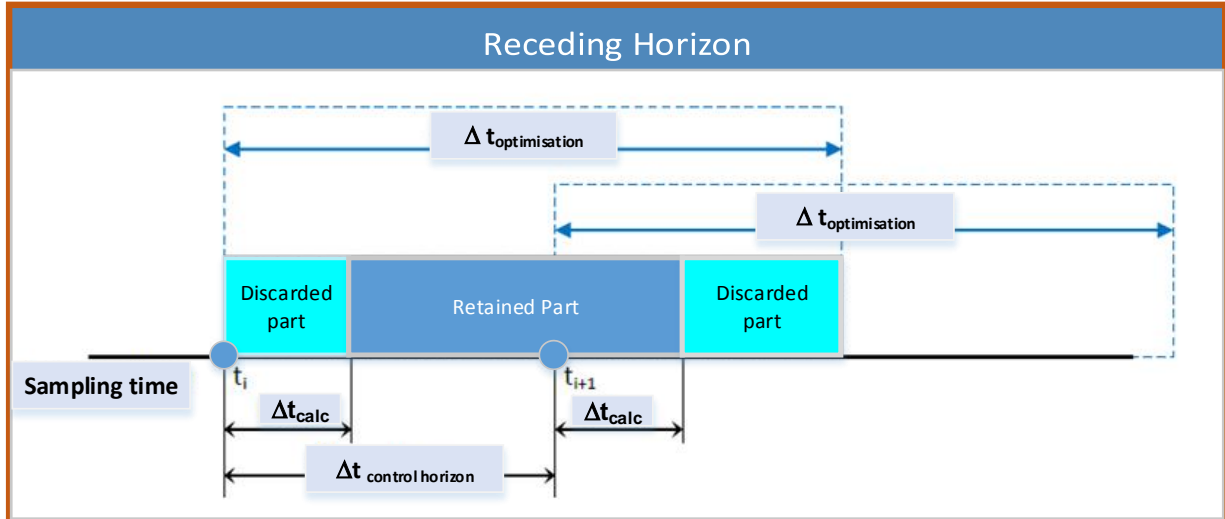


Figure 59.0: Receding horizon

As introduced in the literature survey in Chapter-3 the concept of the receding horizon illustration is described above (figure-59). In the context of sampling points t_1 and $t_1 + \Delta t_{\text{calc}}$ shown above, an optimisation problem is solved over the horizon, $t_{\text{optimisation}}$ and after a period of $t_1 + \Delta t_{\text{calc}}$, which is the time required to solve the problem, the optimal control signal just reached at, is applied to the building up until a new signal from the next optimisation problem is reached at. Therefore, it is obvious that the control signals generated at sampling point i and are between $t_i + \Delta t_{\text{calc}}$ and $t_{i+1} + \Delta t_{\text{calc}}$ are applied while the rest are discarded.

With this in mind, the concept summarised above in the introduction is illustrated in figure-60 below. As can be seen in the figure, the simulation horizon builds up from step-1 to step-3, i.e. from t_0 to t_2 , in three steps as it tries to solve optimisation problem and generate control signals (prediction of set point values for the supervisory variables).

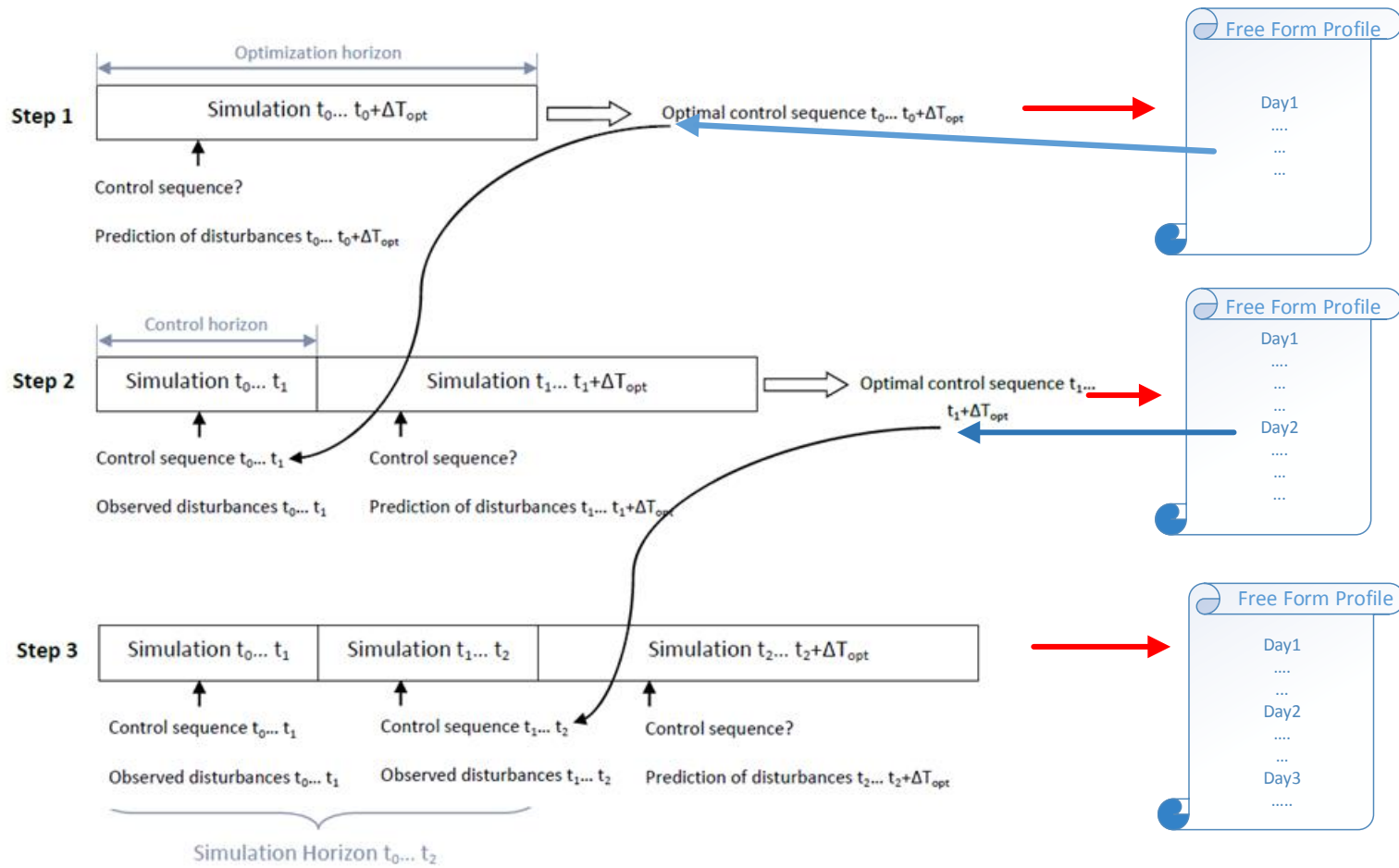


Figure 60.0: MPC with IESVE

In stage-1, the optimisation problem gets solved over a period of length equalling to $t_0 + \Delta T_{Opt}$, where ΔT_{Opt} is the length of the optimisation horizon; in stage-2 the controller advances the optimisation problem to period between t_1 and $t_1 + \Delta T_{Opt}$, where $t_1 - t_0$ is the control horizon.

At this stage it is worth noting that, the simulation has to be reinitialised at t_0 and should run all the way to t_1 using the outcome of the optimisation process in stage-1. This stage is critical because the room loads at a given time k depend on current and past temperature set points, therefore the optimisation for the future requires the history of the past (Gayeski, 2002).

And finally the optimisation problem shifts forward to period from t_2 and $t_2 + \Delta T_{Opt}$ and the same logic applies to the following stages.

Although in receding horizon signals are discarded, as illustrated in figure 46 above; in this work no signal is being discarded and ΔT_{Opt} is negligible compared to the length of the optimisation horizon. Therefore, the impact of discarded signal can safely be considered negligible.

As shown in the image, the communication between the optimisation routine and the simulation takes place via the Free Form Profile, therefore at the end of an optimisation period, the controlled signals are recorded on the profile and the simulation reads these at the beginning of the next initialisation stage.

6.3 Implementation of MPC

6.3.1 Assumptions

It is assumed that there is a perfect weather prediction and the number of occupants will stay at the current level of 3 people during the optimisation week.

6.3.2 Economic Optimisation Model

All optimisation problems need to define the problem variable, objective function and constraint function. In this work, the problem variables are the room temperature set points,

the slab core air entering temperature and the precooling start time. The objective function is the total energy cost of the system over 24 hours and the constraints are comfort and defined ranges of the temperature and Precooling start times.

6.3.3 Cost Function

As shown in the previous chapter, the energy consumption of the building model used in this thesis is dependent on zone temperature set point trajectory, the precooling start time and the slab core entering temperature. Therefore the cost function (the objective function) is given by:

$$\sum_{k=0}^N w * R(k) * Q^*(\vec{Tz}(k), Te(k), Tpc(k)) \text{ ----- (Eq-15)}$$

The constraints are:

$$T_{z,\min}(k) \leq T_z(k) \leq T_{z,\max}(k), \text{ which is controlled via } -0.5 \leq \text{PMV} \leq 0.5$$

$$T_e(t) \in (8, 12)$$

$$T_{pc}(t) \in (18, 20)$$

$$T_{z(t)} \in (22, 25)$$

where:

R (k) is the electricity cost

\dot{Q} is the optimal cooling plant consumption at time k, which depends on current conditions and the zone set points $T_z(k)$

$\vec{Tz}(k)$ is the zone temperature set point vector for time k

$T_e(k)$ is the slab core entering temperature

$T_{pc}(t)$ is the precooling temperature

N is 24 for a day's optimisation horizon

w is a waiting factor

6.3.4 Optimisation Using Exhaustive Search Method

The IES Optimise™ tool has a Genetic Algorithm support and it could have easily been used in this work, instead Exhaustive Search Method is used for finding the minimal cost.

There are two reason why Exhaustive search method is selected, the first is the problem at hand is simpler, is being optimised over a day optimisation horizon. In addition it is a search and test algorithm that works for black box optimisation (Zhao et al, 2013) and it is suitable for problems with reasonable computational time (Zhao et al, 2013, citing Kolda, et al. 2003 and Sinha, 2008). The optimisation problem at hand has multiple constrains and it results in comparatively small search space. For example, the precooling temperature search space is between 03:00am & 08:00am and for 30 mins of discrete interval the number of search steps is 10 for daily control and the optimisation simulation period is 24 hours. It seems the exhaustive search time is feasible for real-time simulation (Zhao et al, 2013).

The second reason is, it is intended to demonstrate that, building service managers could do similar model predictive control, in order to find the optimal control strategy for the next day operation, as long as they can manipulate the simulation output file through some computer script. It is felt that the notion of using Genetic Algorithm for a problem of this magnitude could be off putting for practitioners of the average day to day building operation.

In this work, Lua scripting is used to drive the exhaustive search method.

6.3.4.1 Optimal Search Logic

The exhaustive search method looks for the minimum cost control signals, with in the comfort band, but when comfort is outside the allowable comfort band, it tries to find the control signals that give the minimal comfort value in the search space.

Mathematically this is expressed as: cost control signals:

$$J = \min (f_{\text{Energy}}(x, t) \text{ when comfort is met})$$

$$J = \min (|f_{\text{PMV}}(x, t)|) \text{ otherwise,}$$

this basically gives priority to comfort when constraints are not met.

6.3.5 Terms of Reference for MPC

The following conditions have been taken into consideration for MPC run:

<u>Entities</u>	<u>Assumed Values</u>	<u>Remark</u>
Occupied Weekdays zone control (9am-5pm)	PMV control [-0.5 – 0.5] Temperature control [20, 24]	
Non occupied weekday zone control (5pm to midnight)	PMV [-2, 2] Temp control [28]	After mid night the set point could be lower depending when precooling starts
Comfort assumptions	Met = 1, air speed = 0.137 Summer clo = 0.7	
Weather	Denver	
Schedules	People, lighting and equipment	See table-5 (chapter 3)
Optimisation week	August 11 to 15	
Perfect weather prediction	n/a	
Constant level of internal gains throughout the simulation week	n/a	

Table 16: Optimisation terms of reference

6.4 Results

The result of the simulation are shown in table-17 and figures 61 to 67 show the MPC result compared to the base case.

Variable	March 11	March 12	March 13	March 14	March 15
Slab Core Air Entering (°C)	8	11	8	10	8
Precooling Temp Set point (°C)	18	20	19	19	18
Precooling Start Time	03:00	03:00	03:00	03:00	03:00

Demand Limiting period	12:00 – 17:00				
Normalised Peak Cost Ratio	50	0	30	60	65

Table 17: MPC results

6.5 Discussion of results

The result of the MPC simulation shows over all the peak time demand has reduced by 43.26% and the “peak” peak time energy consumption it has been reduced by 50%. On majority of the days, the number of hours chillers are off during peak time is over 3 hours. On day two of the simulation, the entire load has been shifted to the early morning off peak period (see figure-64) taking advantage of the cooler outside air. Also, on day two of the simulation, the precooling temperature and the slab core air entering temperature are higher than the rest of the days in the simulation week.

The result for day three, Wednesday 13th of Aug indicates, as the result of a cooler night (the coldest night of the simulation week see figure-65), it did not need mechanical precooling.

Generally, the results show great improvement on the baseline in two terms:

- Peak Load shifting - as shown in the figure, almost 50% of the on-peak load has been shifted to the off-peak period
- Peak Load Limiting - The maximum load of the MPC controlled system, during the peak time has been reduced down to ~43%

This result is in agreement with other results of previous other works on controlling the building thermal mass using the MPC.

6.5.1 Conclusion

The results of MPC shows, considerable amount of potential saving could be achieved over the conventional control strategies. Moreover, the energy storage in hollow core slabs and the optimal discharge of it, is shown to be done more effectively with MPC than conventional control strategies. Therefore, it can be concluded that the wider use of hollow core slab could be possible if it is coupled with a predictive system. The saving achieved through the use of the predictive system could potentially pay back the investment in relatively shorter times.

The use of whole building simulation tool for MPC has shown good results and the potentials are there for it to be employed more often, in a day to day management of buildings through optimal control. However at the moment, the computational resource and the computational time needed with the use of the tool could be a bottleneck for systems requiring instantaneous prediction.

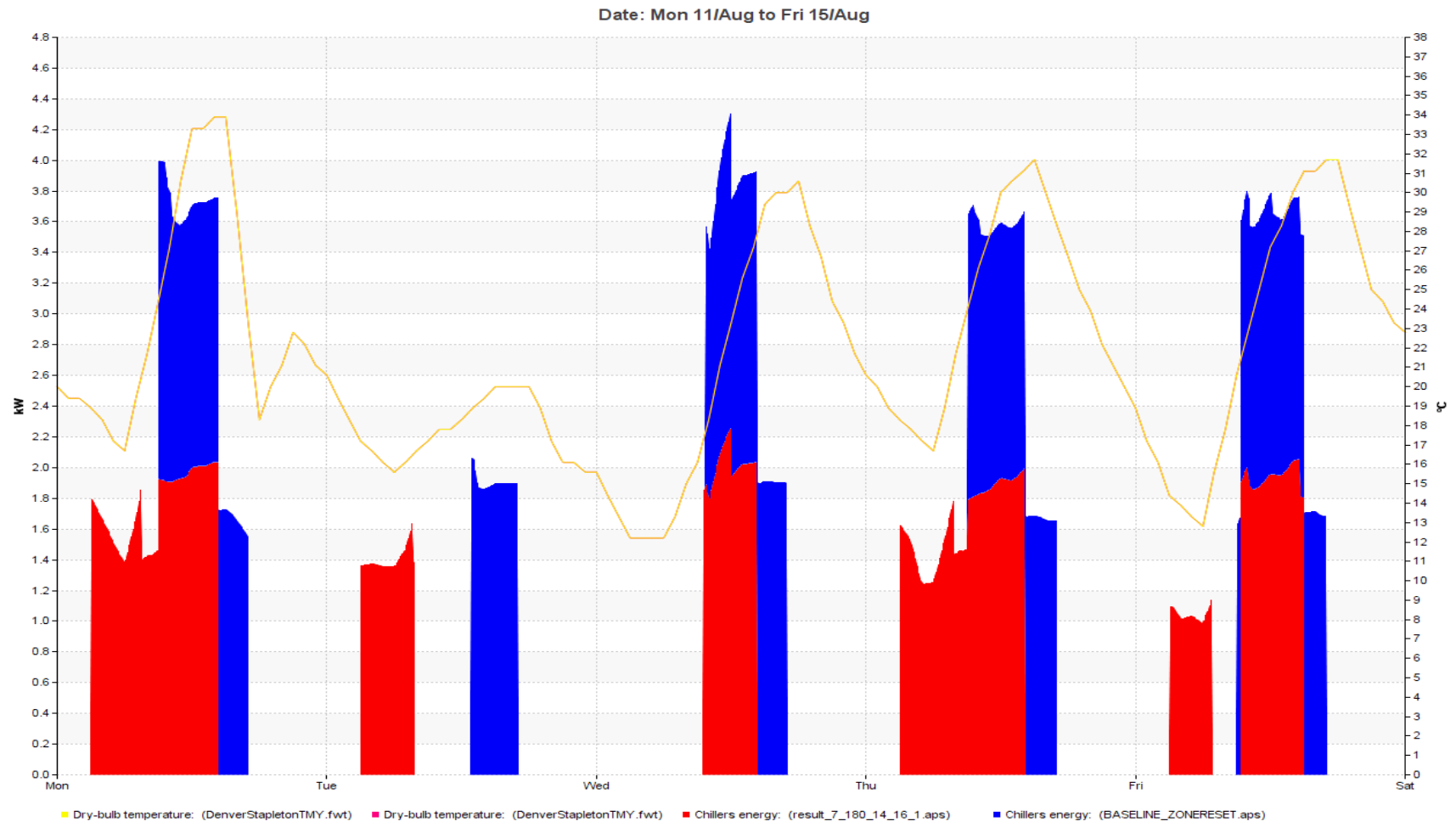


Figure 61 MPC Result showing load shifting and peak demand limiting (the red area is the MPC result while the blue area represents the baseline). The dry bulb temperature for the day is shown and it seems the energy consumption is shows correlation to it.



Figure 62: Result of MPC showing demand limiting and peak shifting, compared to the baseline. It also shows the zone temperature for the day. (red baseline, blue MPC)

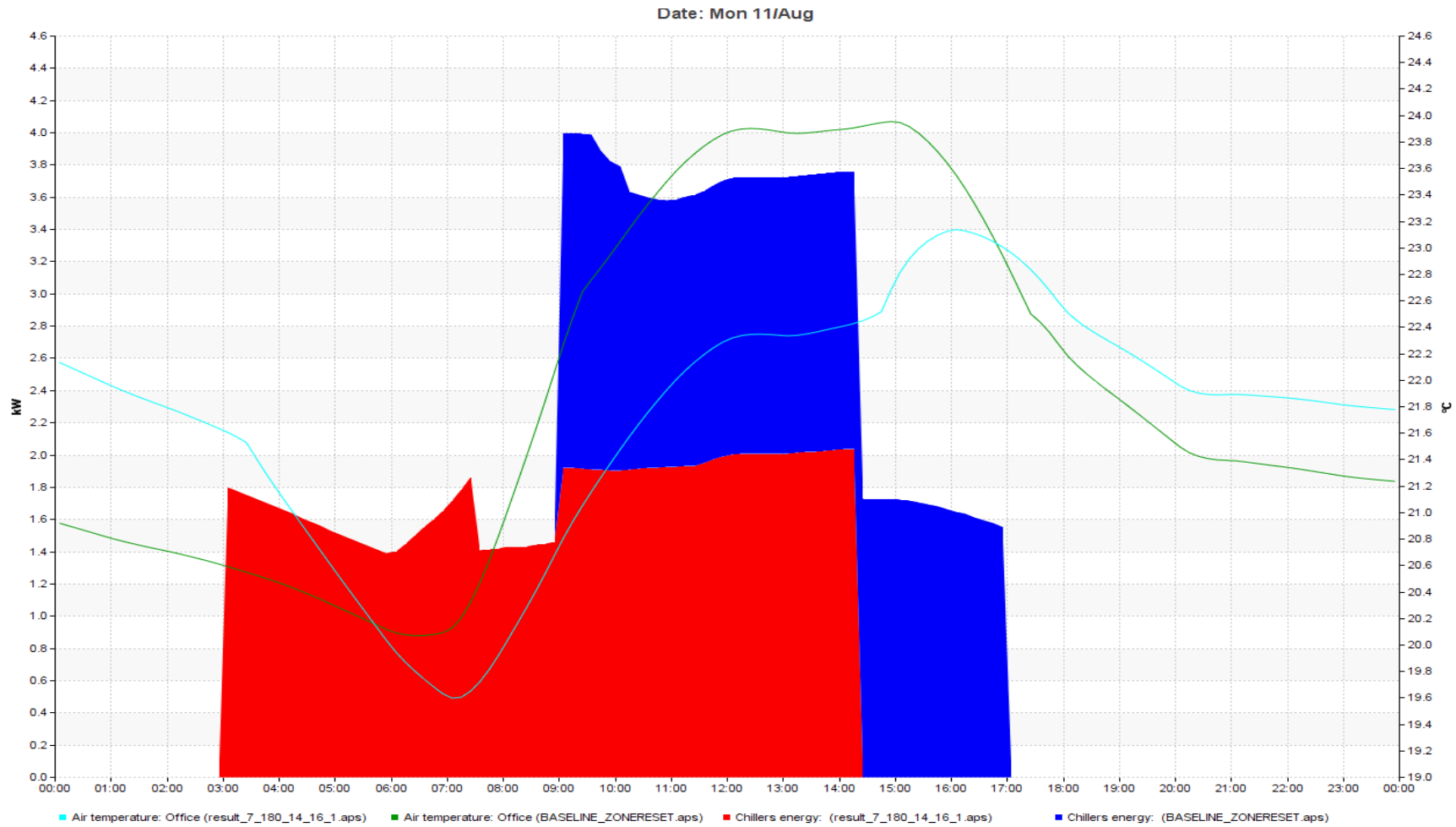


Figure 63: MPC result for Monday (day one of simulation) showing peak load reduction and shifting to off peak hours (red MPC, blue baseline)

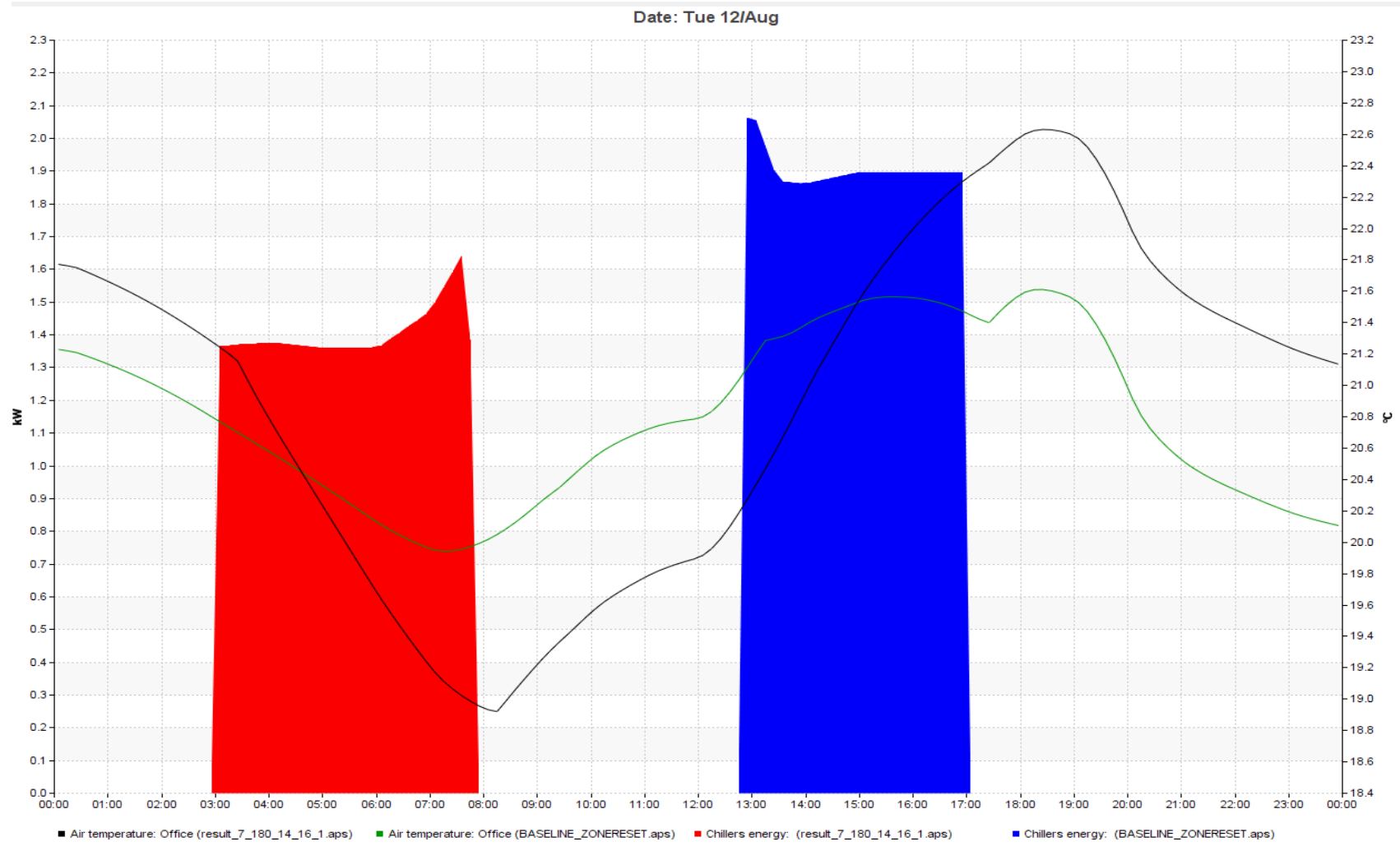


Figure 64: MPC result for Tuesday day two of simulation. Almost all the chiller load has been taken during early mornings (the lines are for dry bulb temperature) (red MPC, Blue, baseline)

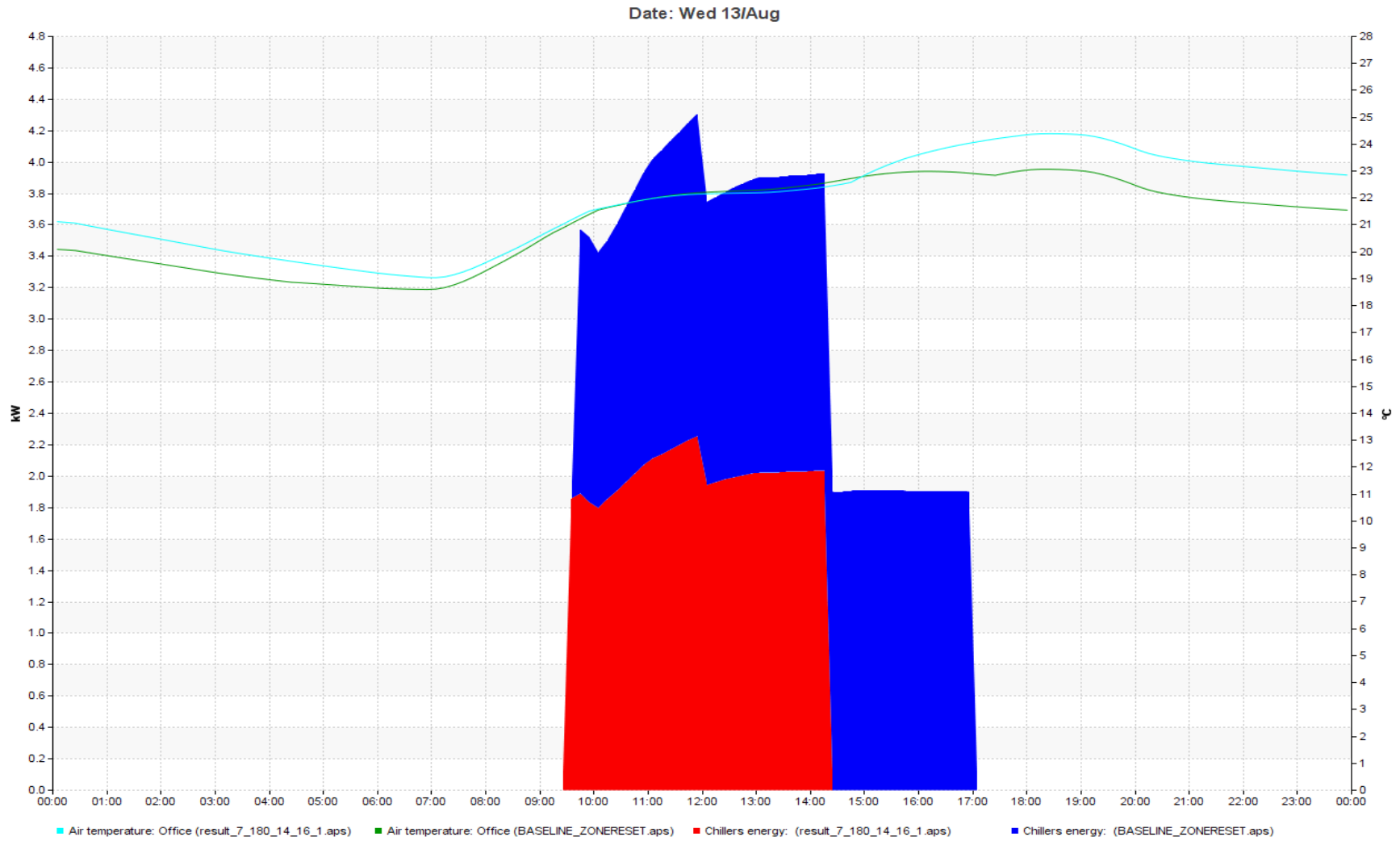


Figure 65: MPC result for Wednesday, day 3 of simulation (red MPC, blue baseline)

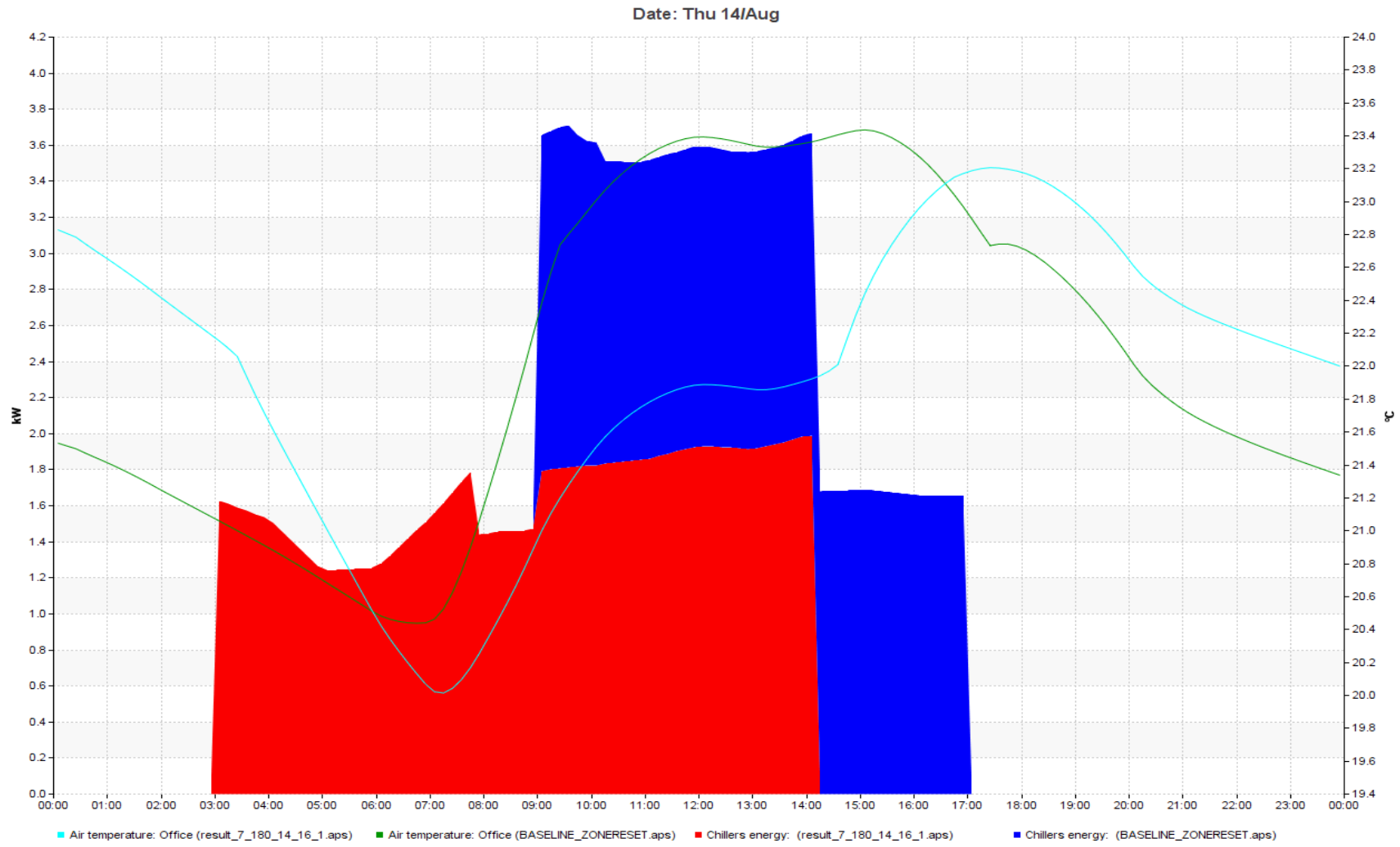


Figure 66: MPC result for Thursday, day 4 of simulation (red MPC, blue baseline)

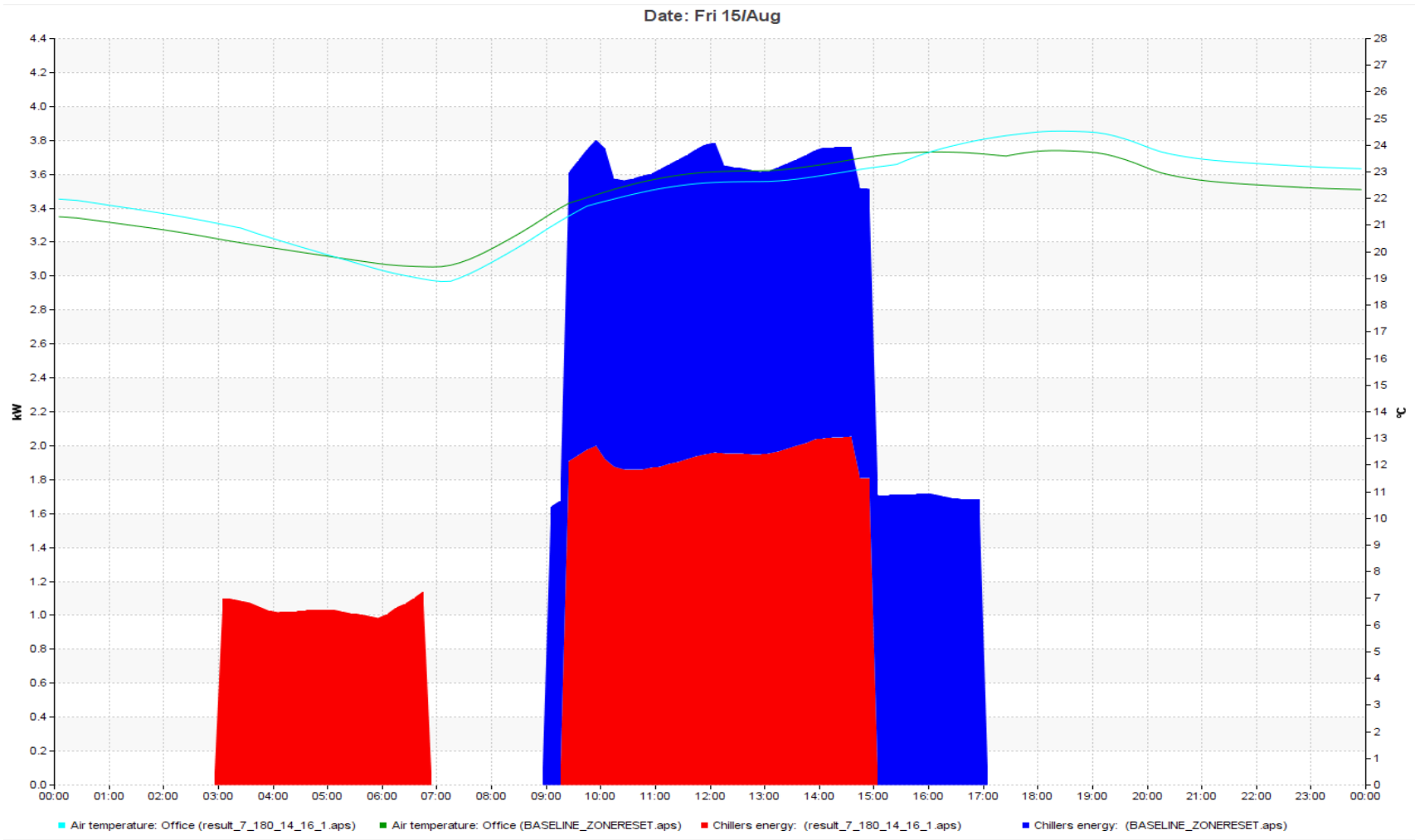


Figure 67: MPC result for Friday day 5 of the simulation (red MPC, blue baseline) On Friday, although there is chiller load during peak time for MPC, its peak value is less than the baseline's peak value.

7 Conclusion

7.1 Modelling a Hollow Core Slab

A hollow core slab thermal model has been developed in IESVE and validated using published experimental data and has been used as a basis for the case studies. In order to refine the model, the THERM tool was used to calculate the effective thermal conductivity and enhance the accuracy and performance of the model. The thermal conductivity calculated using THERM is 26% more than what is used as default in the simulation tool, and hence the capacity of the hollow core slab is increased by the same proportion. Therefore, the study concludes thermal modelling in one dimensional simulation tool can be improved by using a 2D simulation output.

Also the impact of the ‘Bend’ section of the hollow core on heat transfer has been investigated, against the backdrop of differing claims about its impact. Previous works quoted enhanced heat transfer performances in the range of 2 to 50 times that of the straight section. Based on this study, these claims could not be corroborated. Instead the study concludes the bend section has no impact on heat transfer at all and this corroborates with other study done by Barton et al, 2002.

7.2 Parametric Study

Parametric study of the problem variables that affect the daily zone cooling load, has been conducted through the use of the IES-Optimise tool and the results of the study was used as an input to the development of the Model Predictive Control. Over 60,000 simulations have been run over the course of the study and numerous results have been enumerated. This process has enabled the enumeration of various strategies through the variation of control variables and it painted pictures of the impact of the various variables on cost and comfort. Even without MPC, this exercise itself could be used by building service managers or engineers to try out differing scenarios.

From the parametric study, it is observed that the daily cost of electricity is highly dependent on precooling start time, precooling temperature set point, slab core entering temperature & zone temperature set point:

$$E_k = f(\overrightarrow{Setpoint_k}, PCStartTime_k, SlabEnteringAirTemp_k) \text{ ----- (Eq-16)}$$

However, the conclusion of the study is, only the zone temperature trajectory could determine how stored energy is discharged and; even when all the parameters are set at the optimal value, the effectiveness of precooling and the discharge of stored energy highly depends on the zone temperature set point that controls the demand limiting trajectory. Therefore, the study concludes that optimisation of zone temperature set points in conjunction with Time of Use electricity cost, can be used as a proxy to optimally control cooling plants and air handling systems.

7.3 The Use of Whole Building Simulation Tool and MPC

Whole building simulation tool has been used to implement MPC and results are encouraging. The MPC produced control signals that reduced the peak demand and peak load by 50%. The conclusion reached in this respect is that, the success of hollow core slab, as energy saving means, depends on how it's charging and discharging is predictable based on the conditions the next day. The use of MPC can be a valuable aid in this respect.

The use of the IESVE free form profiles to overcome the limitation of “preconditioning”, time step synchronisation and data operability has proved valuable and this work will pave the way for further refinement of the approach, with the view that synchronisation at finer times step level could be possible. As demonstrated in this work, by doing prediction over a day's horizon, building service managers could plan their building operation successfully and reliably, through the use of similar approach, as long as they can assemble a realistic model of their building, through measurement and calibration.

The MPC implemented here, for instance, could be used to complement Weather Compensated Controllers which are forward looking but do not consider the current state of the building. Through calibration of these controllers or daily adjustment of their control systems, based on the MPC run, they can be made to take the current state of the building into account.

As computing resources are made more and more powerful, the scope for using whole building simulation tool for MPC will be prominent either as a collaboration with reduced order model or stand alone. In any case, the thermal response of the real building can only be closely approximated by integrated simulation tool than a custom made thermal response model and hence a bigger role for it (whole building simulation tools) in MPC.

The potential cost saving demonstrated through demand limiting and peak load shifting is a considerable amount that warrants further study to make the use of hollow core slabs more common than it is now. A potential 50% saving over the baseline makes the investment in hollow core slabs attractive, but this needs to be coupled with a control system that predicts the future operation of the slab to optimally charge or discharging it; however, predictive control has always been the challenge.

Generally, the saving quoted here depends on the type of the building, its use, the weather, the utility rate structure, the building thermal capacitance, the occupancy pattern and part-load characteristics of the cooling plant (Braun, 1990).

7.4 Future Work

I propose the following points be studied in the future so that, there is a clear understanding of the ‘cost benefit’ of employing an air activated hollow core slab:

- Although energy consumption is a function of the control variables as shown in equation 16, the complex interaction of the variables and the linearity or otherwise of the function given above need to be further investigated so that accurate measurements of the influence of each variable on energy consumption is known. The

parametric study conducted did not involve Monte Carlo sensitivity study, however in the future conducting this study will be crucial.

- Hollow core slab, showed a potential for saving energy cost, but its economic viability should be compared to the already know cost saving measures in HVAC. For instance, how does hollow core slab perform against a water side economiser? What is the magnitude of fan energy used by hollow core slab system compared to other cost saving measures? These kind of studies need to done in order to qualify the overall benefits or lack of it, of a hollow core system.
- How does air activated hollow core system compare to the performances of a radiant system, where embedded pipes are used to circulate cooling or heating water?

I propose the following point should be considered in the near future:

- IESVE needs to facilitate the data operability and time step synchronisation of its tools with other tools, such as MatLab so that control algorithms are developed outside of the IESVE. This will facilitate further developments of MPC for building control, enabling tighter control on predictions horizons and control horizons, so that faster decisions are made in reaction to change of disturbances in the horizon.

References

- Andersson, L.O, Bernander K.G., Isfalt E, and Rosenfeld A.H., (1979). Storage of heat and coolth in hollow-core concrete slabs, Swedish experience, and application to large, American-style buildings;
- Barton, P, Beggs, C.B., Sleigh, P.A., (2002) A theoretical study of the thermal performance of the TermoDeck hollowcore slab system,
- Oró , E., Gracia, A. de, Castell, A., Farid, M.M., Cabeza, L.F. (2003). Review on phase change materials (PCMs) for cold thermal energy storage applications
- Mehling, H, Cabeza, LF. Heat and cold storage with PCM.(2008) An up to date introduction into basics and applications. Springers-Verlag Berlin Heidelberg
- Castell, A, Martorell, I, Medrano, M, Pérez, G, Cabeza, LF. (2010) Experimental study of PCM in brick constructive solutions for passive cooling. Energy Build
- Zhang, Y., Zhou, G., Lin, K., Zhang, Q., Di H. (2007). Application of latent heat thermal energy storage in buildings: State-of-the-art and outlook. Building and Environment, vol. 42, pp. 2197-2209
- Heim D., Clarke J.A . (2004). *Numerical modeling and thermal simulation of PCM–gypsum composites with ESP-r*. Energy and Buildings, Vol. 36(8), pp. 795–805.
- Neeper, DA (2000). Thermal dynamics of wallboard with latent heat storage. Solar Energy, Vol. 68(5), pp. 393–403.
- Peippo,K, Kauranen,P, Lund, PD. (1991) Multicomponent PCM wall optimized for passive solar heating. Energy and Buildings, Vol. 17(4), pp. 259–70.
- Pasupathya, Velraja, R., Seenirajb, R.V. (2005). Phase change material-based building architecture for thermal management in residential and commercial establishments A.

Asan, H. (2005) Numerical computation of time lags and decrement factors for different building materials

BRE, (2006). BR 489 Part L Explained – The BRE Guide. Garston: Building Research Establishment (BRE).

CIBSE, (2005b). CIBSE knowledge series: KS3 – Sustainable low energy cooling: an overview. London: Chartered Institute of Building Services Engineers.

CIBSE, (2006a) Guide A: Environmental Design. Chartered Institute of Building Services Engineers.

Clarke, J. A., Johnstone, C. M., Kim, J. M. and Tuohy, P. G. (2009). The EDEM methodology for housing upgrade analysis, carbon and energy labelling and national policy development;

Warwick, D. (2010). Integrating Active Thermal Mass Strategies in Responsive Buildings

Corgnati, S. P., & Kindinis A. (2006). Thermal mass activation by hollow core slab coupled with night ventilation to reduce summer cooling loads

Aschehoug, O. & Andersen, I. (2008). Integrating Environmentally Responsive Elements in Buildings

Yang, L. & Li, Y. (2008). Cooling load reduction by using thermal mass & night ventilation

Seshadri, B., Dubey, S. and Pun, W. M. (2013). Numerical Study of a Concrete Core Temperature Control (CCTC) Building for Tropics

Zmeureanu, R. & Fazio, P (1988). Thermal Performance of a Hollow Core Concrete Floor System for Passive Cooling

Braun, J. E. (2006) Reducing Energy Costs & Peak Electrical Demand through Optimal Control of Building Thermal Storage

Pfafferott, J, Henze, G.P, , Herkel, S, & Felsmann, C. (2007). Impact of adaptive comfort criteria and heat waves on optimal building thermal mass control

Ren, M.J. & Wright, J.A. (1997). A Ventilated Slab Thermal Storage System Model

Henze, G. P., Le, T.H., Florita, A. R. & Felsmann, C. (2007). Sensitivity Analysis of Optimal Building Thermal Mass Control

Asan, H. & Sancaktar, Y.S. (1997). Effects of Wall's thermophysical properties on time lag and decrement factor

Li, Y. & Xu, P. (2006). Thermal Mass Design in Buildings – Heavy or Light?

Balaras, C.A. (1995). The role of thermal mass on the cooling load of buildings. An overview of computational methods

Sourbron, M. (2012). Dynamic thermal behaviour of buildings with concrete core activation

Young, Chae, Tae. Richard, K. Strandb. (2013) Modelling ventilated slab systems using a hollow core slab: Implementation in a whole building energy simulation program.

Demand Shifting With Thermal Mass in Light and Heavy Mass Commercial Buildings, Peng Xu, 2007

Braun, James, E. (2003). Load Control using Thermal Mass

Lee, Kypung-ho. & Braun James E. (2007). Model-based demand-limiting control of building thermal mass,

Braun, James, E, Montgomery, Kent, W. & Chaturvedi, Nitin. (2001). Evaluating the performance of Building Thermal Mass Control Strategies,

Lee, Kyoung-ho & Braun, James, E. (2007) Model-based demand-limiting control of building thermal mass,

Jingran Ma, Joe Qin , Timothy, Salsbury & PengXu, (2011). Demand reduction in building energy systems based on economic model predictive control,

Lee, Kyoung-ho. and Braun, James, E.,(2007) Development of methods for determining demand-limiting setpoint trajectories in buildings using short-term measurements,

Jan Široky , Frauke Oldewurtel , Jirí Cigler , Samuel Prívvara (2013).Experimental analysis of model predictive control for an energy efficient building heating system

Jiri Cigler, (2013) Model Predictive Control for Buildings

Pramod, B.Salunkhe, Prashant, S.Shembekar. (2012) A review on effect of phase change material encapsulation on the thermal performance of a system

Shan K. Wang. (2001). Hand book of air conditioning and refrigeration, 2nd edition,

Antonis, M., Psarompas, (2001) Solar wall energy performance assessment

Moor, T. (2008) SIMULATION OF RADIANT COOLING PERFORMANCE WITH EVAPORATIVE COOLING SOURCES TIMOTHY MOORE

Sourbro, Maarten.(2012). Dynamic thermal behaviour of buildings with concrete core activation

Armstrong, Peter, R., Leeb, Steven, B., Norford, Leslie K (2006). Control with building mass Part I & II

Zhao, Jie., Lam, Pho, Khee., Ydstie, B. Erik. (2013) **ENERGYPLUS MODEL-BASED PREDICTIVE CONTROL (EPMPC) BY USING MATLAB/SIMULINK AND MLE+**

Yahiaoui, A., Hensen, J., Soethout, L. and Paassen A.H.C. (2006). Model based optimal control for integrated building system

May-Ostendorp, Peter, Gregor., Henze, P., Corbin, Charles, D., Rajagopalana, Balaji., and Clemens, Felsmann. (2011), Model predictive control of mixed-mode buildings with rule extraction

Oldewurtel, Frauke (2011), Stochastic Model Predictive Control for Energy Efficient Building Climate Control

MITAEAS, G. P. & STEPHENSON, D. G. (1967). Room thermal response factor

THERM, 2D Software, https://windows.lbl.gov/software/therm/7/index_7_3_2.html

IESVE Optimise,

http://www.iesve.com/research-learning/research-flyers/optimise_flyer_mar12_uk_.pdf

IESVE, <http://www.iesve.com/>

,

